

Ag Sintering Die and Passive Components Attach for High Temperature Applications

by

Fang Yu

A dissertation submitted to the Graduate Faculty of
Auburn University
in partial fulfillment of the
requirements for the Degree of
Doctor of Philosophy

Auburn, Alabama
May 7, 2016

Keywords: Ag sintering, die attach, high temperature packaging

Copyright 2016 by Fang Yu

Approved by

R. Wayne Johnson, Chair, Emeritus Professor of Electrical & Computer Engineering
Michael C. Hamilton, Associate Professor of Electrical & Computer Engineering
John L. Evans, Professor of Industrial & System Engineering
Dong-Joo Kim, Associate Professor of Materials Engineering

Abstract

With an increasing demand for SiC and GaN high power devices and high temperature electronics operating in extreme environments, traditional solder materials are reaching their limitations in performance. Compatible, high temperature materials are required for attachment of semiconductor die and passives to the thick film metallized substrate pads. In addition, there is a strong desire to eliminate high lead containing solders in Si power device packaging for use over conventional temperature ranges. Low temperature Ag sintering technology is a promising method for high performance lead-free die attachment. Due to its high thermal and electrical conductivity and high melting point, sintered Ag die attach has received much attention for assembly of power modules and for high temperature (300°C) applications. Previous work with Ag sintering has required pressure during the sintering process or been limited to small area die. In chapter 3, the pressureless sintering of micro-scale silver paste is examined for larger (8mm x 8mm) area die. Experimental combinations included: Si die metallization (Ag and Au); thick film substrate metallization (Au, Ag and PdAg); and sintering temperature.

For Au metallization (die and/or substrate), the initial shear strength results were good with 8mm x 8mm die sintered at lower temperatures (200 °C). The shear strength was beyond the limit of the shear test machine (100 kg), corresponding to >15.3 MPa. However, after aging for 24 hours at 300°C, the shear strength dropped significantly. An SEM was used to characterize cross sections of as-built and aged sample. The decrease in die shear strength with high

temperature sintering (250°C and 300°C) or high temperature aging is attributed to surface diffusion of Ag along the Au surface resulting in a dense Ag layer adjacent to the Au surface and a depletion layer within the die attach adjacent to the dense Ag layer. Shear failures occurred through the depleted region.

For Ag metallization (die and substrate), no decrease in shear strength was observed with 300°C aging. Shear strength of 8x8cm² dies was >100 kg (>15.3 MPa) as-built. The shear strength remained >15.3MPa after 8000 hours of 300°C aging.

The pressureless sintering process for large die (8 mm x 8 mm) and suitable metallization were demonstrated to provide high reliability die attach by using micro-size Ag sintering. The resulting die attach layer had approximately 30% porosity.

In chapter 4, passive component (chip resistors) attachment with pressureless Ag sintering was explored. Due to termination geometry differences between resistors and dies, different processing procedures and parameters were developed.

For PtAu terminated resistors, the mean shear force of as-built samples on thick film Ag metallized substrates was 90 N, but dropped to 18.6 N after 1500 hours at 300°C. Formation of a dense Ag layer near the PtAu resistor termination and a void region near the thick film metallization was seen in cross-sections after 1000 hours at 300°C

For PdAg terminated resistors with a plated Ni/Au finish, the initial shear force results were low due to Ag diffusion along Au metallization surface. For PdAg terminated resistors with Ag thick film substrates, the initial shear force was approximately 60 N and remained in the range of 50-70 N during aging at 300°C for 1500 hours. A new thick film metallization (Au+Ag) was developed to enable the use of thick film Au interconnect metallization.

In chapter 5, a low temperature pressure-assisted rapid sintering process was developed, which include a 150°C, one-minute pre-dry and a 300°C one-minute sintering process. The reduction in the sintering time allowed the use of a flip chip thermo-compression bonder for automated die attach instead of hydraulic hot press. The porosity was decreased from 30% to 15% with application of a low pressure (7.6 MPa) during a one minute sintering process. The shear strength for a 3 mm x 3 mm die was 70 MPa and the 8 mm x 8 mm die could not be sheared off due to a 100 kg shear module force limit. Both the Ag and Au metallization (die and substrate) were studied. Furthermore, a new substrate metallization combination was found that allows the use of Au thick film metallized substrates. High temperature (300°C) storage tests for up to 2000 hours aging were conducted and results were presented.

Acknowledgments

First and foremost, I would like to express my sincere appreciation to my advisor, Dr. R. Wayne Johnson, for his invaluable guidance, support and encouragement during my Ph. D study and research at Auburn University. I have been amazingly fortunate to have such a highly respected advisor who gave me the freedom to explore, and constantly help me with inspiration and ideas when my steps faltered. His pleasant personality and professional research attitude set an excellent model for my future career.

My co-advisor, Dr. Michael Hamilton, has been always there to listen, help and give advice. I am deeply grateful to him for the supporting of my research and guidance on laboratory maintenance. I am also thankful to him for carefully reading and commenting on my papers and this dissertation. I would like to thank all the committee members, Dr. Robert Dean and Dr. Dong-Joo Kim for their valuable time and assistance.

I would also like to thank Dr. Charles David Ellis, Michael J. Palmer, my fabulous colleagues and friends Kun Fang, Zhenzhen Shen, Jinzi Cui, Zhangming Zhou, and George Hernandez for their cooperative support and continual assistance through this research.

Most importantly, I would like to thank my family, to whom this dissertation is dedicated, have been a constant source of love, concern, encouragement and strength all these years. I have to give a special mention for the support given by my parents Zongde Yu and Yugui Cui for their continuous love and encouragement throughout my life.

Table of Contents

Abstract	ii
Acknowledgments.....	v
List of Tables	x
List of Figures.....	xi
CHAPTER 1 INTRODUCTION	1
1.1 Application of High Temperature Electronics.....	1
1.1.1 Oil, Gas and Geothermal Well Logging.....	1
1.1.2 Automotive	2
1.1.3 Aircraft and Space Exploration.....	3
1.2 High Power and High Temperature Devices	4
1.3 High Temperature Electronics Packaging	6
1.3.1 Die Attach.....	6
1.3.2 Electrical Interconnection.....	10
1.3.3 Packaging Body.....	11
CHAPTER 2 LITERATURE REVIEW: Ag Sintering Paste for Die Attach.....	12
2.1 Mechanism of Sintering.....	12
2.2 Ag Sintering Paste for Die Attach	13
2.2.1 Pressure Micron-Ag Paste.....	14

2.2.2	Pressureless Micro-Ag Paste.....	15
2.2.3	Pressureless and Pressure Nano-Ag Paste	16
CHAPTER 3 PRESSURELESS SINTERING		18
3.1	Review of Pressureless sintering	19
3.2	Test Vehicle and Process	20
3.3	Process Development Results and Discussion.....	22
3.3.1	Au Die Metallization, Au Substrate Metallization	22
3.3.2	Au Die Metallization, Ag Substrate Metallization	25
3.3.3	Ag Die Metallization, Au Substrate Metallization	27
3.3.4	Ag Die Metallization, Ag Substrate Metallization	29
3.3.5	Ag Die Metallization, PdAg Substrate Metallization	31
3.4	Long Term Aging Study	33
3.5	Further characterization with Au metallization	36
3.6	Discussion	39
3.7	Conclusion	41
CHAPTER 4 COMPONENT ATTACH WITH PRESSUELESS SINTERING		43
4.1	Introduction.....	43
4.2	Test Vehicle	44
4.3	Process Overview.....	45
4.4	Process development and Initial Screening	46
4.4.1	Resistor with PtAu termination.....	46
4.4.2	Resistor with PdAg termination with plated Ni/Au finish.....	52
4.4.3	Resistor with PdAg termination.....	53

CHAPTER 5	PRESSURE SINTERING	64
5.1	Review of Pressure Sintering Methodology	64
5.2	Test Vehicles.....	67
5.3	Assembly and Characterization Process	68
5.4	Process Optimization	70
5.4.1	Pre-dry Condition:	70
5.4.2	Sintering Temperature and Sintering Time:	71
5.4.3	Sintering Pressure vs. Shear Strength:	74
5.4.4	Porosity versus Sintering Pressure.....	75
5.5	Assembly Results with Different Metallization.....	77
5.5.1	Ag Die Metallization, Au Substrate Metallization	77
5.5.2	Au Die Metallization, Ag Substrate Metallization	78
5.5.3	Ag Die Metallization, Ag Substrate Metallization	81
5.5.4	Ag Die Metallization, Au + Ag Substrate Metallization	82
5.6	Conclusion	85
CHAPTER 6	RELIABILITY OF PRESSURE SINTERING	86
6.1	Literature Review of Reliability for sintered Ag.....	86
6.2	Test vehicles (Materials/Substrates)	87
6.2.1	Substrate Metallization	87
6.2.2	Die Metallization	89
6.3	Assembly and Characterization Process (Process summary)	89
6.3.1	Ag Paste Deposition.....	89
6.3.2	Pressureless Sintering Process [116]	89

6.3.3	Fast Pressure-Assisted Sintering Process []	89
6.3.4	Die Shear Testing.....	90
6.3.5	SEM Analysis	91
6.4	Reliability of pressureless sintering.....	91
6.4.1	Thermal Aging and Thermal Cycling Test Conditions.....	91
6.4.2	Thick Film Substrates: Aging.....	92
6.4.3	DBC: Aging	93
6.4.4	Thick Film metallization: Thermal cycle.....	95
6.4.5	DBC: Thermal cycle	96
6.5	Reliability of pressure sintering.....	97
6.5.1	Thick Film metallization: Aging.....	98
6.5.2	DBC: Aging	102
6.5.3	DBC: Thermal cycling.....	104
6.6	CONCLUSION.....	105
CHAPTER 7 CONCLUSION AND FUTURE WORK.....		106
7.1	Pressureless Sintering	106
7.2	Component Attach with Pressurless sintering	106
7.3	Pressure Sintering	107
7.4	Future Work.....	108
REFERENCES		109

List of Tables

Table 1-1 High Temperature Applications -].....	4
Table 1-2 Key semiconductor materials properties . (*)means measured at 300 K.	5
Table 2-1 Commercial entities from the semiconductor industry involved in the use of sintered Ag technology for die-attach (in alphabetical order) [65]	14
Table 5-1. Summary of recent literature on pressure-assisted Ag sintering processes.....	66

List of Figures

Figure 1-1 Cross section of EP-SOIC or EP-QFP.	7
Figure 1-2 Graphical representation of the conventional process vs. the TLPS technique [40]. ...	9
Figure 2-1 Three stages of solid state sintering: left: initial stage, center: intermediate stage, right: final stage (Courtesy EPMA) [59]	13
Figure 2-2 An Ellingham diagram for the reduction of metal oxides.....	16
Figure 3-1 Sintering profile of three different sintering temperature 200°C, 250°C, 300°C. Set 10 °C/min ramp rate and soap for 1 hour.....	21
Figure 3-2 Au die with Au substrate sintered at 200°C, 250°C, 300°C, respectively, and aged at 300°C for 24 hours.....	23
Figure 3-3 Cross section microstructure of sintered and aged sample: Au substrate + 200nm e-beamed Au die. (a.) 200°C sintering for 1 hour. (b.) After 300°C aging for 24 hours.	24
Figure 3-4 Details of non-porous layer and depletion region.....	24
Figure 3-5 Cross section of lamination samples: 200nm Au metallized die with Au metallized substrate. (a.) 130°C dry for 30 min and 200°C sintered with pressure for 1 hour. (b.) Aged at 300°C for 24 hours.....	25
Figure 3-6 Au die with Ag substrate sintered at 200°C, 250°C, 300°C, respectively, and aged at 300°C for 24 hours.....	26

Figure 3-7 Cross section microstructure of sintered and aged sample: Ag substrate + 200nm e-beamed Au die. (a.) 200°C sintering for 1 hour, (b.) After 300°C aging for 24 hours.	27
Figure 3-8 Ag die with Au substrate sintered at 200°C, 250°C, 300°C, respectively, and aged at 300°C for 24 hours.	28
Figure 3-9 Cross section microstructure of sintered and aged sample: Au substrate + 300nm e-beamed Ag die. (a.) 200°C sintering for 1 hour, (b.) After 300°C aging for 24 hours.	29
Figure 3-10 Ag die with Ag substrate sintered at 200°C, 250°C, 300°C respectively. And aged at 300°C for 24 hours.	30
Figure 3-11 Cross section microstructure of sintered and aged sample: Ag substrate + 300nm e-beamed Ag die. (a.) 200°C sintering for 1 hour, (b.) After 300°C aging for 24 hours.	31
Figure 3-12 Ag die with PdAg substrate sintered at 200°C, 250°C, 300°C, respectively, and aged at 300°C for 24 hours.	32
Figure 3-13 Cross section of PdAg substrate with Ag die. (a.) Sintered at 200°C for 1 hour. (b) Aged at 300°C for 24 hours.	33
Figure 3-14 Porosity calculation with as a function of aging time.	34
Figure 3-15 Microstructure of Ag metallization die with Ag thick film substrate sample at high temperature (300°C) reliability test and porosity calculation.	35
Figure 3-16 Cross Section of a Ag die assembled on a PdAg substrate after 1000 hours at 300°C.	36
Figure 3-17. Cross sections of Au metallized Die on Au metallized substrate, sintered at 200°C for 1 hour. (a) after 30 minutes aging at 300°C, (b) after 1 hour aging at 300°C.	37
Figure 3-18. Cross sections of Au metallized Die on Au metallized substrate, sintered at 200°C for 1 hour. (a) after 30 minutes aging at 250°C, (b) after 4 hours aging at 250°C.	38
Figure 3-19. Cross sections of Au metallized Die on Au metallized substrate, sintered at 200°C for 1 hour then aged after 1500 hours at 200°C.	39

Figure 3-20. Cross section of samples aged in nitrogen for 24 hours. 200nm Au die with Au substrate sintered at 200°C.....	41
Figure 4-1. Sintering profile of three different sintering temperatures 200°C, 250°C, 300°C. Ramp rate was 10°C/min and dwell for 1 hour.....	46
Figure 4-2. Shear force of PtAu resistor sample sintered at 200°C, 250°C, 300°C, and aged for 100 hours, 250 hours, (a) Au substrate, (b) Ag substrate.	48
Figure 4-3. PtAu resistor with Au metallized substrate 200°C sintered for 1 hour without post-print drying.....	49
Figure 4-4. TGA analysis of weight loss of Ag sintering paste. Ag paste was placed in Pt pan and temperature was ramped at 50 °C/min with air flow rate of 50 ml/min.	49
Figure 4-5 Post-printing-dry method: shear force of PtAu resistor sample sintered at 200°C, 250°C, 300°C, and aged for 100 hours or 250 hours on (a) Au substrate and (b) Ag substrate.	51
Figure 4-6 Au substrate failure analysis. Au substrate with PtAu resistor sintered at 300°C with post-print drying step, then aged at 300°C for 250 hours.	52
Figure 4-7. Box plot of shear force for PdAg resistor with plated Ni/Au finish assembled on Au substrate showing shear force of samples as-built and aged for 100 hours or 500 hours.....	53
Figure 4-8. Shear force of as-built PdAg resistors (Supplier A) attached to Ag and PdAg thick film metallized substrates. Assembly process: post-print drying and pressureless sintered at 300°C for one hour. Results for samples aged for 100, 250, 500 hours are also shown.....	54
Figure 4-9. (Top) schematic cross-section showing resistor, termination and solder structure to aid in location determination of (Bottom) SEM image and elemental analysis (weight percentage) of the substrate-side failure surface after shear testing. The sample was as-built PdAg terminated resistor (Supplier A) on a Ag substrate.....	55
Figure 4-10. Shear force of as-built PdAg resistors (Supplier B) attach separately with Ag, Au + Ag and PdAg thick film metallized substrates. Assembly process: post-print drying and pressureless sintered at 300°C for one hour.....	56

Figure 4-11. Sample of PdAg resistor (Supplier B) with Ag metallized substrate sintered at 300°C for 1 hour.....	57
Figure 4-12. Sample of PdAg resistor (Supplier B) with PdAg metallized substrate sintered at 300°C for 1 hour.....	58
Figure 4-13. Sample of PdAg resistor (Supplier B) with Au + Ag metallized substrate sintered at 300°C for one hour.....	59
Figure 4-14. Shear force of Ag substrate with PtAu resistor sintered at 300°C for 1500 hours. .	60
Figure 4-15. Ag metallized substrate with PtAu terminated resistor sintered at 300°C, then aged at 300°C for 1000 hours.....	61
Figure 4-16. Shear force of PdAg resistors (Supplier B) with Ag metallized substrate aged for 1500 hours.....	61
Figure 4-17. Cross section of PdAg (Supplier B) with Ag metallized substrate aged at 300°C for 1000 hours.....	62
Figure 5-1 Temperature and force profile of pressure-assisted sintering, exhibiting a 3 °C/s ramp rate and sintering/force application dwell time of 60 seconds.....	69
Figure 5-2. TGA of weight loss of Ag sintering paste. Ag paste was placed in a platinum pan with a temperature ramp of 50 °C/min and with air flow rate of 50ml/min.	71
Figure 5-3. Box plot of shear strength versus sintering temperature and sintering time at 7.6 MPa sintering pressure. 3mm x 3 mm Ag metallized SiC die assembled on Ag thick film metallized substrates following a 150°C one-minute pre-dry.	73
Figure 5-4. Box plot of shear strength versus sintering pressure.....	75
Figure 5-5. Porosity of sintering Ag under different sintering pressure.	76
Figure 5-6. Cross-sectional SEM image of die attach layer for as-built sample with 3 mm x 3 mm Ag metallized die on a Ag thick film substrate sintered at 300°C with 3.8 MPa for one minute.	77

Figure 5-7. Image of fracture surface of 8 mm x 8 mm Ag metallized die with Au thick film metallized substrate.....	78
Figure 5-8. (a) Cross-sectional SEM image of die attach layer for an 8mm x 8mm Au metallized die with Ag thick film substrate that was sintered at 300°C with 7.66 MPa pressure for one minute. (b) Cross-sectional SEM image of sample that was aged at 300 °C for 1 hour.	80
Figure 5-9. (a) Cross-sectional SEM image of die attach layer of as-built sample that was 8 mm x 8 mm Ag metallized die with Ag thick film substrate sintered at 300°C with 7.66 MPa for one minute. (b) Cross-sectional SEM image of sample aged at 300°C for 1 hour.	82
Figure 5-10. SEM image and EDS elemental analysis of Au + Ag thick film layer of an as-built sample. The spectra are given in weight percent.	83
Figure 5-11. (a) Cross-sectional SEM image of die attach layer of as-built sample that was 8 mm x 8 mm Ag metallized die with Au + Ag thick film substrate sintered at 300°C with 7.66 MPa for one minute. (b) Cross-sectional SEM image of sample aged at 300°C for 1 hour.	85
Figure 6-1. SEM image and EDS elemental analysis of Au + Ag thick film layer of an as-built sample. The spectra are given in weight percent.	88
Figure 6-2. Temperature and force profile for pressure-assisted fast sintering, exhibiting a 3°C/s ramp rate and sintering/force application dwell time of 60 seconds.	90
Figure 6-3. Thermal cycling temperature profile.....	91
Figure 6-4. Cross sectional SEM image of die attach layer for 300°C 1500 hours aged sample with Ag metallized Si die on Au+Ag metallized substrate.....	93
Figure 6-5. Cross sectional SEM image of die attach layer after 2000 hours aging at 300°C. Sample was Ag metallized SiC die on Ni/Ag metallized DBC substrate (a) overview, (b) close-up.....	94
Figure 6-6. (a) Cross-sectional SEM image of die attach layer of sample that was 8mm x 8mm Ag metallized die with Ni/Pd/Ag metallized DBC substrate sintered at 300°C 1 hour without pressure. (b) Cross-sectional SEM image of sample aged at 300°C for 2000 hours.	95

Figure 6-7. Cross-sectional SEM image of die attach layer of sample with 8mm x 8mm Ag metallized Si die and Ag thick film metallized substrate after cycles from -55°C to 300°C (a) 750 cycles, (b) 1000 cycles.	96
Figure 6-8. DBC substrate showing progressive failure of Cu-to-alumina interface with increasing number of thermal cycles.	97
Figure 6-9. Cross-sectional SEM image of die attach layer of sample that was 8mm x 8mm Ag metallized SiC die with Ag metallized DBC substrate after 300 cycles from -55°C to 300°C.	97
Figure 6-10. Cross-sectional SEM image of die attach layer of sample that was 8mm x 8mm Au die with Ag substrate sintered at 300°C with 7.6 MPa pressure for one minute and aged at 300°C for (a) 24 hours, (b) 500 hours.	99
Figure 6-11. Cross-sectional SEM image of die attach layer of sample that was 8mm x 8mm Ag die with Ag substrate sintered at 300°C for one minute and aged at 300°C for: (a) 24 hours, (b) 1500 hours.	100
Figure 6-12. Shear strength of 3 mm x 3 mm Ag metallized die with Ag thick film substrate pressure-assisted (7.6 MPa) sintered at 300°C for one minute and aging time from initial to 1500 hours.	101
Figure 6-13. Cross-sectional SEM image of die attach layer of 8mm x 8mm Ag metallized die with A Ag thick film substrate pressure-assisted (7.6 MPa) sintered at 300°C for one minute and aged at 300°C for: (a) 24 hours. (b) 2000 hours.	102
Figure 6-14. Cross-sectional SEM image of die attach layer of 8mm x 8mm Ag metallized SiC die with Ni/Pd/Au metallized DBC substrate pressure-assisted (7.6 MPa) sintered at 300°C for one minute. (a) As-built, (b) Aged for 250 hours at 300°C.	104
Figure 6-15. Cross-sectional SEM image of die attach layer of 8mm x 8mm Ag metallized SiC die with Ag metallized DBC substrate pressure-assisted (7.6 MPa) sintered at 300°C for one minute and aged at 300°C for 2000 hours.	104

CHAPTER 1 INTRODUCTION

High temperature electronics (HTE) refers to the devices or systems operating in high-temperature environments, usually defined as above 125°C, outside of the “traditional” temperature range -55°C to +125°C [1]. There is no agreement as to the realm of high temperature among experts due to the application differences, such as the sensor in the combustion chamber of a jet engine may experience 300°C or higher, whereas the power devices in the flight surface actuator system may operate at temperature of 200°C. The high operating temperature can be attributed to the ambient environment (combustion chamber, oil, gas and geothermal well logging, surface of Venus), power dissipation (power transistor, RF amplifier, etc.), or a combination of both (automotive).

1.1 Application of High Temperature Electronics

Many industries need electronics that can work reliably and durably at high temperatures or extreme harsh environments. The down-hole oil and gas industry is the oldest, and currently still the largest application of high-temperature electronics [2]. This and other applications for automotive, aircrafts and space exploration will be discussed below.

1.1.1 Oil, Gas and Geothermal Well Logging

Oil and natural gas account for 63% of the energy consumed in the United States in 2013, fueling the American economy [3]. The Annual Energy Outlook 2015 [4] indicates that they will continue to play a vital role in the U.S. energy portfolio for the next several decades. Reliable exploration and production technologies are needed to effectively and economically access these resources in an environmentally way. The global geothermal gradient is generally 25 °C/km depth, in some areas even more. As the reserves of easily accessible nature resources continue to

decline, downhole exploration goes ultra-deep, the ambient temperature becomes higher up to 200°C, with pressure greater than 25 kpsi [2].

Due to the extreme temperature environment, it has been a difficult task for downhole electronics to implement control and monitoring. In the oil exploration and oilfield development, down-hole drilling is significant in a wide range of applications. While drilling or soon thereafter, measurements, including temperature, pressure, subsurface electrical resistivity, radiation, and inclination are needed to determine the characteristics of the formation, the type of rock in the formation, whether hydrocarbons are adequate etc. Incorrect readings cause expensive errors in locating oil and gas deposits in the earth, predicting the life and working time of a well, determining the suitability of a drilling location, and establishing the production volume of the well. Reliability is paramount, otherwise, the device will need regular or more frequent replacement and increased drilling cost due to the extreme temperature environments. Packaging poses significant challenges for the materials used in drilling.

The monitoring and data acquisition for enhanced geothermal systems (ESG) must operate at temperatures ranging from 150°C to 300°C [5]. The enhanced and supercritical geothermal systems require downhole gauges tolerating up to and even beyond 400°C in Iceland and New Zealand [6]. Correspondingly, high temperature packaging to interface with the elements of the electrical system is required.

1.1.2 Automotive

As a transition from mechanical or hydraulic systems to electronically controlled systems, by-wire technology in automobiles has been under way for almost a decade (More Electric Vehicles). Besides, current power electronics in automotive are transitioning from silicon to wide bandgap (WBG) devices to meet efficiency, cost, volume, and weight targets. The operating

temperature of electronics depends on location, power dissipation etc., ranging from 150°C to 300°C. Heat sinking is required in underhood temperature above 125°C. The integrated power transistors and smart power devices in the actuator are expected to operate at 175°C to 200°C [7].

Hybrid and Electric Vehicles (HEV/EV) are regarded as one of the most effective ways to reduce CO₂ emissions and fossil fuel use. The power electronics in an HEV can share the cooling water from the internal engine to remove heat from the power electronics. The engine coolant is nominally 105°C or higher [8]. Accordingly, the power devices junction temperature must operate at 150°C to 175°C [9]. A secondary lower temperature direct liquid cooling structure was integrated with IGBT modules to achieve efficient thermal management [10], but this adds weight, cost and complexity. Also, since EVs do not have a primary cooling loop, the option is to circulate fuel or adding a water-cooling system, which complicates the design, decreases reliability, and adds cost and weight. Therefore letting the electronics operate hot is potentially more advantageous than complex cooling system.

1.1.3 Aircraft and Space Exploration

There is a transition from bleed-air from the engine to the More Electric Airplane (MEA). Boeing's 787 has installed a 'More-Electric Architecture' for energy management and pneumatic pumps [11]. Hydraulic actuation is being replaced with electro-mechanical actuators (EMAs) or electro-hydrostatic actuators (EHAs) [12]. Also, the electric motor driven cabin air compressors are taking the place of the gas driven turbines, whose size is close to 100 kW.

In order to decrease the wiring harnesses complexity and weight in airplanes, a distributed system is more preferable than a centralized control system, which could reduce the complexity by one or more orders and several hundred pounds. The engine controls should be placed in proximity with the engine, with temperatures ranging from -55°C up to 225°C [12].

In space exploration, for the Venus mission of NASA’s Solar System Exploration Roadmap, electronics and packaging technologies may be required to survive at least 460°C for more than 90 hours [13] [14].

Table 1-1 shows some high-temperature applications and summarize their operational temperatures, power, and technologies and minimum duration.

Table 1-1 High Temperature Applications [15-18]

High Temperature Electronics Application	Peak Ambient	Chip Power	Current Technology	Future Technology	Minimum Duration
Deep-Well Drilling Telemetry					
Oil and Gas	300°C	<1 kW	SOI	SOI & WBG	Few hours-years
Geothermal	600°C	<1 kW	NA	WBG	Few-100 hours
Automotive					
Engine Control Electronic	150°C	<1 kW	BS & SOI	BS & SOI	8000 operation hours, 10 years “shelf”
On-cylinder& Exhaust Pipe	600°C	<1 kW	NA	WBG	
Electric Suspension & Brake	250°C	>10 kW	BS	WBG	
Electric/Hybrid Vehicle PMAD	150°C	>10 kW	BS	WBG	
Turbine Engine					
Sensors, Telemetry, Control	300°C	<1 kW	BS & SOI	SOI & WBG	Thousands of hours
	600°C	<1 kW	NA	WBG	
Electric Actuation	150°C	>10 kW	BS & SOI	WBG	
	600°C	>10 kW	NA	WBG	
Spacecraft					
Power Management	150°C	>1 kW	BS & SOI	WBG	1000 hours
	300°C	>10 kW	NA	WBG	
Venus & Mercury Exploration	550°C	~1 kW	NA	WBG	
Industrial					
High Temperature Processing	300°C	<1 kW	SOI	SOI	
	600°C	<1 kW	NA	WBG	

BS=bulk silicon, SOI=silicon-on-insulator, WBG=wide bandgap (semiconductor)

1.2 High Power and High Temperature Devices

Due to its bandgap energy of 1.12 eV, silicon becomes intrinsic and loses the characteristics of pn junction at 200°C to 350°C, depending on the doping levels. Silicon-on-insulator (SOI) technology is required when temperatures approach 200°C because leakage currents become a challenge. The limit on low breakdown voltage requires a large Si die area when building higher voltage rating MOSFETs and Schottky diodes [19].

The superior performance of SiC or GaN surpass Si's limits, such as the high breakdown voltage, lower switching losses, higher current densities and high thermal conductivity, [20][21]. With a bandgap of >3 eV (shown in Table 1-2), SiC devices have been demonstrated to work functionally at 600°C [22]. Advances in wide bandgap semiconductors allow the fabrication of high temperature compatible sensors [25] and high power devices. To implement high power or high temperature chips into actual application, integration and packaging for these devices are essentially required.

Table 1-2 Key semiconductor materials properties [23] [24]. (*) means measured at 300 K.

Wide Bandgap Materials	4H- SiC	6H- SiC	Si	GaN	GaAs
Thermal conductivity (W/cm·K)	4.9 (7)	4.9 (7)	1.3 (1.3)	1.3 (1.1)	0.5 (0.55)
Bandgap (eV)	3.26 (3.26)	3.03 (3.02)	1.12 (1.1)	3.39 (3.44)	1.42 (1.43)
Saturated electron velocity (10^7 m/s)	2.0	2.0	1.0	2	1.0
Electron mobility	1000 (700)	600 (330- 400)	1450 (1400)	2000 (900)	8500 (8500)
E_b (MV/cm) (Break down field)	2.2	2.4	0.3	5.0	0.4
Electronic maximum operation temp. (°CC)	750	700	150	>750	350
CTE (ppm/K)	5.12	5.12	2.6	5.73	5.4-7.2
Process maturity	Medium	Medium	Very high	Very low	High
Lattice constant (Å)	3.073	3.081	3.94	3.189	4.00

In regard to Silicon Carbide (SiC) electronics, publications cover the study of low power devices, such as sensors [25] with demonstrated stable operation up to 500°C and op-amps [26] characterized up to 350°C. Tsuyoshi etc. packaged SiC JFETs (Junction Gate Field Effect Transistors) and SBDs (Schottky Barrier Diodes) and tested the static and transient

characteristics up to the temperature of 400°C. A 4 kW converter system was confirmed to operate up to 250°C.

1.3 High Temperature Electronics Packaging

In order to assure the high performance and reliability of devices or systems “enjoying” such high temperature operation, corresponding packaging materials and techniques have to be compatible with more severe thermal and electrical constraints.

The mainly considerations for high temperature electronics assembly and packaging are:

- Electrical connection (signal and power)
- Heat removal
- Mechanical protection and integration
- Practicality and cost
- Undesirable materials (e.g. Pb)

1.3.1 Die Attach

Die attach is the physical attachment of the die to the package or substrate to provide a mechanical connection of the die to the substrate, electrical connection and a thermal path for removing heat during operation as shown in Figure 1-1. In the case of conventional application, polymers such as epoxy adhesives are the most common material for die attach. Due to the intrinsic high thermal and electrical resistivity of polymers, ceramic particles can be added to increase thermal conductivity while retaining electrical insulation. Ag and Au particles are added if electrical conductivity is needed.

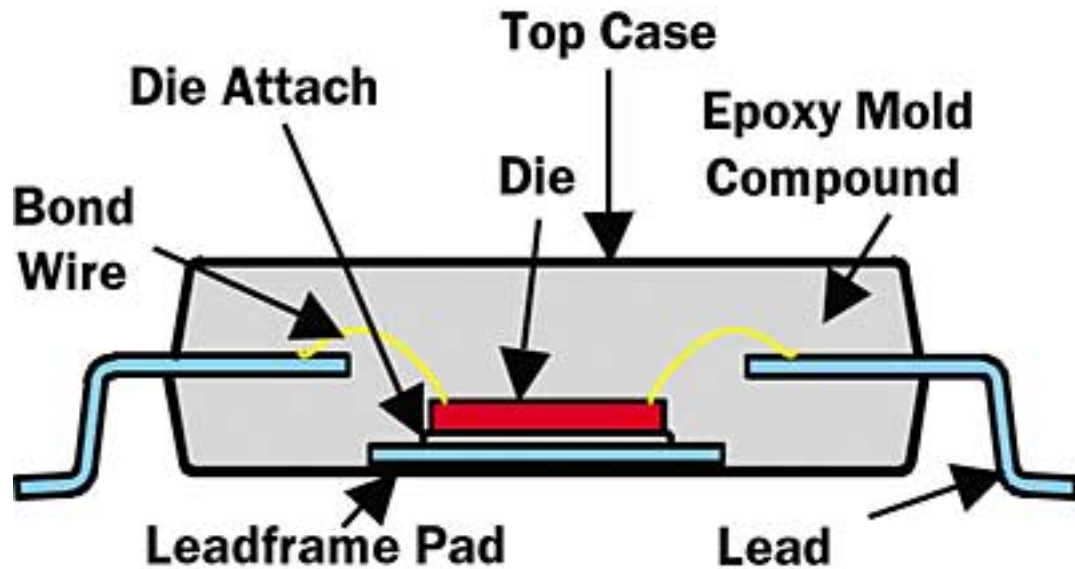


Figure 1-1 Cross section of EP-SOIC or EP-QFP [27].

The benefits of conductive adhesives are low curing temperature, low elastic modulus, lower stress concentrations on the die, easy to work with and low cost. But still the electrical and thermal conductivity is lower compared with metallic solder. Besides, the reduced strength at elevated temperatures and decomposition (depends on formulation, temperature, atmosphere) limit the use of polymer die attach in high temperature applications. Johnson, et al. have confirmed that conductive adhesive die attach is suitable for under-the-hood automotive application at 175°C in air[28]. Riches, et al. have demonstrated polymer die attach material at 250°C for 2000 hours in nitrogen.

For the high temperature environment, metallic die attach materials and techniques such as solders, brazes, transient liquid phase (TLP) and sintering are more common. Lead-Tin is an important die attach material for high temperature applications ($\leq 225^\circ\text{C}$), especially for large size die. However, lead compounds have been regarded as one of the chemicals posing the greatest threat to human life and the environment [29].

AuGe die attach was proven to work reliably on Au thick film metallized Si_3N_4 ceramic substrates with Ti/Ti:W/Au metallized Si die [30]. The mean shear strength decreased from 3.96 to 3.33 kg/mm² after aging 3000 hours at 300°C, a decrease of only 16%. Formation of Au-Si-Ge ternary eutectic (melting point 326°C) limits the application temperature to 300°C. Palmer et al. [31] demonstrated AuGe die attach of Si die to thick film Al_2O_3 substrates at 300°C for 2000 hours. Chidambaram et al. found the growth of Ge phase in Au matrix at high temperature lead to a degradation of shear strength [32].

AuSi die attach was evaluated on both Si [33] and SiC dies [34]. During the bonding process, defects such as delamination, voids were not unusual. Process optimization was performed to achieve the 100% bonded area [35] and vacuum soldering was used to minimize voids [36].

Zinc based alloys are of research interest due to the comparative low cost. Rettenmayr, et al, evaluated the microstructure evolution and the mechanical properties of Zn-Al alloy with additives of Ga or Mg [37]. Egelkraut, et al. studied the ZnAl_5 on bare copper and nickel metallization [38]. In both cases, a strong decrease of shear strength with time was observed. Kim et al. [39] reported the Zn-Sn alloys with different loadings of Sn (20, 30, 40%) on AlN-direct bond copper substrate. After reflow at 260°C, the shear strength was about 30 MPa to 40 MPa.

Liquid transient phase (TLP) bonding is a joining process, which involves a low melting point element or alloy that forms intermetallics or diffuses into the materials that need to be joined; in the process the composition of the liquid changes, resulting in its solidification. The advantage of TLP bonding over soldering or brazing is the ability to form high temperature joints at low processing temperatures as shown in Figure 1-2. The TLPS material primarily consists of

a high melting point base metal (constituent B) and a low melting point additive (constituent A). At a processing temperature T_p , which is below the melting point of the base metal powder B, while above that of additive A, the liquid phase of A formed to enhance the mass transportation rates and densification. Finally, the equilibrium bulk composition formed a solid joint [40]. In the case of typical soldering or brazing, the processing temperature must exceed the liquidus temperature of the alloy by 30-40°C. During cool down from the solidus temperature builds CTE induced stress into the joint. However, TLP has its limitation: the assembly process can be minutes to hours, depending on the material system to allow the intermetallic formation or diffusion to occur.

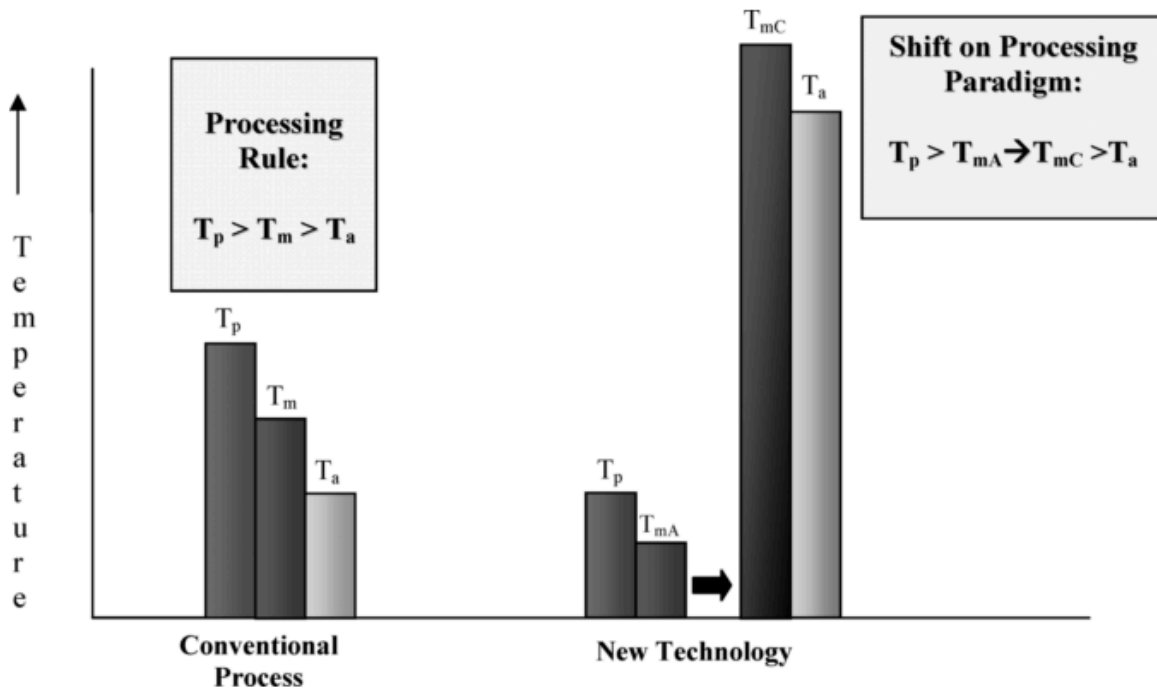


Figure 1-2 Graphical representation of the conventional process vs. the TLPS technique [40].

Ag-In has been widely studied due to the low process temperature and high operation temperature. Quintero, et al. evaluated an In-Ag paste on direct bond copper (DBC) for TLP bonding. The 250°C annealing for 1 hour yielded a system with a thermal stability up to 400°C or

above [40]. Au-Sn is another TLP bonding material which has drawn much attention. Johnson et al. [41] developed the Au-Sn die attach with 20 μm Ag plated on either the backside of SiC or DBC substrate to provide enough Au for the TLP bonding. Reliability of 400°C was achieved on DBC substrates with electroplated Ni and Au, but Kirkendall voiding was observed with electroless Ni:P/Au.

The Au-In alloy (multiple layers of Au and In deposition) was reported to have a low process temperature of 200°C, that produced a high temperature 454°C bonding [42]. Grummel, et al. [43] studied the Au-In TLP bonding with indium thin film layer deposition on the back side of SiC die. The threshold pressure was >3 MPa to achieve high bonding strength with the most preferable At. % In being 0.667.

1.3.2 Electrical Interconnection

Wire bonding is the most common method for connecting the semiconductor die pad and package or substrate bond pad by using metallic wires. Au, Al and more recently Cu wire are commonly used for wire bonding. The major concern is the compatibility of the metals used for the wire and the bond pad metallization. At high temperature, failures related to poor compatibility are intermetallic compound (IMC) growth at the boundary interface, which creates a brittle area, and diffusion (Kirkendall effect), which creates voids to decrease the bonding strength and conductivity. The famous “purple plague” is the most representative failure, which refers to the IMC growth of Au wire and Al metallized pad and Kirkendall voids develop at elevated temperature.

There is an impetus to use the same metal for the bond pad and the bond wire, also known as monometallic bond, to avoid the compatibility issue. For example, Al (1.5% Si) wires are currently used in the package of SOI devices with Al pads for 225°C. If this is not possible,

the selection of metals is critical in the design of the interconnection system. For Au wire bonding, with Al pad metallization, a barrier layer is needed to the Al pad, such as electroless Ni/electroless Pd/immersion Au [44], [45], electrolytic Cu/Ni/Au [46] or electroless Ni/Au [47].

Other wire bonding combinations have also been reported, such as Ni wire on SiC devices with Ni pads [48], Pd wire on Ti/Pd and Ti/Au pads [49], CuPd wire with ENEPIG (Electroless Nickel 3um Electroless Palladium 0.3um Immersion Gold 0.01um) bond pad metallization.

1.3.3 Packaging Body

Different from the molding compound used in plastic packages for conventional temperature ranges, high temperature electronics are typically packaged in hermetic ceramic and metal packages [50], [51]. Alumina and AlN packages with refractory metallization are commercially available. AlN provides a better CTE match with Si, SiC and GaN devices compared to Al₂O₃, which leads to potentially higher reliability during thermal cycling [52].

Metal packages, such as Kovar, Cu and stainless steel, can be sealed by resistance or laser welding. A SOI sensor module packaged with hermetically sealed metal package was reported to sustain functionality after 500 hours at 250°C and 500 cycles of -55°C~250°C [53]. A package using a combination of ceramic and metal has been implemented for a SiC sensor for 500°C [54], [55] and 600°C [56] applications.

CHAPTER 2 LITERATURE REVIEW: Ag Sintering Paste for Die Attach

For decades, high lead solders have been used for high temperature (<225°C) die attach. AuSi and AuGe eutectics and liquid phase transient (LPT) bonding with AuSn have been studied for higher temperatures, but they are hard solders and high cost. Ag sintering technology is being considered a promising replacement for high lead solder for high temperature and high power applications. Sintered Ag offers a number of advantages: 1) low processing temperature; 2) high temperature compatibility; 3) high thermal conductivity; and 4) high electrical conductivity. Compared to its high melting point (1233k (960°C)), Ag sintering paste can be processed at significantly low temperature range from 200°C to 300°C, which is close to other Pd-free alternatives in the market. Also its high melting temperature suggests that silver has potential capability of high temperature operation. Besides, Ag possesses the best electrical conductivity and second best thermal conductivity, making it suitable to high temperature packaging. In March 2016, the price of Ag is up proximately 1/80 of Au and 1/60 of Pt [57]. Being a single phase system, sintered Ag shows better mechanical strength and reliability. These characteristics are advantages for sintered Ag application of high power and high temperature electronics.

2.1 Mechanism of Sintering

“Sintering is the process of compacting and forming a solid or porosity-controllable mass of material by heat and/or pressure without melting it to the point of liquefaction. Sintering happens naturally in mineral deposits or as a manufacturing process used with metals, ceramics, plastics, and other materials” [58]. During sintering, atomic diffusion allows the neighboring fine powder particles to hold together which gives the compact sufficient driving force. At the sintering temperature, necks were formed and the grains grew at the contact surface [59] as

illustrated in Figure 2-1 below. Without a liquid phase involved, chip swimming during bonding process can be avoided, thus increasing the accuracy of die attach. In this dissertation, unless specially stated, Ag sintering die attach means the process of assembly die by using Ag sintering paste.

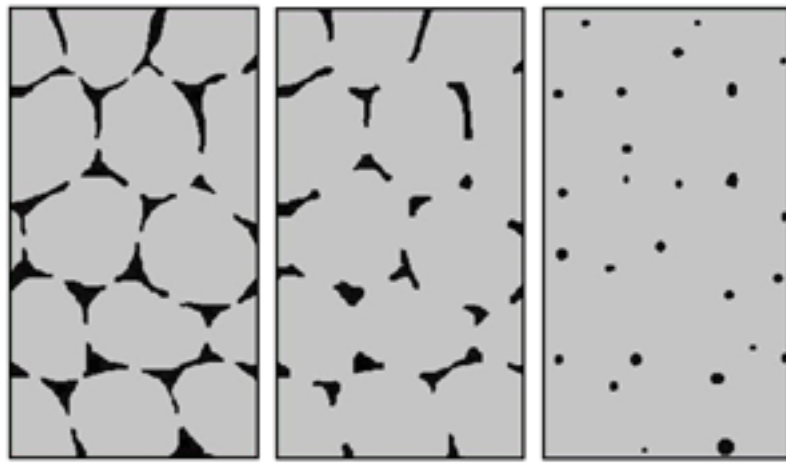


Figure 2-1 Three stages of solid state sintering: left: initial stage, center: intermediate stage, right: final stage (Courtesy EPMA) [59]

2.2 Ag Sintering Paste for Die Attach

Silver sintering technology for die attach was pioneered in Europe for power die attach, also known as the low-temperature jointing technique and dates back to the late 1980s [60-62]. However, this process required pressures of 9 to 40MPa during sintering at temperatures of approximately 250°C [63], [64]. This complicates the manufacture process and increases the cost of production. Also when pressure is applied, the brittle chips and substrates may be cracked or broken. Attempts have been made to reduce or eliminate the need for pressure by using nanoscale-Ag particles in the mid-2000s when the nano-Ag paste was developed. Commercial available Ag sintering pastes were summarized in the Table 2-1 [65].

Table 2-1 Commercial entities from the semiconductor industry involved in the use of sintered Ag technology for die-attach (in alphabetical order) [65]

Sintered Ag suppliers	Semiconductor companies using sintered Ag	End users using sintered Ag
1. Alent "Alpha"	1. Danfoss Silicon	1. Ford Motor
2. Applied Nanoparticle Laboratory Inc.	2. Hitachi	2. Magneti Marelli
3. Dowa Electronics	3. Infineon Technologies (previously known as Siemens AG)	3. Nissan Motor
4. Henkel	4. Luminus Devices	4. Robert Bosch
5. Heraeus	5. ON Semiconductor	5. Baker Hughes
6. Namics	6. Semikron Elektronick	
7. NBE Technologies	7. Shindengen Electric Manufacturing	
8. Nihon Handa		
9. Nihon Superior		
10. Senju Metal		

2.2.1 Pressure Micron-Ag Paste

H. Schwarzbauer [60] [62] used silver plate-like power particles, with a granule size of 15 μm , and a bulk density of approximately 1.9 g/ml. The powder was suspended in cyclohexanol as solvent in a weight ratio of approximately 2:1. In the year of 2004, he [66] patented another paste by using terpineol or ethylene glycol ether. W. Baumgartner and J. Fellingner [67] developed a Ag sintering paste mixed with cyclo-hexanol and menthol at weight ratio of 1:1, which was determined to not volatilize too quickly, i.e. the paste could be stored longer. This type of Ag sintering paste normally require 9 MPa at 180-250°C [60], or 40 MPa at 240°C [68].

2.2.2 Pressureless Micro-Ag Paste

One approach to produce pressureless Ag sintering paste was by adding an endothermically decomposable Ag compound. According to the Ellingham diagram shown in Figure 2-2, all metals with a negative value of ΔG may be oxidized to form a stable metal oxide. The oxides with positive ΔG are not stable and are easily decomposed to elemental metals. Silver oxide (Ag_2O) is stable at low temperature and decompose at higher temperatures because of the positive value of G at higher temperatures. W. Schmitt [69], [70] from Heraeus invented a pressureless Ag sintering paste composited of 70%-90% metal powder (flakes or powers of particles with dimensions of in the range of 0.1-10 μm , preferably 0.3-3 μm), 1%-20% endothermically decomposable metal compound and 5-20% by weight of a solvent having a boiling point or range above 220°C. The endothermically decomposable metal compound can be silver carbonate, silver lactate, silver formate, silver citrate, silver oxide (for example Ag_2O). The silver compound can easily reduce to metallic Ag above 250°C to bridge the Ag fillers and allow sintering to occur. A pressureless process was demonstrated: 8 mm² die were placed onto a lead frame. After being dried at 100°C for 20 minutes, sintering took place at 250°C for 45 minutes [70].

Another approach to eliminate the application of pressure is to increase the weight percentage of Ag fillers in the Ag sintering paste. Kuramoto et al. investigated a pressureless sintering process for 600 μm^2 LED die attach with Ag paste containing 92.6 % weight percent of micrometer size Ag particles. They also found the flake-like shaped Ag particles (8 μm) exhibits high bonding strength than round shape particle (0.3 μm), which were dispersed in diethylene glycol monobutylether. The combination of two particle types with an optimized ratio yielded higher shear strength than flake-like Ag particle alone [71].

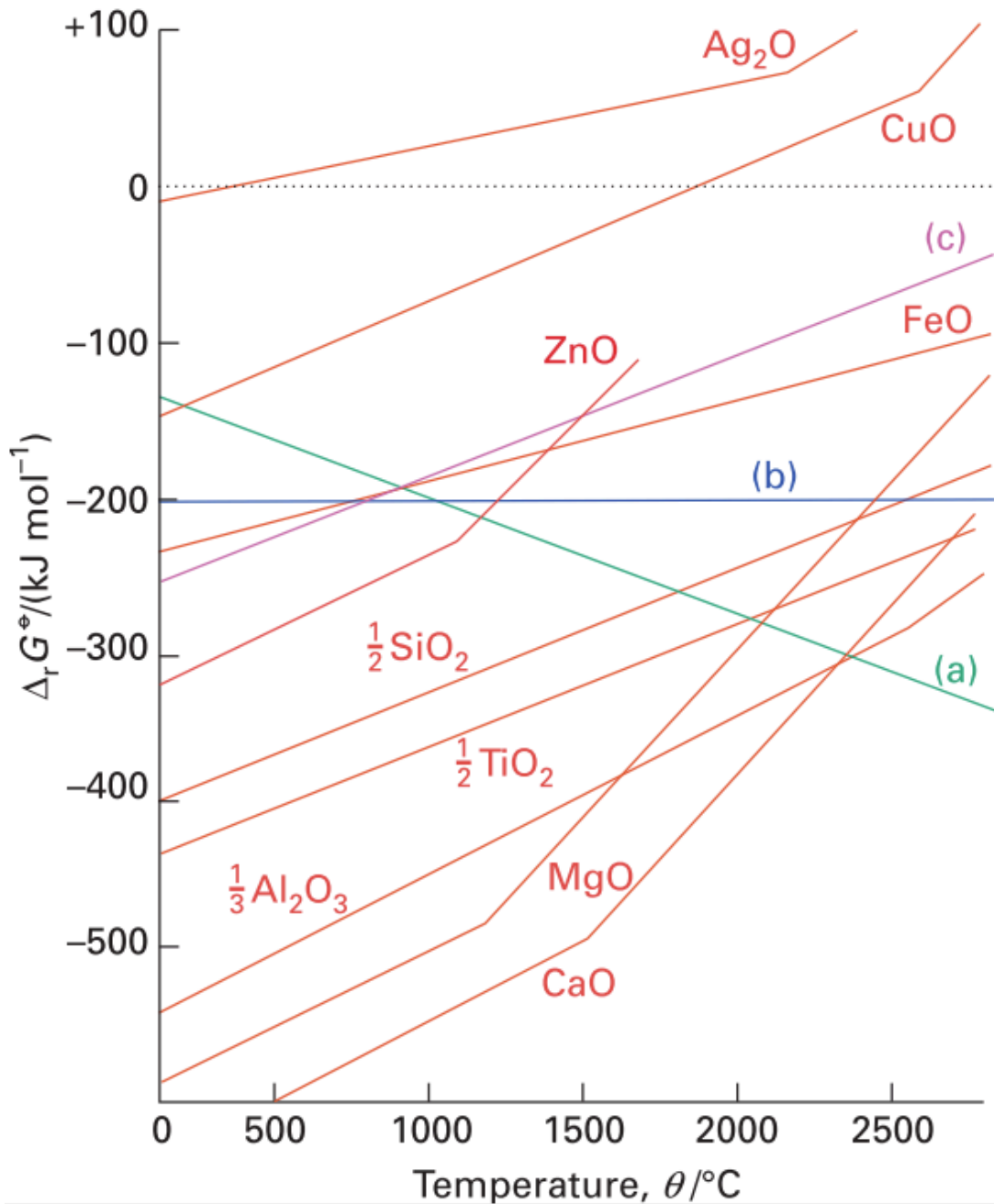


Figure 2-2 An Ellingham diagram for the reduction of metal oxides [72].

2.2.3 Pressureless and Pressure Nano-Ag Paste

Another approach to produce Ag sintering paste that requires less sintering pressure is to reduce the particle size to the nanoscale to increase the sintering driving force. The diameters of

Ag nanoparticles are preferably 100 nm [73]. Typically, the compositions of nano Ag sintering paste are passivated Ag nanoparticles with capping agents, surfactant, binder, dispersant, thinner and solvents etc. to prevent agglomeration. In early studies, pressure was still needed even use nano Ag paste [74]. Lu et al. produced and examined a nano Ag sintering paste containing 30 nm Ag particles [75]. With this paste, pressureless sintering process was implemented on small dies (1.71 mm x 1.38 mm and 2.26 mm x 2.26 mm) with shear strength up to 38 MPa. However, for large die 6 mm x 6 mm [76] and 10 mm x10 mm die [77, 78], pressure was still needed. To reach a shear strength >30MPa and good electrical performance, 3 MPa lamination pressure was needed during sintering [79].

CHAPTER 3 PRESSURELESS SINTERING

Thick film hybrid modules have been used for high temperature applications since the mid-1970's [80] and continue to be used today [81]. Compatible, high temperature materials are required for attachment of semiconductor die and passives to the thick film metallized substrate pads. Due to its high thermal and electrical conductivity and high melting point, sintered Ag die attach has received much attention for assembly of power modules and for high temperature applications. Low temperature Ag sintering technology provides a lead-free die attachment compatible with high temperature (300°C) applications. Previous work with Ag sintering has required pressure during the sintering process or been limited to small area die. In this chapter, the pressureless sintering of micro-scale silver paste is examined for larger (8mm x 8mm) area die. Experimental combinations included: Si die metallization (Ag and Au); thick film substrate metallization (Au, Ag and PdAg); and sintering temperature.

For Au metallization (die and/or substrate), the initial shear strength results were good with 8mm x 8mm die sintered at lower temperatures (200°C). The shear strength was beyond the limit of the shear test machine (100 kg), corresponding to >15.3 MPa. However, after aging for 24 hours at 300°C, the shear strength dropped significantly. An SEM was used to characterize cross sections of as-built and aged sample. The decrease in die shear strength with high temperature sintering (250°C and 300°C) or high temperature aging is attributed to surface diffusion of Ag along the Au surface resulting in a dense Ag layer adjacent to the Au surface and a depletion layer within the die attach adjacent to the dense Ag layer. Shear failures occurred through the depleted region.

For Ag metallization (die and substrate), no decrease in shear strength was observed with 300°C aging. Shear strength of 8x8cm² dies was >100 kg (>15.3 MPa) as-built. The shear strength remained >15.3MPa after 3000 hours of 300°C aging.

3.1 Review of Pressureless sintering

Silver sintering technology for die attach was pioneered in European for power die attach. However, this process required pressures of 20 to 40MPa during sintering at temperatures of approximately 250°C [82-84]. This complicates the manufacture process and increases the cost of production. Also when pressure is applied, the brittle chips and substrates may be cracked or broken. Attempts have been made to reduce or eliminate the need for pressure by using nanoscale-Ag particles. G. Q. Lu has reported extensively on Ag nano-paste as a die attach material. For small dies (1.71 mm x 1.38 mm and 2.26 mm x 2.26 mm), the pressureless sintering process yielded high shear strength up to 38Mpa [85] and could support high temperature operation of SiC power devices [86]. The Ag substrates (40 MPa) had better adhesion than Au substrates (20 MPa) [87]. However, for large die 6 mm x 6 mm [88] and 10 mm x10 mm die [89], [90], pressure was still needed. To reach a shear strength >30MPa and good electrical performance, 3 MPa lamination pressure was needed during sintering [91].

In this chapter, pressureless sintering of micro-size Ag paste with large (8 mm x 8 mm) die was examined. The intended application was die attach of Si or silicon on insulator (SOI) analog and digital die for use at temperatures up to 300°C. High power applications were not considered. As such, thick film substrates were used and die shear strength was the evaluation metric. High electrical and thermal conductivity are generally not required with these device types and were not measured.

3.2 Test Vehicle and Process

Substrate Metallization: 5.08 cm x 5.08 x 0.64mm thick 96% alumina (Al_2O_3) substrates purchased from Coorstek were used for this experiment. The substrates were metallized with either thick film Au, Ag or PdAg by screen printing. The size of die pad printed was 8 mm x 8 mm. The printed substrates were dried at 150°C for 10 min., then fired at a peak temperature of 850°C for 10 min.

Die Metallization: Silicon wafers were metallized on the backside by e-beam evaporation. For Au metallized die, Ti (50 nm), Ni (200 nm), and Au (200 nm) were sequentially deposited. To evaluate the effect of Au thickness, some wafers were electroplated with 2 μm of Au. For Ag metallized die, Ti (50 nm), Ni (200 nm), and Ag (300 nm) were sequentially deposited on the Si wafer. The wafers were diced into 8 mm x 8 mm test dies.

Sample assembly: The die attach material was Ag sintering paste containing micro-size Ag particles. A 50 μm thickness laser cut stencil was used to print the silver sintering paste on the metallized substrate. A metal squeegee was used on an MPM semiautomatic printer. After printing the Ag paste, test dies were placed in the paste within 10 minutes. A Palmour Products Model 3500 pick and place system was used for controlled die placement.

Pressureless sintering process: Three sintering temperatures: 200°C, 250°C, and 300°C were experimentally evaluated. The oven profile (Figure 3-1) was a 5 °C/min ramp to peak temperature then a 1 hour hold at peak temperature. To evaluate the different material and sintering temperature combinations, as-sintered samples were analyzed by shear testing and cross sectioning. In addition, sintered samples were aged at 300°C for 24 hours, then analyzed by shear testing and cross sectioning.

Pressure sintering process: For comparison, samples were prepared with pressure during sintering. The pressure was applied using a Carver hydraulic press, model #3912 with top and bottom temperature controlled platens. After the die was placed in the Ag paste printed on the metallized substrate, the sample was placed on the lower platen and the temperature was raised to 130°C and held for 30 minutes. Then 4.3 MPa pressure was applied and the temperature was ramped to 200°C and held for 1 hour to complete the pressure sintering process. Silicone pads were used between the sample and the platens to provide cushion and protection.

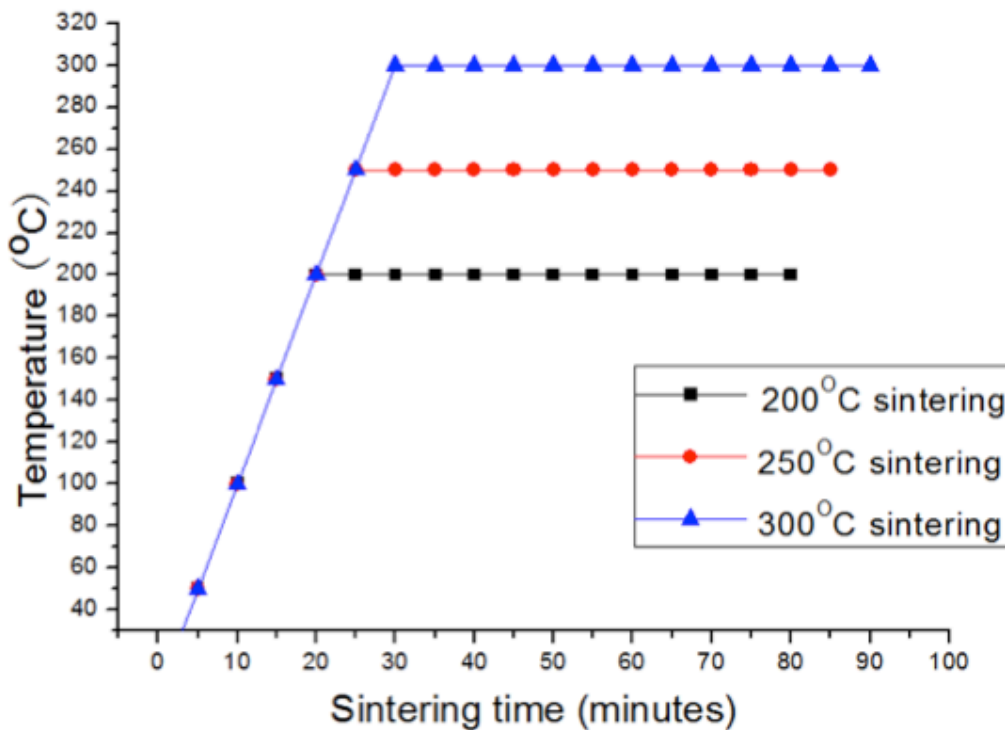


Figure 3-1 Sintering profile of three different sintering temperature 200°C, 250°C, 300°C. Set 10 °C/min ramp rate and soap for 1 hour.

Die Shear Testing: A Dage 2400PC shear tester with a 100kg die shear module was used for die shear testing. In some cases the die could not be sheared with the 100kg applied force. For a 8mm x 8mm die, this corresponds to a maximum test limit of 15.3 MPa.

SEM Analysis: SEM cross sectional analysis was used to examine the sintered Ag microstructure. The sample was diced into two pieces along the center of the die. For samples known to have low shear strength, the die was encapsulated with epoxy prior to dicing to maintain the integrity of the die attach. The cross section was prepared for SEM examination by ion milling with an Ion Tech 22cm Linear Ion Gun.

3.3 Process Development Results and Discussion

3.3.1 Au Die Metallization, Au Substrate Metallization

Good initial results were obtained for samples sintered at 200°C, but samples sintered at 250°C and 300°C had significantly lower shear strengths (Figure 3-2). For the 200°C initial sintering, none of the dies could be sheared (>100kg). After aging, the shear strength dropped significantly for the 200°C and the 250°C sintered samples.

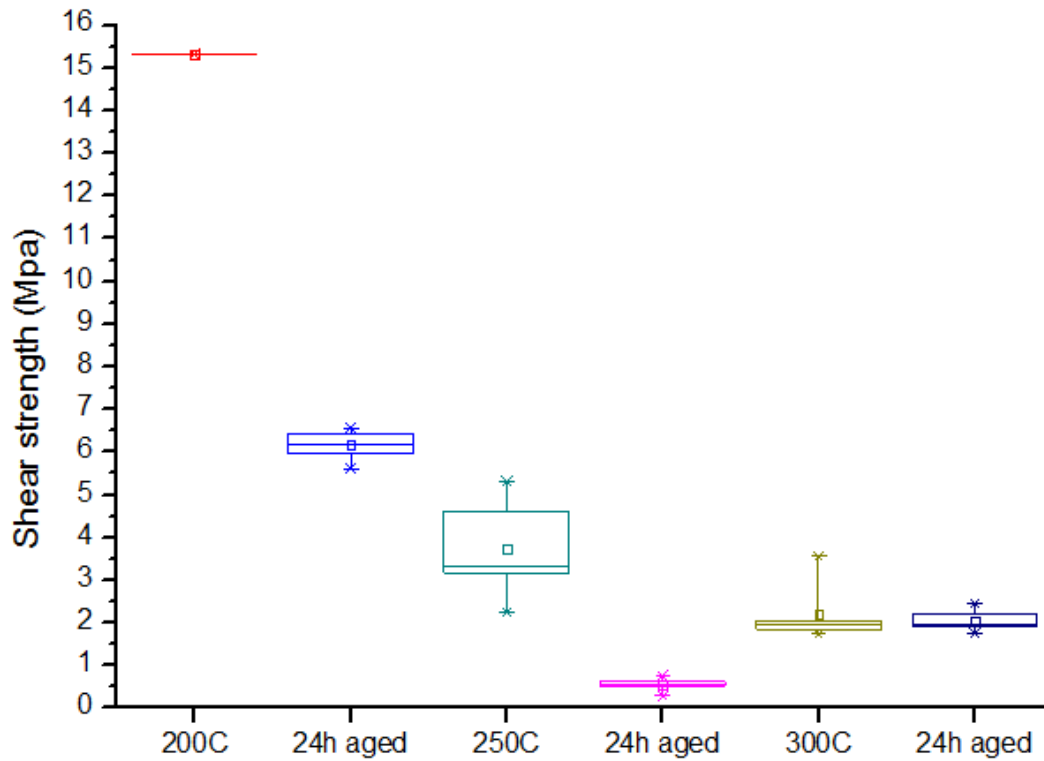


Figure 3-2 Au die with Au substrate sintered at 200°C, 250°C, 300°C, respectively, and aged at 300°C for 24 hours.

To investigate the reduction in shear strength of the 200°C sintered samples with 24 hour aging at 300°C, cross sections of as-sintered and aged samples were examined by SEM (Figure 3-3 and Figure 3-4). After aging, a continuous, non-porous Ag layer was observed adjacent to the die Au metallization with a corresponding depletion region adjacent to the non-porous Ag layer.

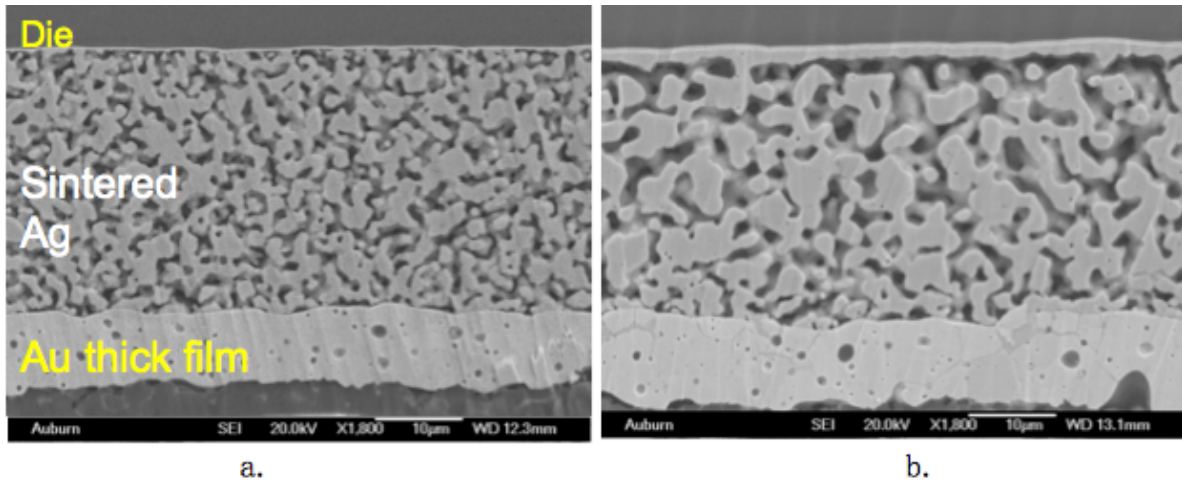


Figure 3-3 Cross section microstructure of sintered and aged sample: Au substrate + 200nm e-beamed Au die. (a.) 200°C sintering for 1 hour. (b.) After 300°C aging for 24 hours.

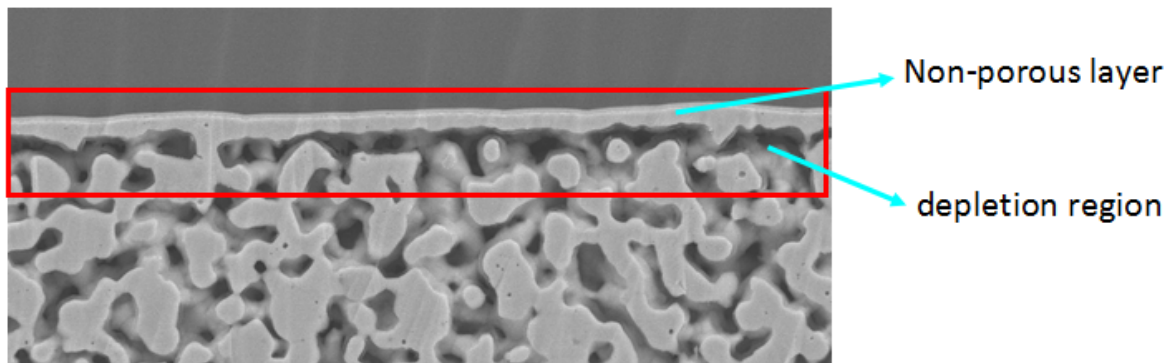


Figure 3-4 Details of non-porous layer and depletion region

For Au die, the formation of the continuous non-porous Ag layer adjacent to the 200nm Au e-beamed layer on the die and the corresponding high-porosity/depletion layer is the cause for the degradation of shear strength. Examination of the fracture surfaces confirmed, a thin, dense Ag layer on the die side of the fracture. Lewis, et. al. have also reported a void free Ag layer on Au substrates [92].

For comparison, Au samples (die and substrate) were assembled with pressure (4.3 MPa) applied during sintering. For both initial and aged (300°C/24 hours) samples, the dies could not

be sheared off of the substrates (shear strength higher than 15.3 MPa). The SEM image of a cross section (Figure 3-5) shows an obviously more dense as-sintered structure than that of pressureless processed sample. Also, the non-porous Ag layer and depletion region are not found in laminated samples after 24 hours of 300°C aging.

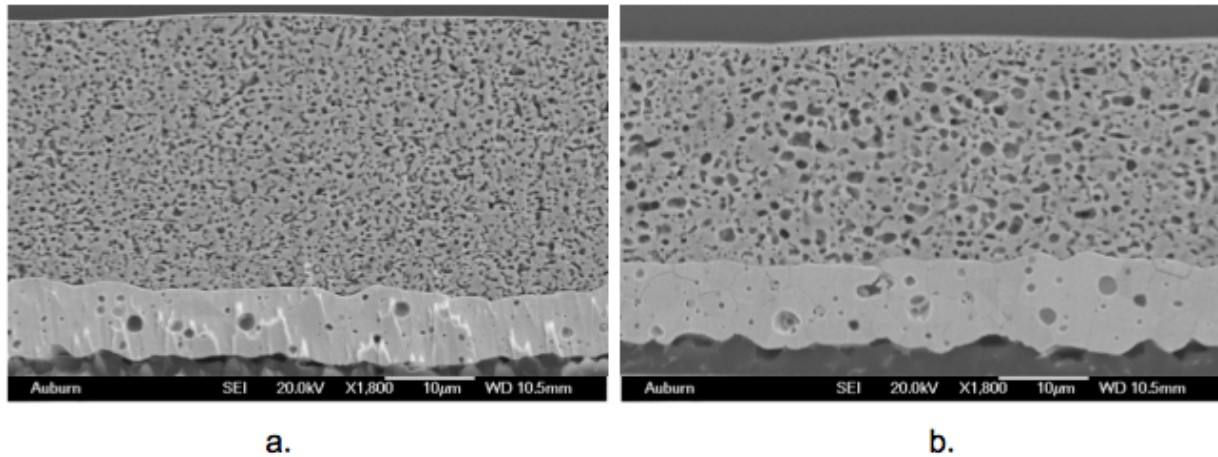


Figure 3-5 Cross section of lamination samples: 200nm Au metallized die with Au metallized substrate. (a.) 130°C dry for 30 min and 200°C sintered with pressure for 1 hour. (b.) Aged at 300°C for 24 hours.

3.3.2 Au Die Metallization, Ag Substrate Metallization

The as-sintered (200°C sintering temperature) sample could not be sheared, but after aging, the shear strength dropped significantly to 4 MPa. Higher sintering temperatures resulted in a decrease in the initial shear strength as shown in Figure 3-6. The results are similar to the Au die/Au substrate metallization combination.

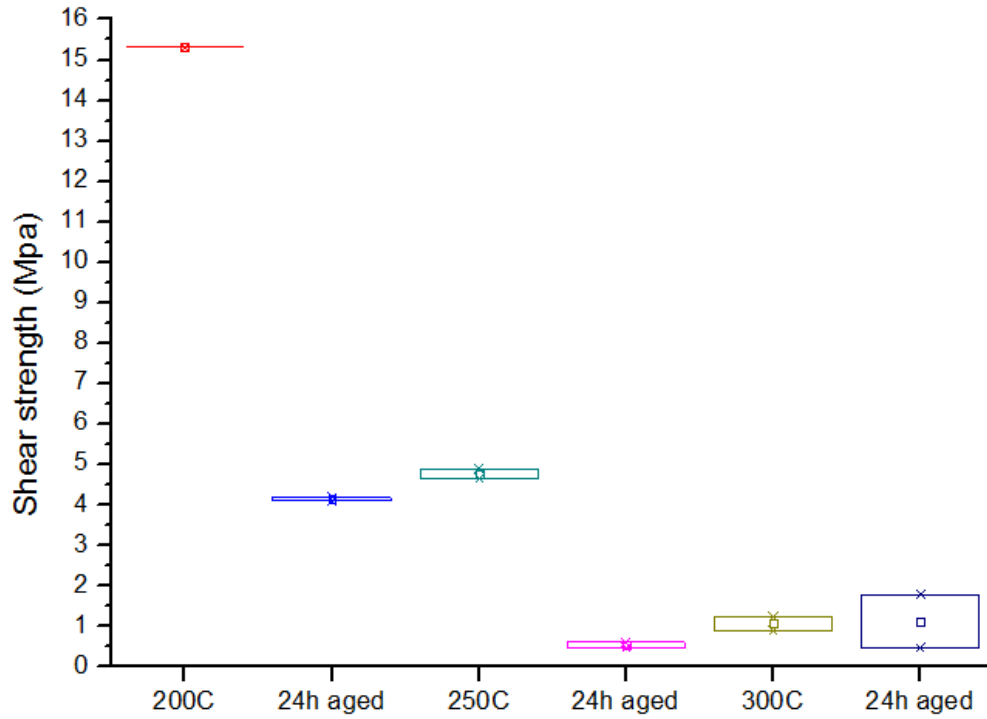


Figure 3-6 Au die with Ag substrate sintered at 200°C, 250°C, 300°C, respectively, and aged at 300°C for 24 hours.

As shown in Figure 3-7, after 300°C aging for 24 hours a depletion region and a continuous, non-porous Ag layer was observed on the die side, similar to the Au die on Au substrate metallization combination Figure 3-4.

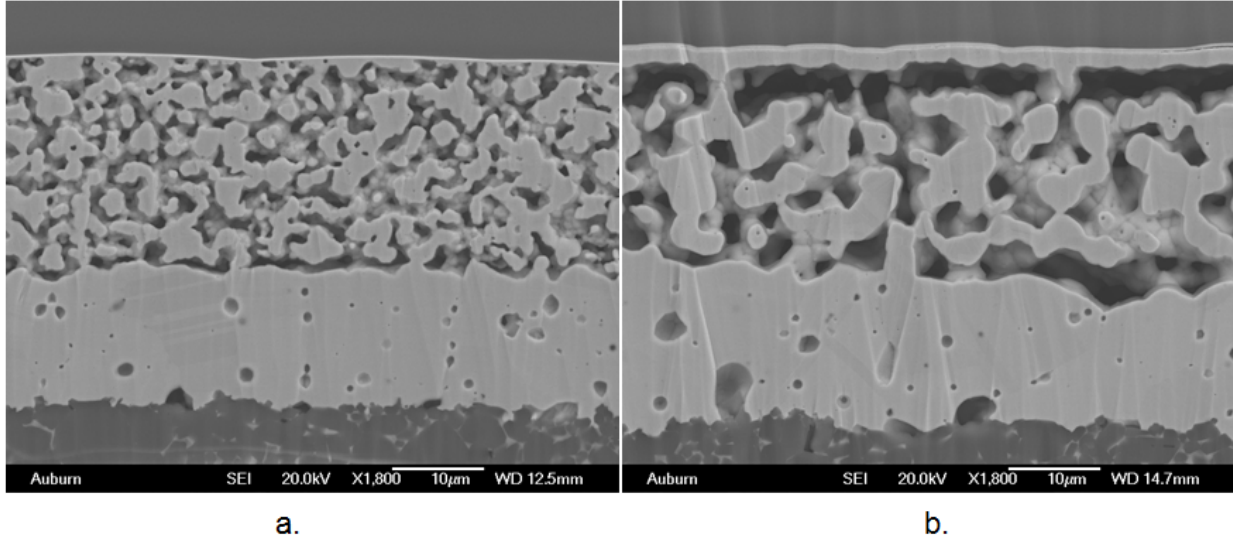


Figure 3-7 Cross section microstructure of sintered and aged sample: Ag substrate + 200nm e-beamed Au die. (a.) 200°C sintering for 1 hour, (b.) After 300°C aging for 24 hours.

3.3.3 Ag Die Metallization, Au Substrate Metallization

The initial result is the same (>100 kg) for all three sintering temperatures. After aging for 24 hours at 300°C, the Ag die bonded to Au substrate had shear strength 12-14 MPa, a decrease with aging (Figure 3-8).

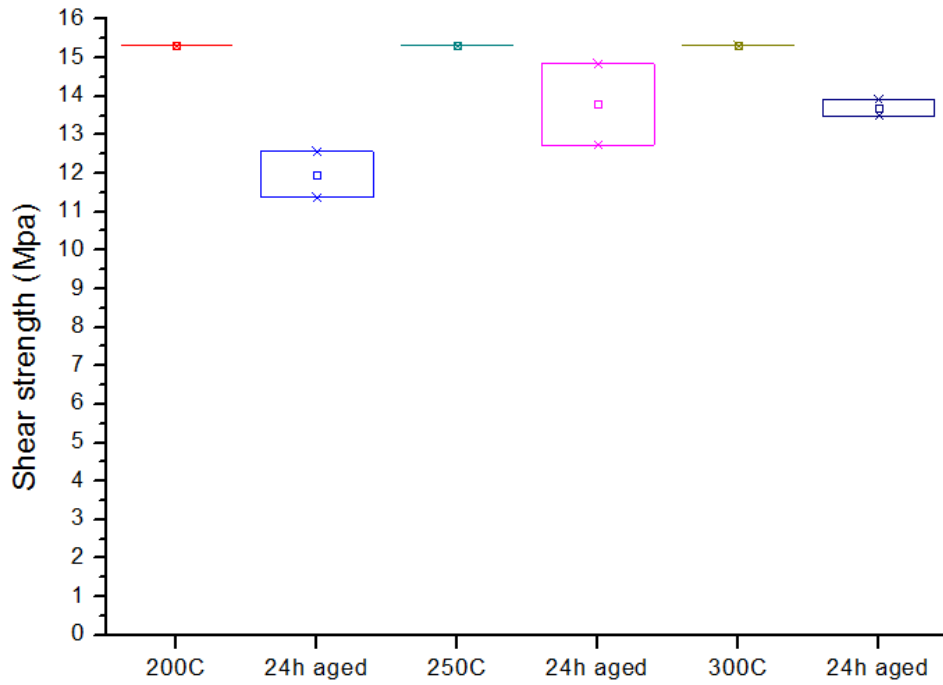


Figure 3-8 Ag die with Au substrate sintered at 200°C, 250°C, 300°C, respectively, and aged at 300°C for 24 hours.

For the Ag die on Au substrates, the SEM cross sections are shown in Figure 3-9. A depletion region and continuous, non-porous layer was observed on the thick film Au side of the sintered Ag. This depletion region corresponds to the decrease in die shear strength, although the decrease is less than observed with a Au metallized die.

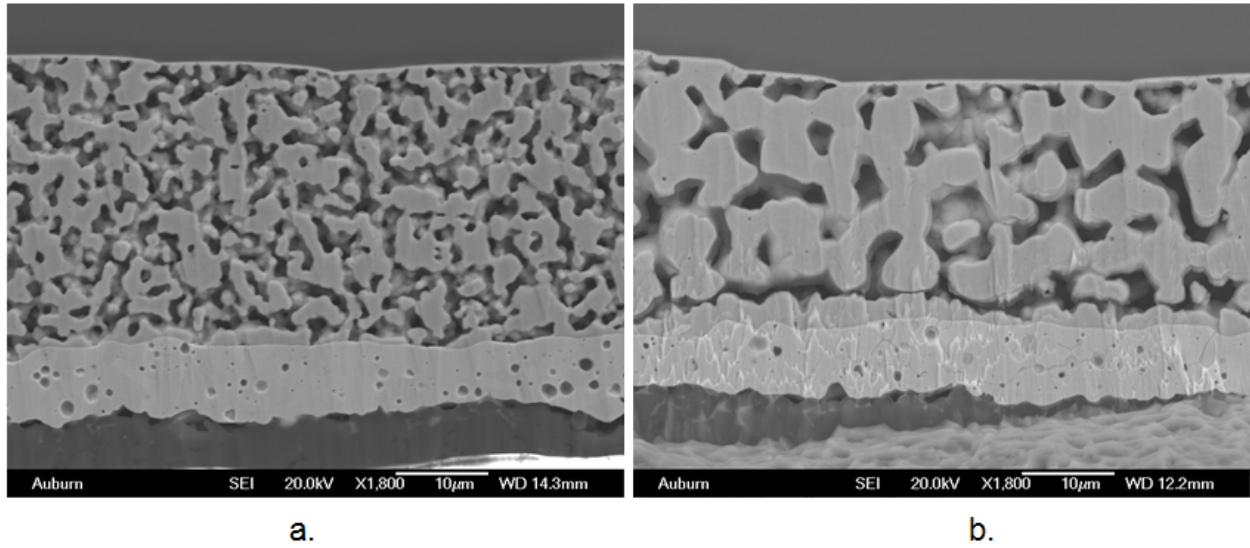


Figure 3-9 Cross section microstructure of sintered and aged sample: Au substrate + 300nm e-beamed Ag die. (a.) 200°C sintering for 1 hour, (b.) After 300°C aging for 24 hours.

3.3.4 Ag Die Metallization, Ag Substrate Metallization

The die shear strength was >100 kg (>15.3 MPa) for all sintering temperatures, both as-sintered and after 24 hours at 300°C (Figure 3-10).

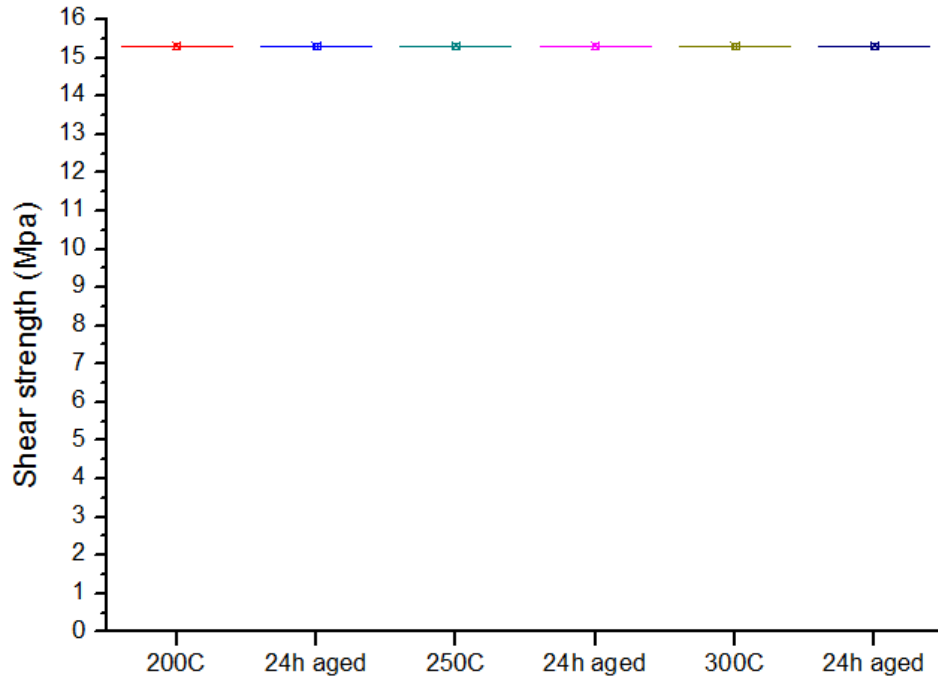


Figure 3-10 Ag die with Ag substrate sintered at 200°C, 250°C, 300°C respectively. And aged at 300°C for 24 hours.

From Figure 3-11, the sintered Ag has a homogeneous porous structure. It is clear that the Ag grains grow larger during the 24 hours 300°C aging. The pore size increases, while the number decreases. No depletion region or continuous, non-porous Ag layer was observed.

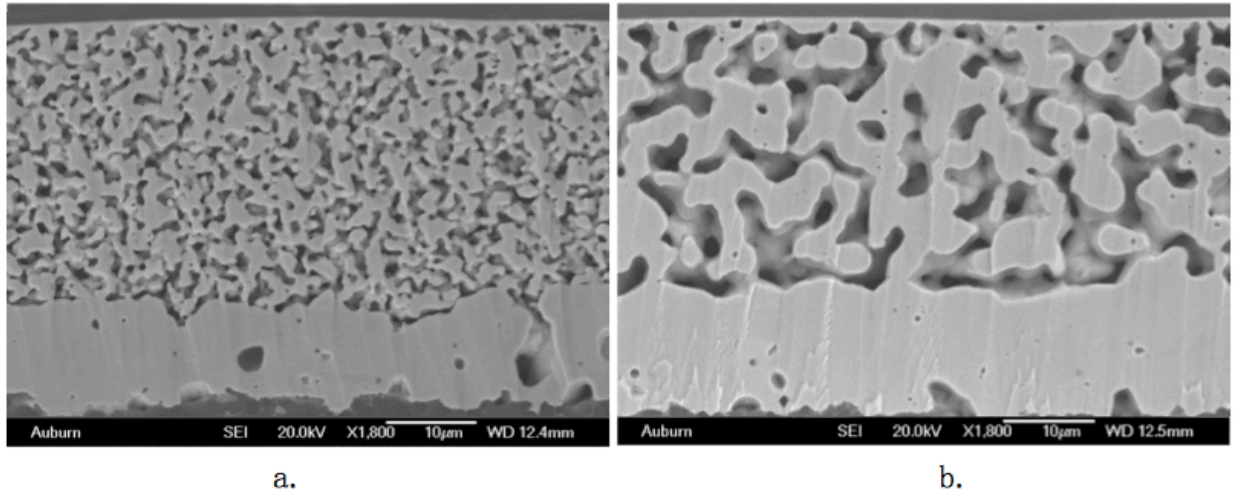


Figure 3-11 Cross section microstructure of sintered and aged sample: Ag substrate + 300nm e-beamed Ag die. (a.) 200°C sintering for 1 hour, (b.) After 300°C aging for 24 hours.

3.3.5 Ag Die Metallization, PdAg Substrate Metallization

The shear test results (Figure 3-12) indicate that a 200°C sintering temperature is insufficient to form the strongest attachment. The shear strength was 8.5 MPa. For 250°C and 300°C sintering, the die could not be sheared. The die could not be sheared for all sintering temperatures after aging for 24 hours at 300°C.

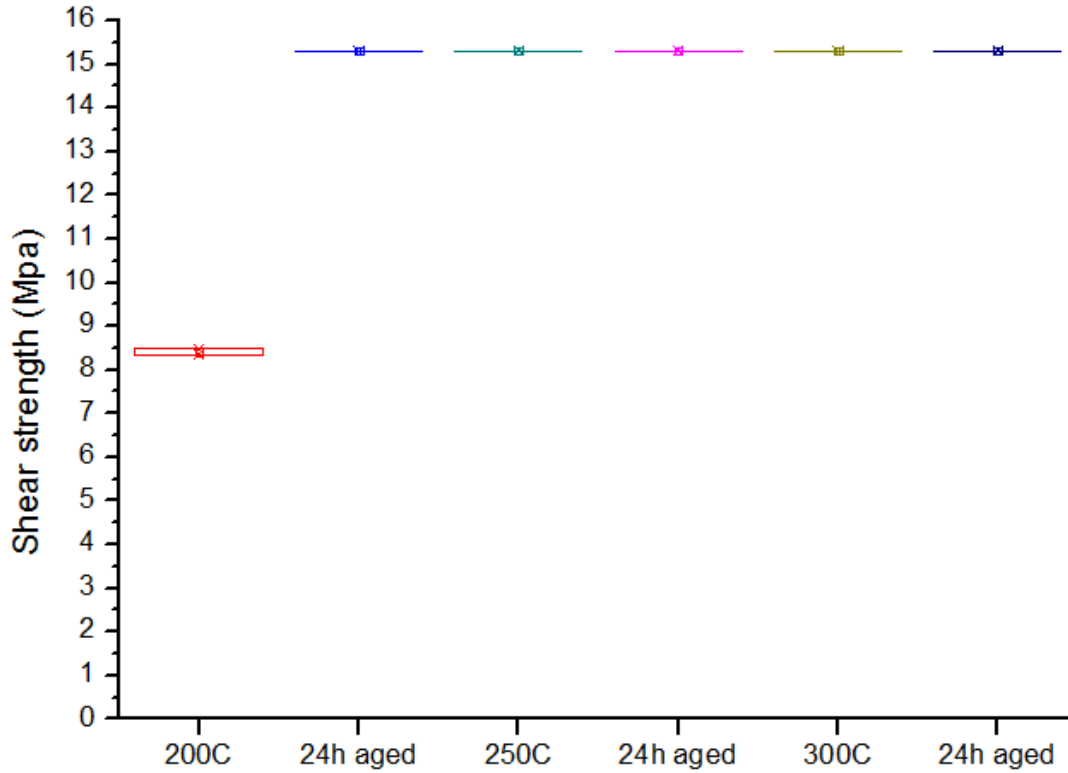


Figure 3-12 Ag die with PdAg substrate sintered at 200°C, 250°C, 300°C, respectively, and aged at 300°C for 24 hours.

Figure 3-13 shows cross sections of the 200°C sintered PdAg sample as-built and after 24 hours at 300°C. Due to the lower strength with 200°C sintering, the as-built sample separated between the Ag die attach and the PdAg substrate during sample preparation indicating reduced adhesion at this interface.

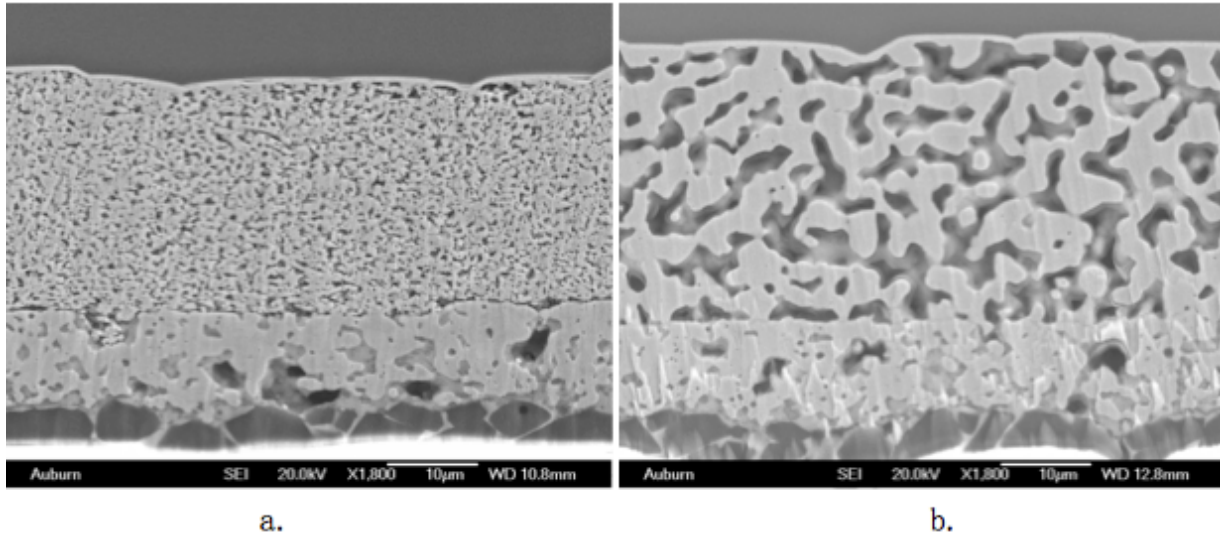


Figure 3-13 Cross section of PdAg substrate with Ag die. (a.) Sintered at 200°C for 1 hour. (b) Aged at 300°C for 24 hours.

3.4 Long Term Aging Study

The reliability test is conducted at 300°C for both Ag and PdAg metallized substrate with Ag metallized die. Both sample groups were assembled using a 300°C, 1 hour pressureless sintering process.

For the Ag metallized substrates, the die could not be sheared at any test interval through 8000 hours. From Figure 3-15, there is little change in the microstructure of the sintered Ag with aging time. Also, no trend of shear strength decrease shows up. The porosities of sintered Ag area are around 30% in Figure 3-14.

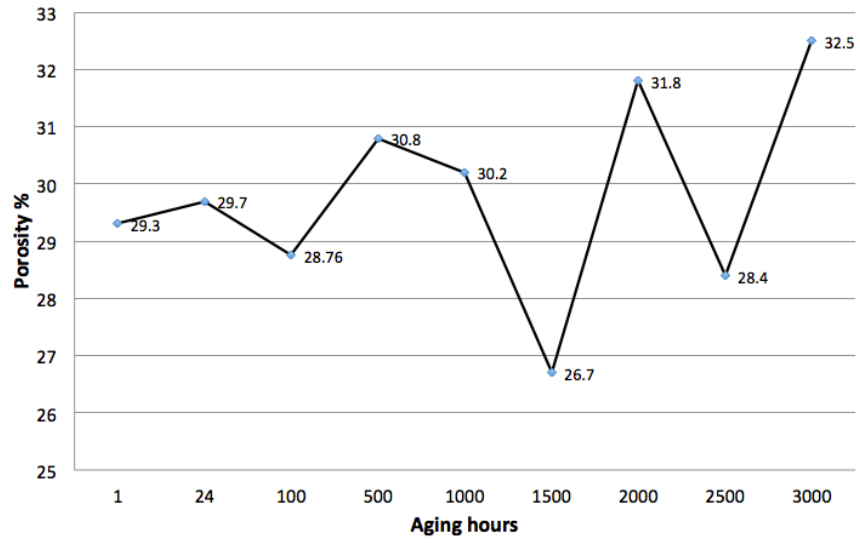


Figure 3-14 Porosity calculation with as a function of aging time.

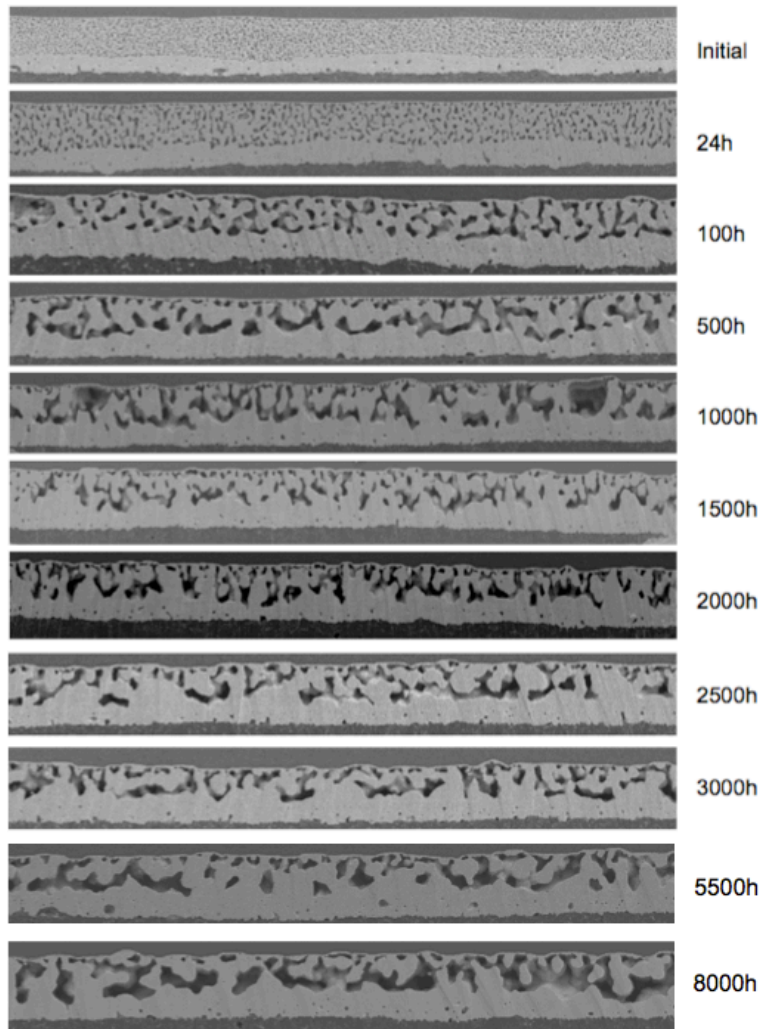


Figure 3-15 Microstructure of Ag metallization die with Ag thick film substrate sample at high temperature (300°C) reliability test and porosity calculation.

For Ag metallized die and PdAg metallized substrates, 1000 hours of high temperature storage testing has been completed. After 1000 hours at 300°C, the Ag metallized die on PdAg thick film substrates could not be sheared at 100kg force. Figure 3-16 shows a cross section of a sample after 1000 hours of aging at 300°C.

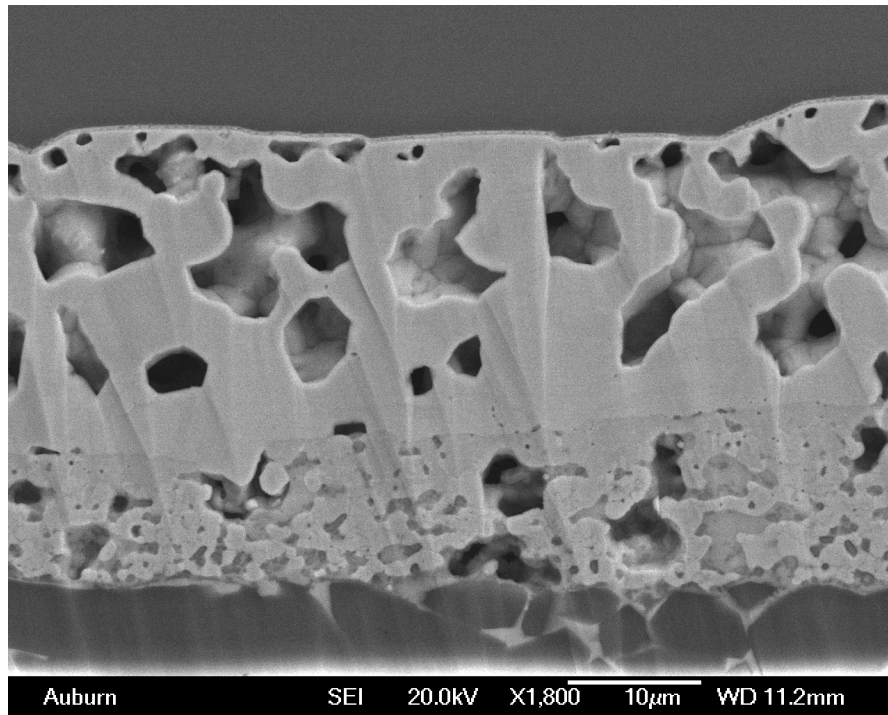
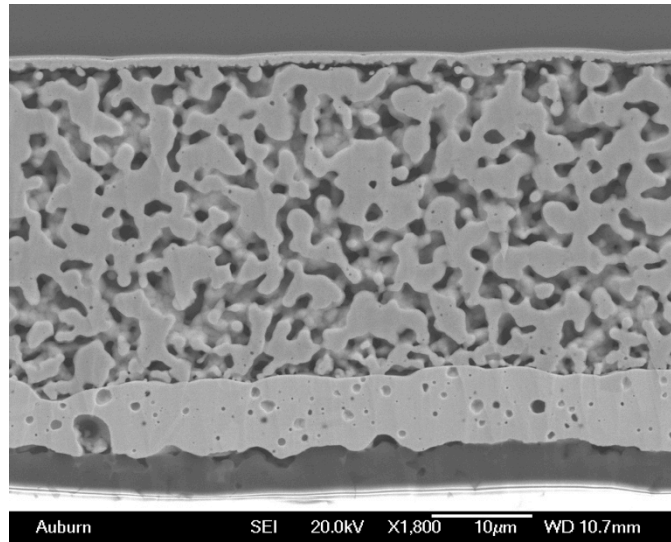


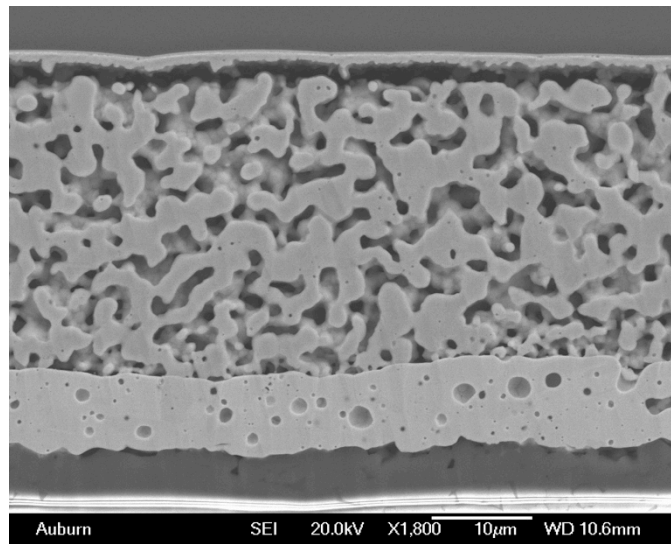
Figure 3-16 Cross Section of a Ag die assembled on a PdAg substrate after 1000 hours at 300°C.

3.5 Further characterization with Au metallization

Samples with Au die and Au thick film substrate metallization sintered at 200°C for one hour were subjected to high temperature storage and cross sectioned. Figure 3-17 shows the progression of the depletion layer formation with aging at 300°C. The depletion layer begins to be pronounced after 30 minutes and was fully developed after only 1 hour. The shear strength after 1 hour was less than 0.3MPa.



(a)

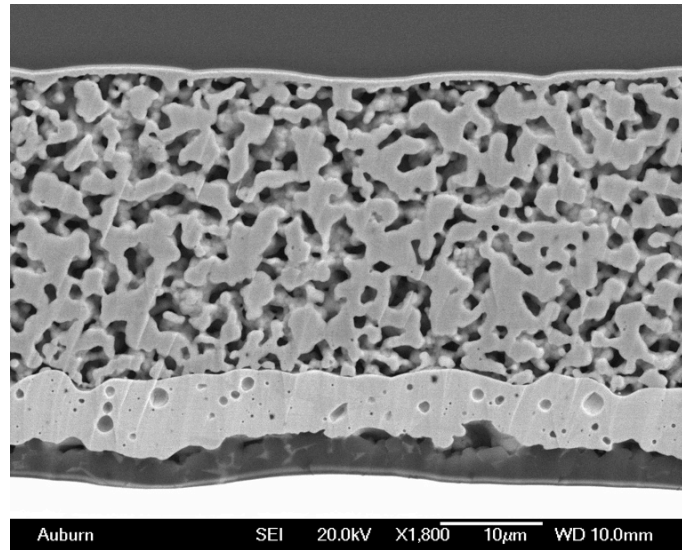


(b)

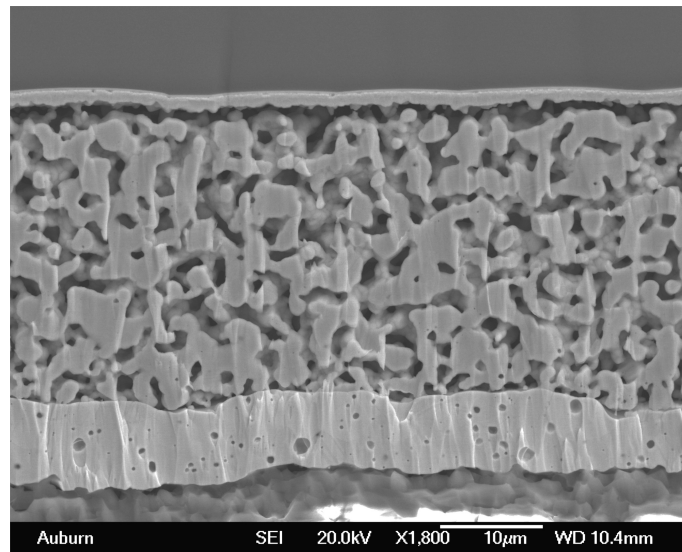
Figure 3-17. Cross sections of Au metallized Die on Au metallized substrate, sintered at 200°C for 1 hour. (a) after 30 minutes aging at 300°C, (b) after 1 hour aging at 300°C.

Figure 3-18 shows the progression with 250°C storage. After 4 hours storage at 250°C, the depletion region was well formed and the die shear strength was 7.9MPa. The rate of depletion region formation was slower than at 300°C. In comparison, Figure 3-19 shows the results after 1500 hours of storage at 200°C. The dense Ag layer has formed on the die side, but

the depletion layer has not formed. The lack of a depletion layer was confirmed by the inability to shear the die with 100kg of force after 1500 hours aging at 200°C.



(a)



(b)

Figure 3-18. Cross sections of Au metallized Die on Au metallized substrate, sintered at 200°C for 1 hour. (a) after 30 minutes aging at 250°C, (b) after 4 hours aging at 250°C.

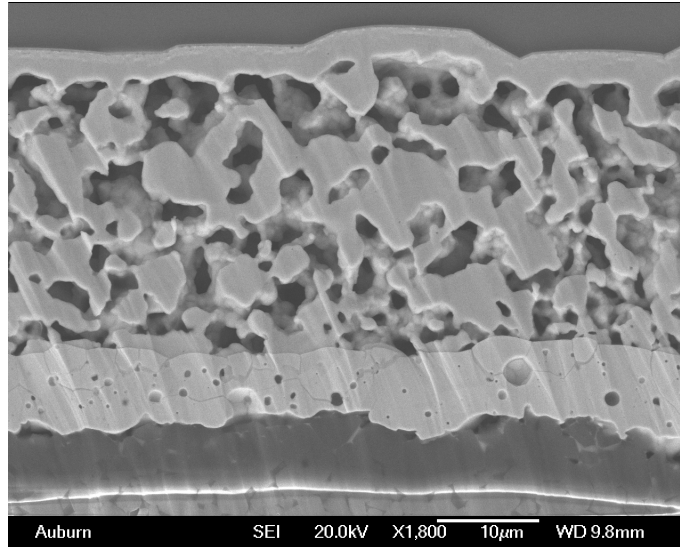


Figure 3-19. Cross sections of Au metallized Die on Au metallized substrate, sintered at 200°C for 1 hour then aged after 1500 hours at 200°C.

3.6 Discussion

Pressureless sintering produces a more porous Ag structure than when pressure is applied during sintering. Since the applications intended in this work are not for power devices, the decreased electrical and thermal conductivity resulting from the porosity is not a concern. With Ag metallized die and Ag or PdAg substrate metallization, the pore size increases with aging at 300°C, but the percent porosity remains relatively constant. Good mechanical strength is maintained.

With Au metallization on the die or the substrate or both, high temperature sintering (250°C and 300°C) and high temperature aging (300°C) yields low shear strengths. A dense Ag layer forms on the Au surface and an adjacent depletion layer forms that is mechanically weak. This dense Ag layer was not observed in as-built samples with 200°C sintering. The cross section revealed areas of Au-to-Ag contact and areas of exposed Au with no Ag. After 24 hours at 300°C, the dense Ag and depleted layers form. The Au is completely covered with Ag. Ag surface

diffuses on Au surfaces at high temperature. This has been observed in Au wire bonds on Ag thick film aging studies at 150°C [93]. Sousa, et. al. have observed Ag diffusion along Au surfaces with Ag adhesives aged at 250°C [94] It is theorized that with 300°C aging of the 200°C sintered sample, Ag diffuses along the exposed Au surface creating a continuous Ag layer. This ‘consumption’ of Ag from the bulk results in a depletion layer. With sintering under pressure, the Ag is much more dense and exposed Au surface is limited after sintering. This limits surface diffusion of Ag on exposed Au with subsequent aging. Thus, no depletion layer is formed and the die shear strength remains high.

Oxygen has been shown to play a role in Ag migration under bias at high temperature [95]. To evaluate the role of oxygen in this mechanism, samples (Au die and Au substrate metallization) were built and initially sintered at 200°C for 1 hour, then the PEO 601 furnace was programmed to age the sample in nitrogen gas flow at 300°C for 24 hours. After the 24 hour aging, the die could not be sheared.

Figure 3-20 is a cross section of the Au die on Au substrate after 24 hours at 300°C in nitrogen. Corresponding to the high shear strength, there is no depletion layer formed. Elimination of oxygen does appear to prevent the formation of this depletion layer.

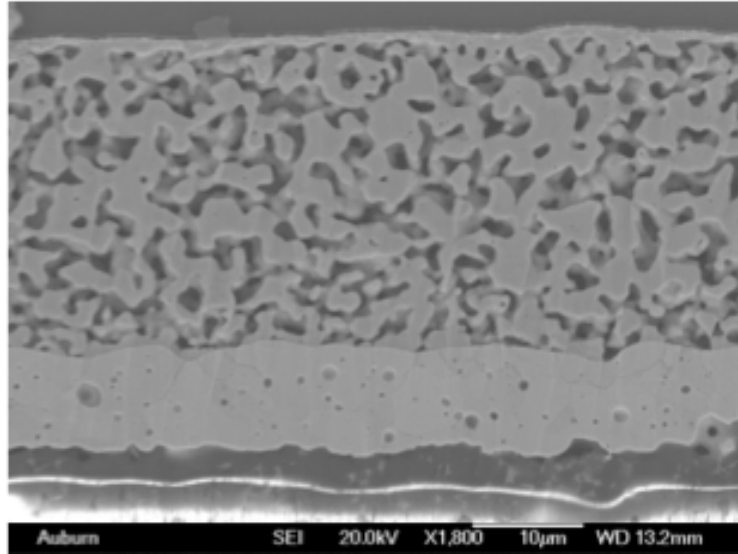


Figure 3-20. Cross section of samples aged in nitrogen for 24 hours. 200nm Au die with Au substrate sintered at 200°C.

3.7 Conclusion

A pressureless Ag sintering process has been demonstrated for larger die (8 mm x 8 mm). While a higher void percentage was observed compared to a pressure process, for non-power device applications the increased porosity is less of an issue. Degradation of shear strength was observed with high temperature sintering and high temperature aging of samples with Au metallization on the die, the substrate or both. Ag surface diffusion was proposed to explain this phenomenon. We observed the formation of a Ag depletion region in the die attach sintered Ag layer with 250°C and 300°C aging and corresponding low shear strength was found with Au metallized die. With storage at 200°C, the depletion region did not form and the shear strength remained high for Au metallized die on thick film Au substrates after 1500 hours. For Ag metallized die and Ag or PdAg thick film metallized, high shear strengths were maintained after high temperature aging at 300°C. Pressureless sintering of micro-scale Ag die attach with Ag die metallization and Ag and PdAg thick film metallization is a viable assembly process for high

temperature die attach of non-power device. For power devices, the impact of the increased porosity on electrical and thermal performance must be determined.

CHAPTER 4 COMPONENT ATTACH WITH PRESSUELESS SINTERING

With an increased demand for high power and high temperature electronics, Ag sintering paste has been considered a promising Pb-free die attach material candidate for these applications. A large amount of research has been performed investigating pressure and pressureless Ag sintering for die attach.

In this work, passive component (chip resistor) attachment with Ag sintering was explored. Due to termination geometry differences between resistors and die, different processing procedures and parameters were developed.

For PtAu terminated resistors, the mean shear force of as-built samples on thick film Ag metallized substrates was 90 N, but dropped to 18.6 N after 1500 hours at 300°C. Formation of a dense Ag layer near the PtAu resistor termination and a void region near the thick film metallization was observed in cross-sections after 1000 hours at 300°C.

For PdAg terminated resistors with a plated Ni/Au finish, the initial shear force results were low due to Ag diffusion along Au metallization surface. For PdAg terminated resistors with Ag thick film substrates, the initial shear force was approximately 60 N and remained in the range of 50-70 N during aging at 300°C for 1500 hours. A new thick film metallization (Au+Ag) was developed to enable the use of thick film Au interconnect metallization.

4.1 Introduction

With increased demand for high power and high temperature electronics, high temperature die attach materials and processes are required. In these applications, sintered Ag offers a number of advantages: 1) low processing temperature (200-300°C); 2) high temperature compatibility (melting point of 960°C); 3) high thermal conductivity; and 4) high electrical

conductivity. In early process development, pressure was required during sintering [96-98]. To simplify the process, pressureless Ag sintering for die attach has been investigated [99-102]. Bai, et al. [99-101] demonstrated pressureless sintering for small die, while Fang, et al. [102] sintered 8 mm x 8 mm die with high shear strength and approximately 30% porosity.

High temperature electronic systems require not only semiconductor devices, but also passive components, such as resistors, capacitors, and inductors. Chip resistor components are present in most electronic assemblies. Hunt et al. [103] assembled PtAg finished chip resistors on composite PTFE ceramic substrates (Ni/Pd/Au finish) using pressureless Ag sintering at 300°C for 30 minutes. The initial shear force was 13 N and after aging at 200°C, the shear force decreased to 5 N. The Sn finished components were pressureless sintered on polyimide substrates (Ni/Pd/Au finish) at 230°C for 5 minutes [103]. The as-built shear force was 9 N and after aging at 85°C/85%RH or 175°C, or thermal cycled from 20°C to 150°C for 1137 hours, the shear force was in the range of 5-7 N.

In this work, passive component (thick film chip resistors) attachment using pressureless Ag sintering was explored. Due to termination geometry differences between resistors and dies, different processing procedures and parameters were developed (compared to previous work with die). Pressureless sintering was studied since applying pressure during sintering to multiple resistors on a substrate would be a processing challenge.

4.2 Test Vehicle

Substrates: 5.08 cm x 5.08 x 0.64mm thick, 96% alumina (Al_2O_3) substrates purchased from Coorstek were used for this experiment. For resistor attach, the pattern on the ceramic substrate was designed to bond 20 resistors. The size of the resistor pad was 2.03 mm x 1.42 mm and the distance between the two termination pads was 2.23 mm. Four types of thick film

metallization were examined: Au, Ag, PdAg, Au+Ag. The conductor paste was printed onto the ceramic substrate by screen printing using an MPM TF-100 semiautomatic printer. The printed substrates were dried at 150°C for 10 min, and fired at a peak temperature of 850°C for 10 min. For the Au+Ag substrates, the first metallization layer of Au thick film was processed using the same procedure. The use of Au thick film for the component pad and interconnect routing eliminates the risk of Ag migration at high temperature and was compatible with Au wire bonding. However, to provide a “Ag” surface layer for the sintered Ag attach, a layer of thick film Ag was printed on the previously printed and fired Au pad. The Ag was dried and fired, creating a Ag-rich top surface on the pad.

Surface mount resistor component: Wrap around jumpers were purchased from two suppliers. Supplier A provided three types of resistor terminations: PtAu, PdAg, and PdAg with plated Ni\Au finish. The dimensions of the resistor (R1206) were length: 3.23 mm, width: 1.60 mm, and thickness: 0.46 mm. Supplier B provided PdAg terminated resistors. The dimensions were 3.18 mm x 1.60 mm x 0.64 mm.

4.3 Process Overview

The Ag sintering paste containing micrometer-size Ag particles was stencil printed onto the metallized ceramic substrate. A 50 mm-thick stencil was laser cut to create 20 pairs of 2.4 mm x 2 mm apertures. An MPM TF-100 semiautomatic printer with a metal squeegee was used to print the Ag paste. The resistor was placed on the printed substrate using a Palomar Products Model 3500 pick and place system with a resistor placement force of 39 mg.

Pressureless sintering process: Three sintering temperatures: 200°C, 250°C, and 300°C were experimentally evaluated. The oven profile (Figure 4-1) was a 10 °C/min ramp to peak temperature then a 1-hour hold at the peak temperature. To evaluate the different material and

sintering temperature combinations, as-sintered samples were analyzed by shear testing and cross sectioning. A Dage 2400PC shear tester with a 100 kg die shear module was used for resistor shear testing. In addition, sintered samples were aged at 300°C for 100, 250, 500, 750, 1000, or 1500 hours, then analyzed by shear testing and cross-sectioning.

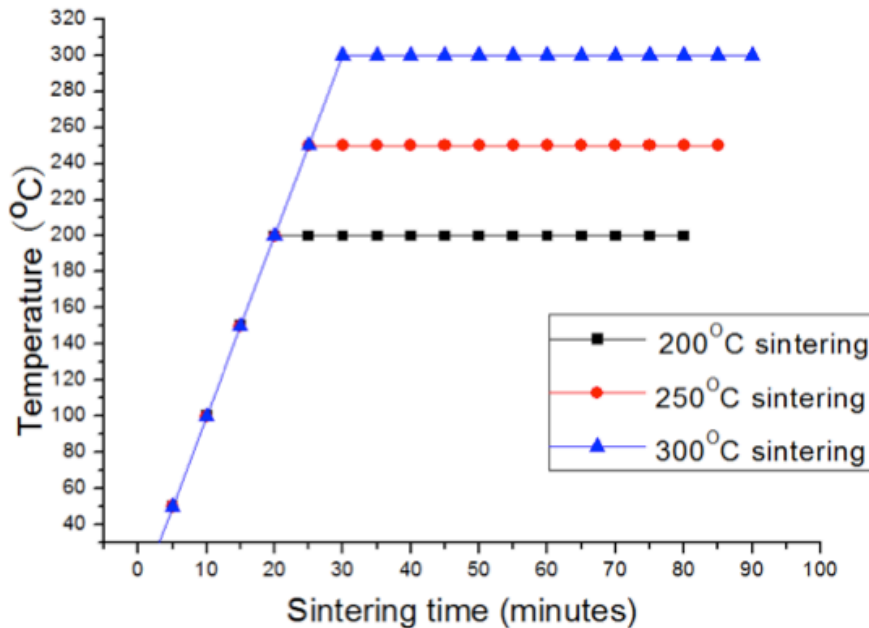


Figure 4-1. Sintering profile of three different sintering temperatures 200°C, 250°C, 300°C. Ramp rate was 10°C/min and dwell for 1 hour.

SEM Analysis: SEM cross-sectional analysis was used to examine the sintered Ag microstructure. The sample was encapsulated with epoxy prior to dicing to maintain the integrity of the resistor attach. The cross-section was prepared for SEM examination by ion milling with an Ion Tech 22cm Linear Ion Gun.

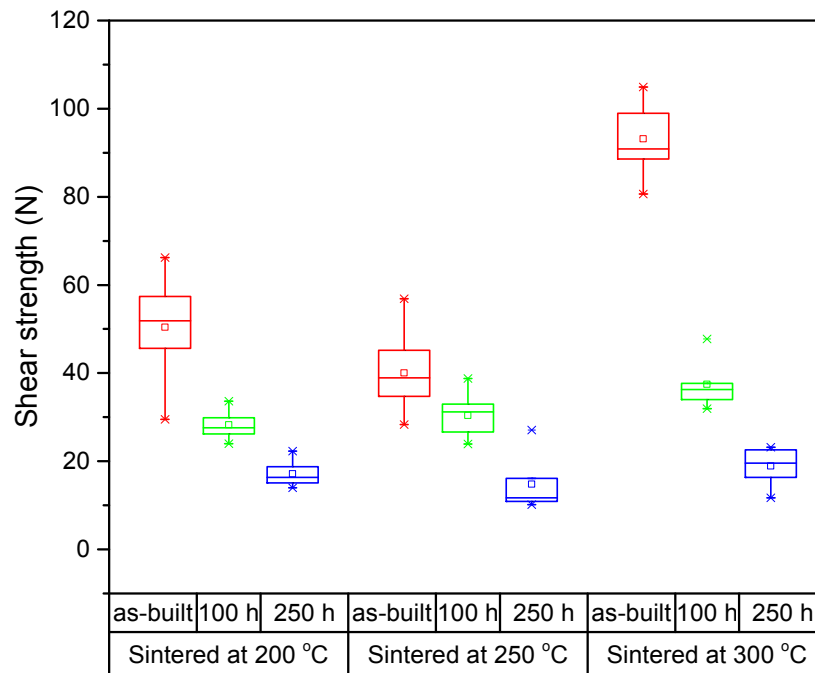
4.4 Process development and Initial Screening

4.4.1 Resistor with PtAu termination.

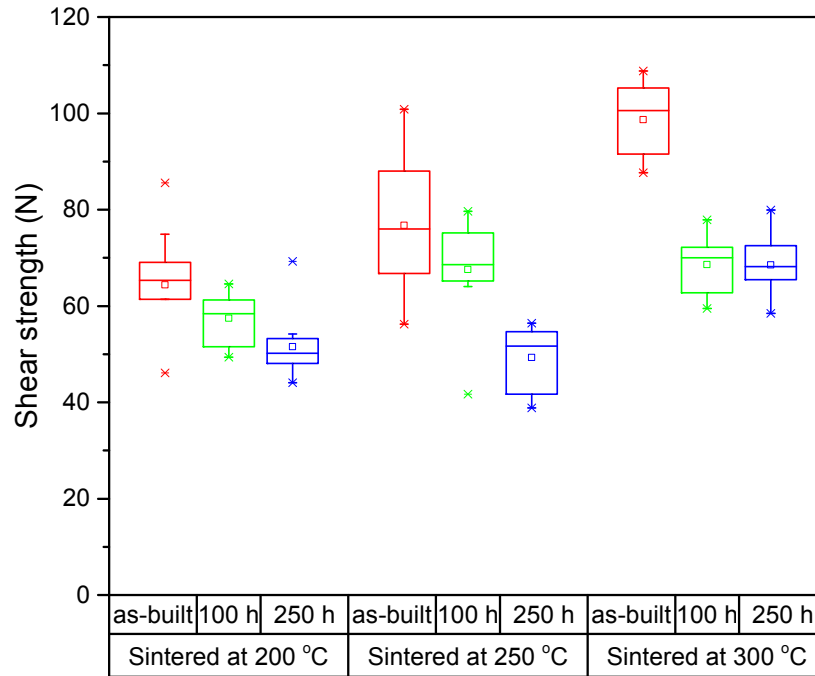
The initial average shear forces for PtAu resistors samples sintered at 200°C, 250°C and 300°C were 50.4 N, 40.0 N and 93.1 N, respectively on Au substrates (Figure 4-2(a)) and 64.4 N,

76.7 N, 98.7 N, respectively on Ag substrates (Figure 4-2(b)). Sintering at 300°C was better than 200°C or 250°C in achieving higher shear force. After aging at 300°C for 250 hours, the shear force on Au substrates decreased significantly, with shear forces comparable for all initial sintering temperatures (Figure 4-2(a)). A decrease in shear force occurred after 250 hours of aging at 300°C for Ag substrate samples, but was less dramatic compared to the Au substrate samples (Figure 4-2 (b)).

Samples were cross-sectioned to characterize the attachment. The thickness of the sintered Ag was only 10 μm as shown in Figure 4-3. The lowest force that could be applied during pick and placement with the Palomar Products Model 3500 was 39 mg. This force squeezed wet paste from under the resistor during placement, resulting in a thin bond layer.



(a) Au Substrate



(b) Ag Substrate

Figure 4-2. Shear force of PtAu resistor sample sintered at 200°C, 250°C, 300°C, and aged for 100 hours, 250 hours, (a) Au substrate, (b) Ag substrate.

In order to increase the thickness of the sintered Ag layer, a post-printing drying step was implemented. Figure 4-4 is a thermogravimetric analysis (TGA) scan of the Ag paste at a rate of 50°C per minute in air (50ml/min) using a Shimadzu TGA-50. The weight loss begins at approximately 50°C. Thus a 50°C drying temperature was investigated. The assembly process used a preheated box oven. The substrate with freshly printed Ag paste was placed into the oven and the door closed. The drying time was defined as the time from closing the oven door until opening the oven door to remove the substrate. A drying time of 5 minutes over dried the Ag paste and the paste did not “wet” the resistor metallization during die placement and the resulting shear force was only 6.1 N. A one-minute post-printing drying step at 50°C was selected based on experimental results. In production, an inline oven or hotplate drying option could also be used instead of a box oven.

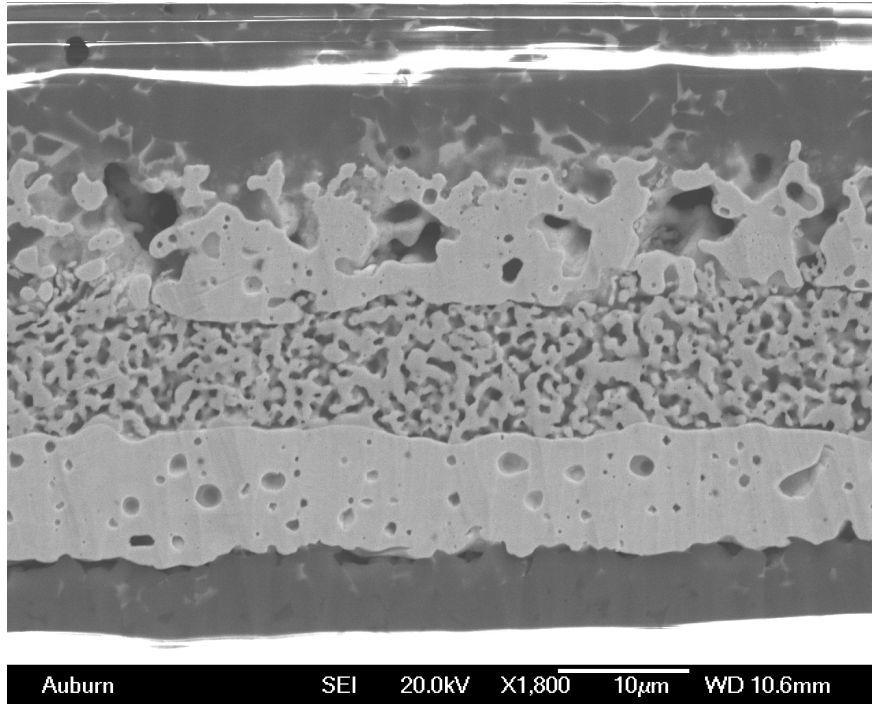


Figure 4-3. PtAu resistor with Au metallized substrate 200°C sintered for 1 hour without post-print drying.

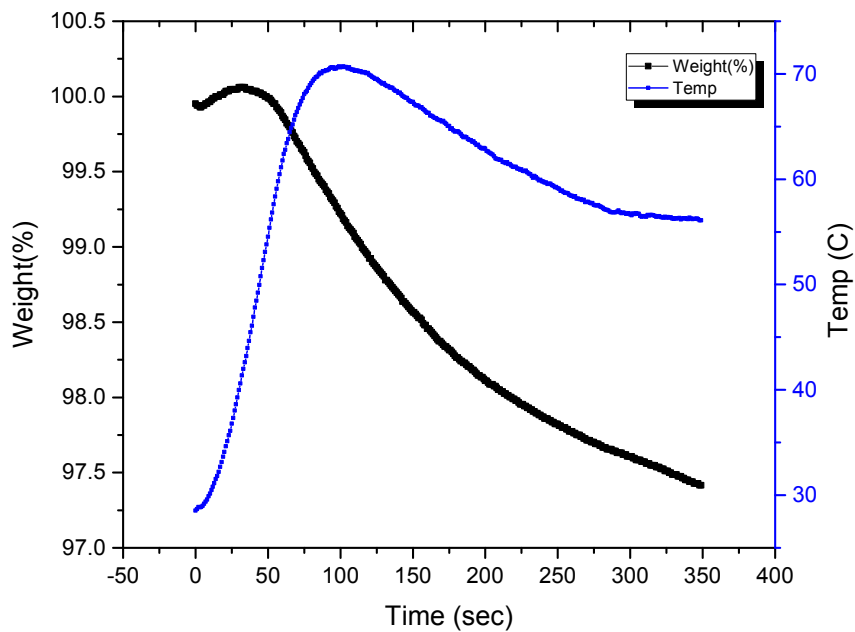
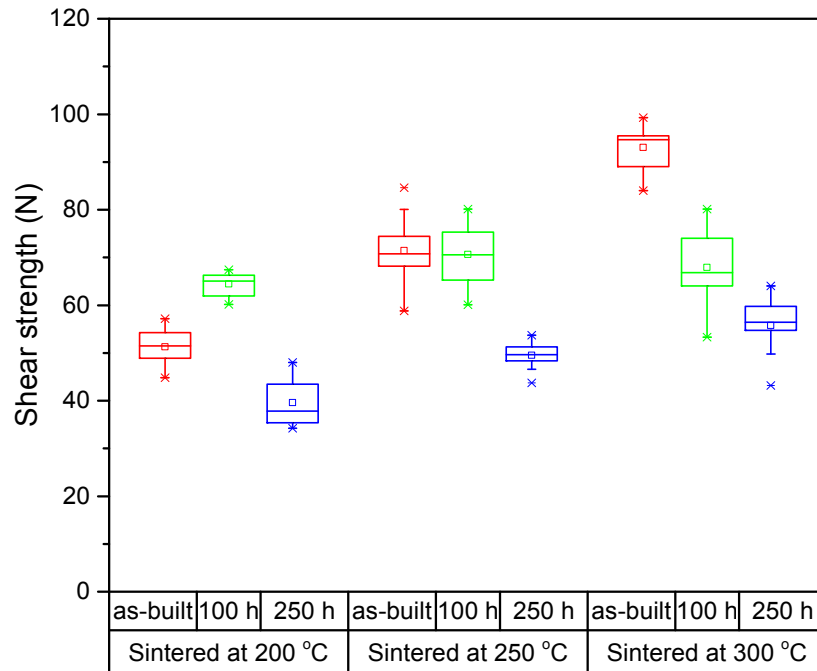
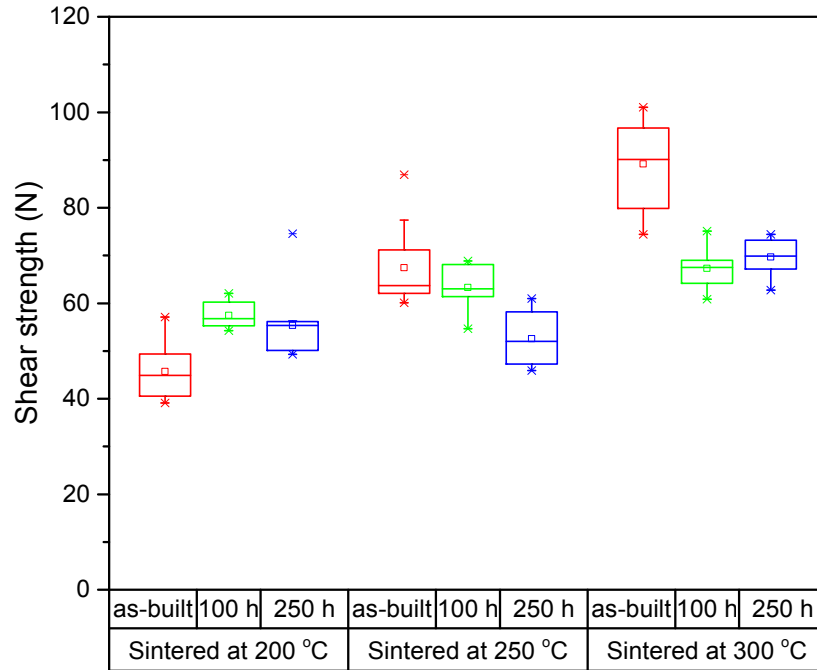


Figure 4-4. TGA analysis of weight loss of Ag sintering paste. Ag paste was placed in Pt pan and temperature was ramped at 50 °C/min with air flow rate of 50 ml/min.

The post-printing drying step increased the thickness of sintered Ag layer. After drying the printed substrate in air at 50 °C for 1 minute, the surface was not as soft as the fresh paste. A sintered Ag thickness of approximately 20 μm was achieved. The post-print drying decreased the degradation of shear force for Au substrate samples (Figure 4-5(a)). For samples on Au metallized substrates, the average shear force was 55.6 N (post-print drying) compared to 18.9 N (no drying step) after being aged for 250 hours. For the Ag metallized substrate, the post-print drying step did not significantly increase the shear force after 250 hours aging at 300°C.



(a) Au Substrate



(b) Ag Substrate

Figure 4-5 Post-printing-dry method: shear force of PtAu resistor sample sintered at 200°C, 250°C, 300°C, and aged for 100 hours or 250 hours on (a) Au substrate and (b) Ag substrate.

To better understand the decrease in shear strength on Au substrates, cross-sectioning of Au substrate samples aged for 250 hours at 300°C was performed (Figure 4-6). A dense Ag layer was found near the Au substrate side, leaving a depletion region in the center of the sintered Ag that weakened the bond.

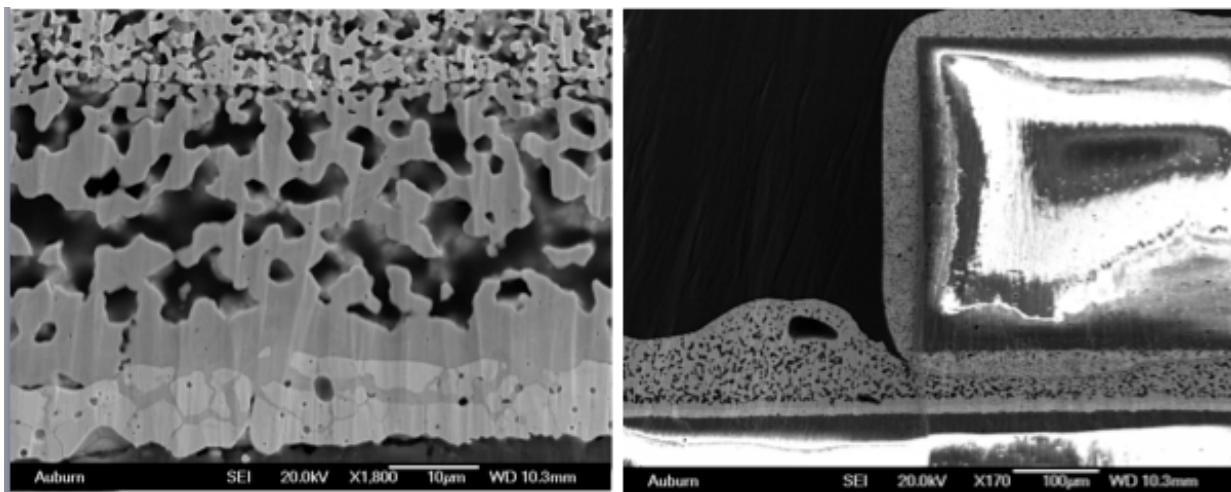


Figure 4-6 Au substrate failure analysis. Au substrate with PtAu resistor sintered at 300°C with post-print drying step, then aged at 300°C for 250 hours.

The formation of a dense Ag layer at the interface to the thick film Au on the substrate was previously observed with pressureless sintering for die attach [102]. Ag diffused along the exposed Au surface creating a continuous Ag layer. This ‘consumption’ of Ag from the bulk resulted in a depletion layer, which was the weakest point of the bond.

4.4.2 Resistor with PdAg termination with plated Ni/Au finish

The PdAg resistors with Ni/Au finish were evaluated early in the experiment, before the development of the post-print drying process. PdAg resistors with Ni/Au finish were assembled on Au and Ag metallized substrate without the post-print drying step. Pressureless sintering temperatures of 200°C and 300°C yielded average initial shear forces of 39.2 N, and 17.2 N, respectively on Au substrates, as shown in Figure 7. The shear strength decreased with aging at 300°C. On Ag substrate metallization, the average shear force was 22.0 N when sintered at 300°C, which was considerably lower than with PtAu resistor terminations. Similar results have previously been reported for pressureless sintered Ag die attach with Au backside metallized die [102]. The PdAg resistors with Ni/Au finish were not used for further testing.

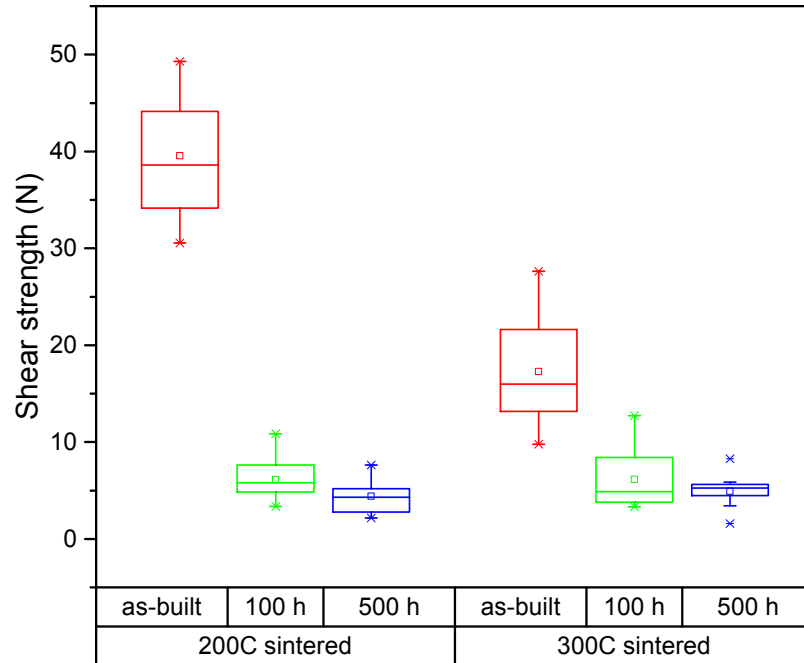


Figure 4-7. Box plot of shear force for PdAg resistor with plated Ni/Au finish assembled on Au substrate showing shear force of samples as-built and aged for 100 hours or 500 hours

4.4.3 Resistor with PdAg termination

PdAg termination resistors from Supplier A were evaluated first. The average shear force of as-built samples was 59.8 N (Ag substrate) and 67.4 N (PdAg substrate) as shown in Figure 8. After aging for 500 hours, the range of shear force decreased to approximately 40 N. All of the failures (initial and aged) were at the PdAg termination metallization-to-resistor ceramic body interface. The fracture analysis is shown in Figure 4-9. The elemental analysis of the imprint region in the middle of the image contained Pd, Ag and Bi, which came from the resistor termination metallization. The weakest point of bonding was in the resistor not the sintered Ag. This resistor was not used for further testing.

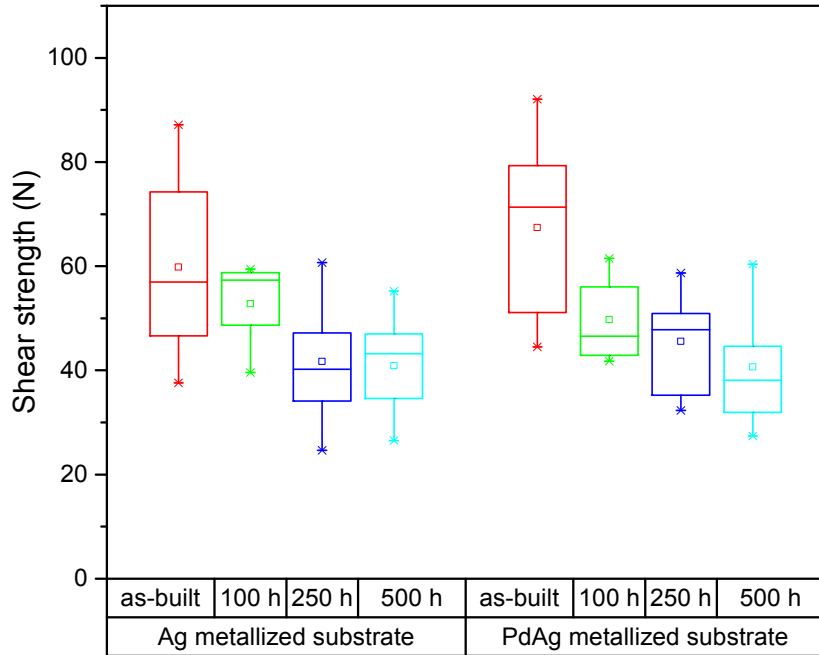
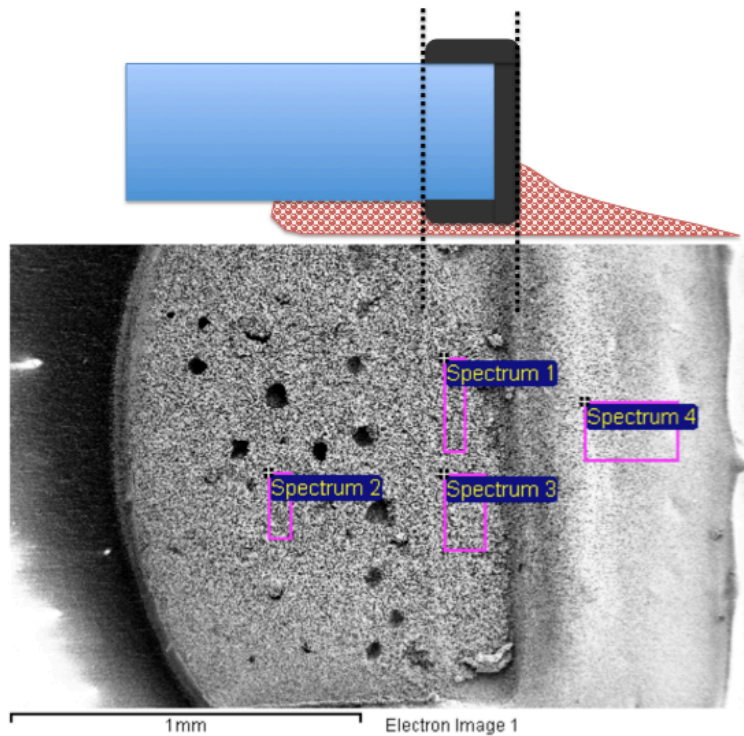


Figure 4-8. Shear force of as-built PdAg resistors (Supplier A) attached to Ag and PdAg thick film metallized substrates. Assembly process: post-print drying and pressureless sintered at 300°C for one hour. Results for samples aged for 100, 250, 500 hours are also shown.



Spectrum	Pd	Ag	Bi	Total
Spectrum 1	16.8	71.7	11.5	100.0
Spectrum 2	0.00	100.00	0.0	100.0
Spectrum 3	15.9	72.4	11.7	100.0
Spectrum 4	0.0	100.0	0.0	100.0

Figure 4-9. (Top) schematic cross-section showing resistor, termination and solder structure to aid in location determination of (Bottom) SEM image and elemental analysis (weight percentage) of the substrate-side failure surface after shear testing. The sample was as-built PdAg terminated resistor (Supplier A) on a Ag substrate.

PdAg resistors from Supplier B were then used. The PdAg resistors were assembled on substrates with Ag, PdAg, Au+Ag thick film metallization. The post-print drying process step was used and the samples were sintered at 300°C for 1 hour. The average initial shear force results are summarized in Figure 4-10. There was no significant difference between the three types of substrate metallization. All of fracture surfaces were in the sintered Ag.

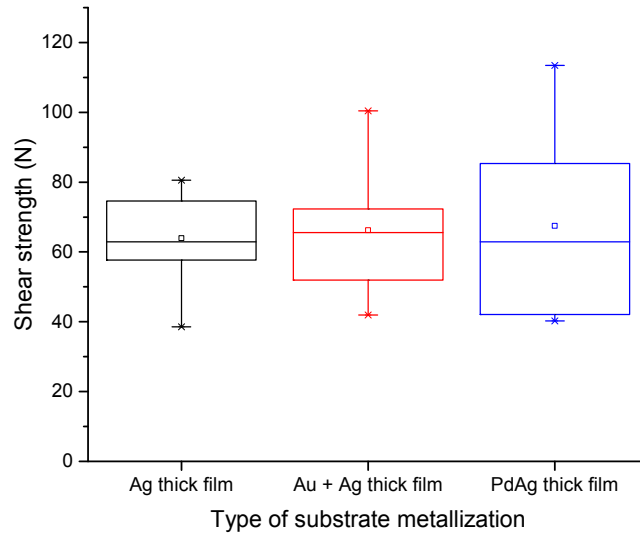
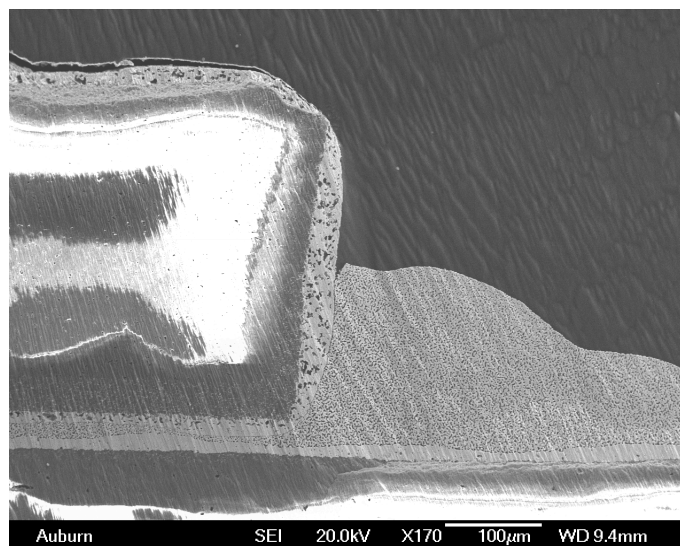
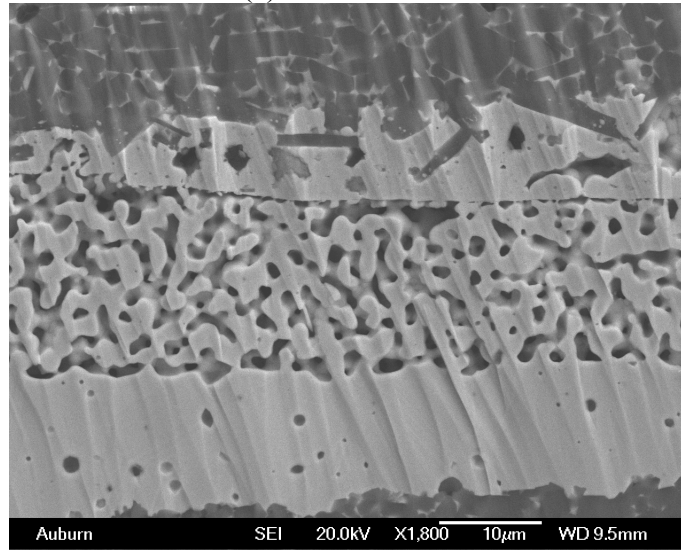


Figure 4-10. Shear force of as-built PdAg resistors (Supplier B) attach separately with Ag, Au + Ag and PdAg thick film metallized substrates. Assembly process: post-print drying and pressureless sintered at 300°C for one hour.

The sintered Ag layer had a homogeneous porous structure. Cross-sections of as-built PdAg resistors attached to Ag, PdAg and Au+Ag thick film metallized substrates are shown in Figure 4-11, Figure 4-12 and Figure 4-13. There was no dense Ag layers or void/depletion regions. The results are similar for all three types of substrate metallization.

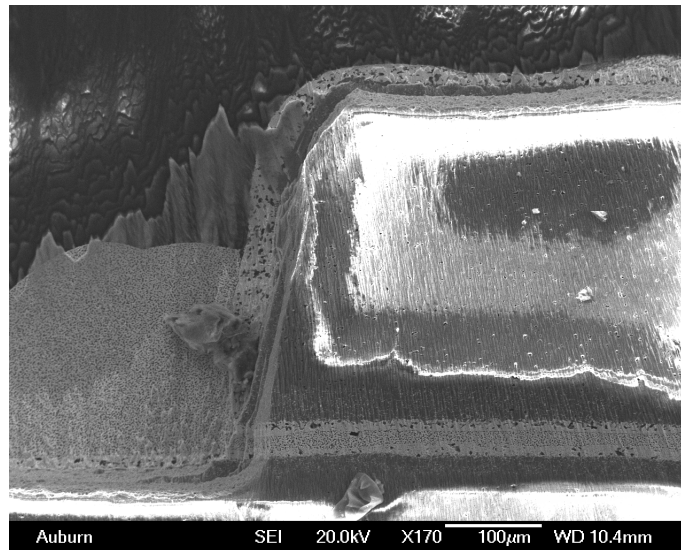


(a) Cross-section

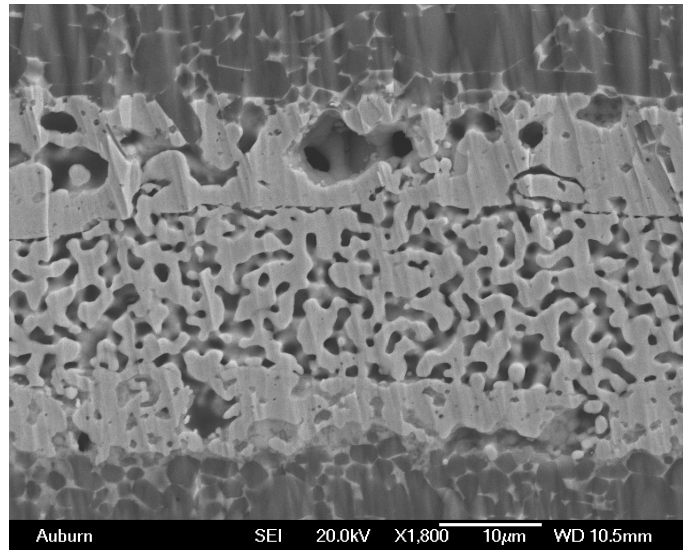


(b) Close-up under resistor termination

Figure 4-11. Sample of PdAg resistor (Supplier B) with Ag metallized substrate sintered at 300°C for 1 hour.

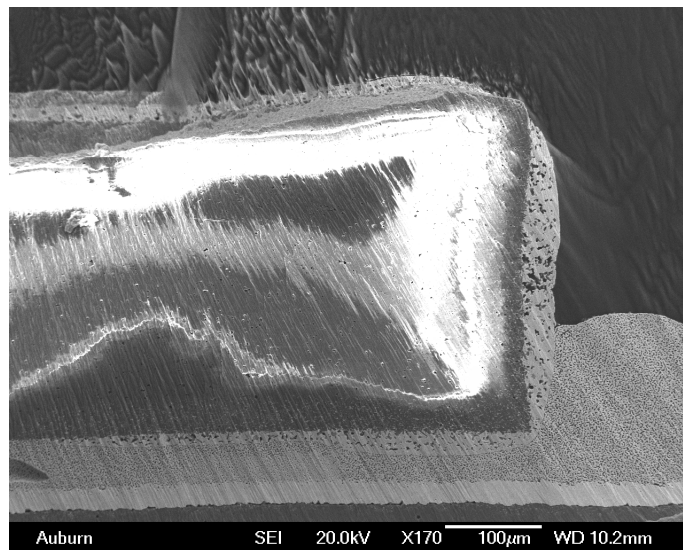


(a) Cross-section

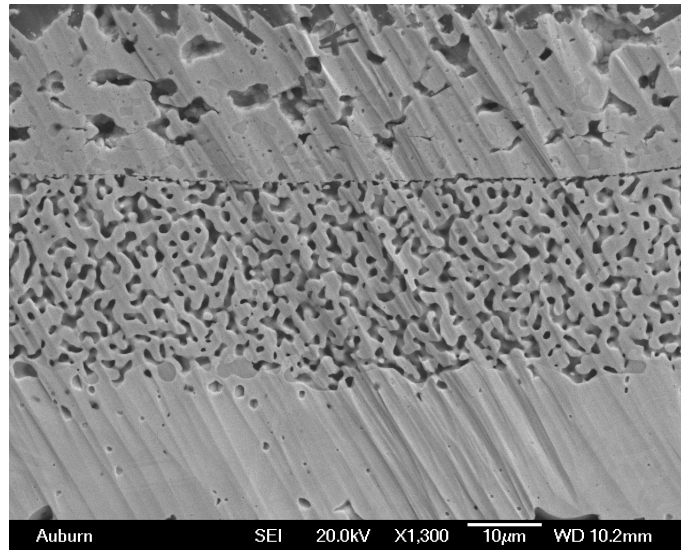


(b) Close-up under resistor termination

Figure 4-12. Sample of PdAg resistor (Supplier B) with PdAg metallized substrate sintered at 300°C for 1 hour.



(a) Cross-section



(b) Close-up under resistor termination

Figure 4-13. Sample of PdAg resistor (Supplier B) with Au + Ag metallized substrate sintered at 300°C for one hour.

Long term aging study

Two sample groups were subjected to long-term (1500 hours) aging at 300°C. One group was the Ag metallized substrate with the PtAu terminated resistor and another group was Ag metallized substrate with the PdAg terminated resistor (Supplier B).

As shown in Figure 4-14, although the initial shear force was high for the PtAu terminated resistors on Ag thick film substrates, it dropped steadily with increasing aging time. After 1500 hours, the attachment had decreased significantly. In order to understand the failure mechanism, the cross-section of a sample aged for 1000 hours was examined (Figure 4-15). A dense Ag layer formed near the resistor side at the PtAu termination leaving large voids in the bulk of the attach layer. Compared to the dense Ag layer formed near the Au thick film substrate in Figure 4-6, the morphology was similar. The formation of a dense Ag layer on an Au or PtAu surface results in voids or depletion layer near the opposing surface.

The shear test result as a function of aging time at 300°C for the PdAg terminated resistors (Supplier B) on Ag thick film metallization was shown in Figure 4-16. There is no degradation in shear force with aging.

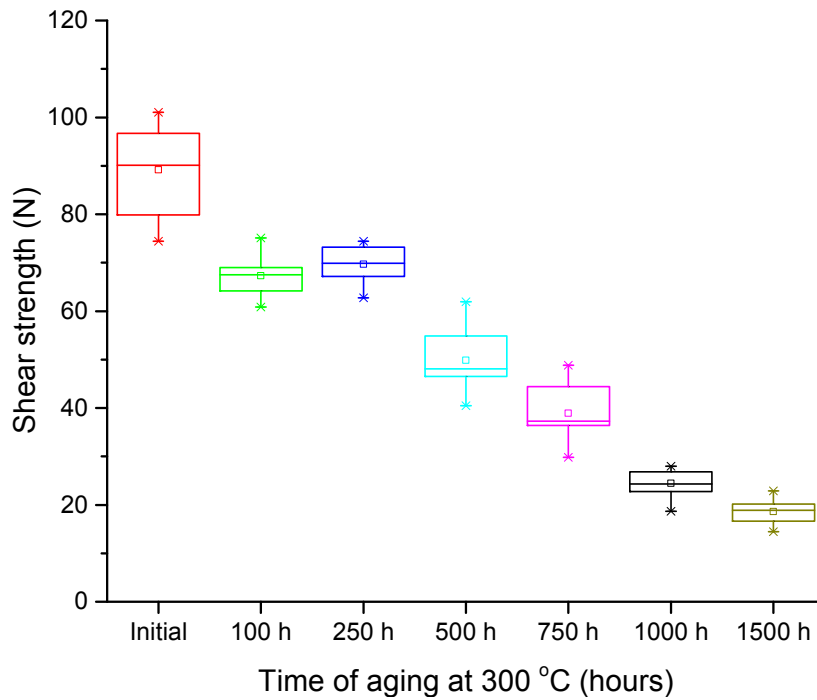


Figure 4-14. Shear force of Ag substrate with PtAu resistor sintered at 300°C for 1500 hours.

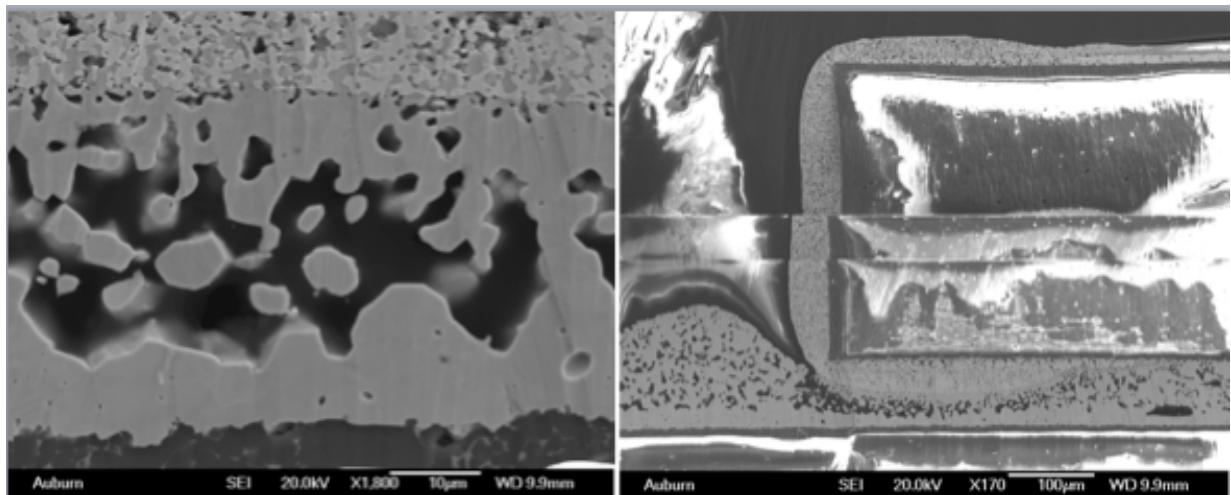


Figure 4-15. Ag metallized substrate with PtAu terminated resistor sintered at 300°C, then aged at 300°C for 1000 hours.

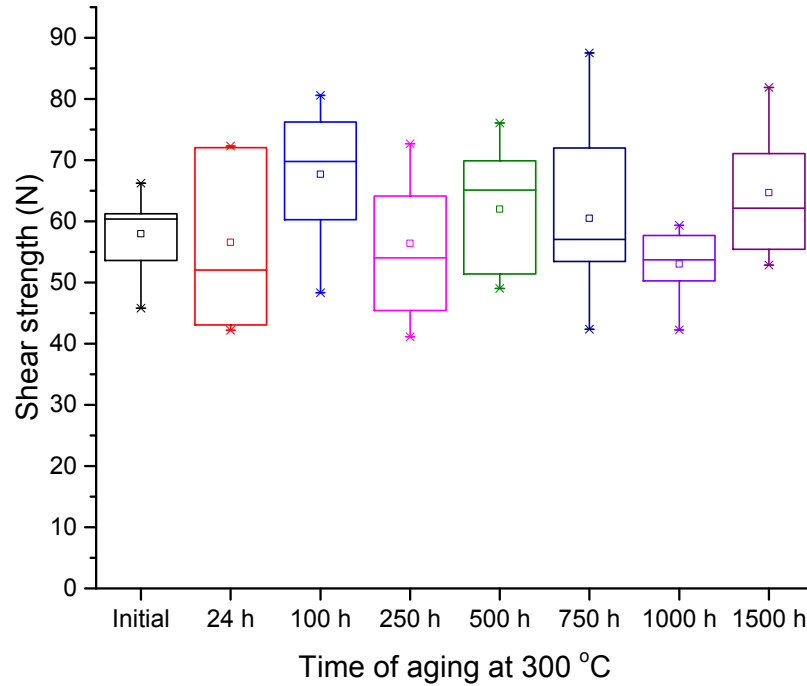
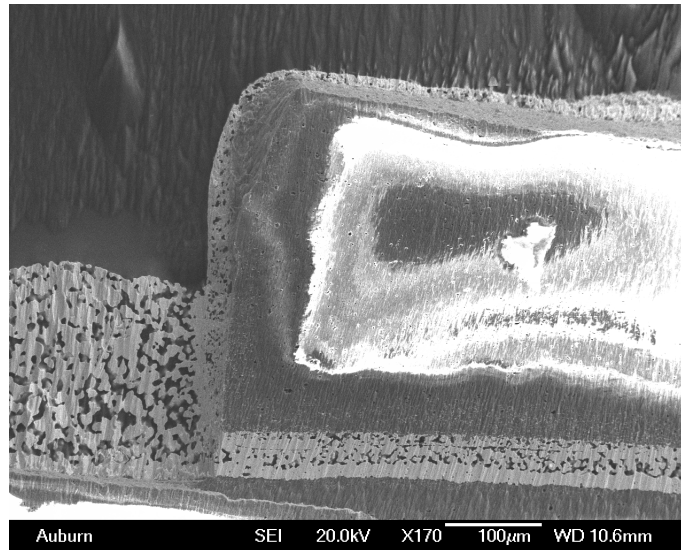
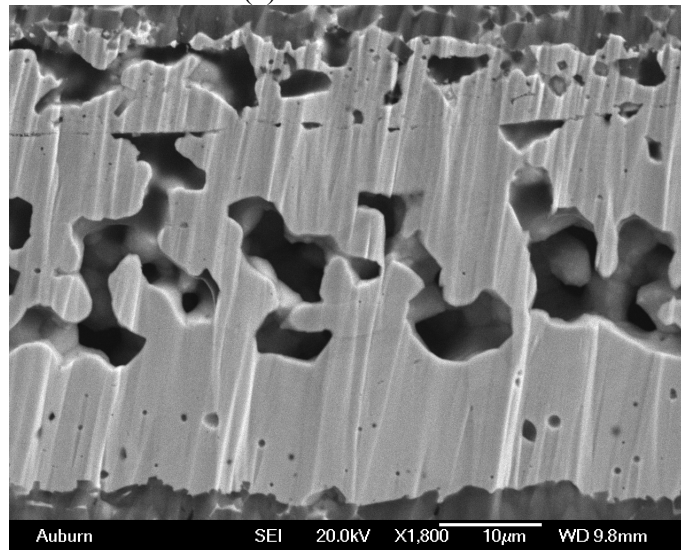


Figure 4-16. Shear force of PdAg resistors (Supplier B) with Ag metallized substrate aged for 1500 hours.

As shown in Figure 4-17, after aging at 300°C for 1000 hours, the pores merged to form a larger porous structure, but no dense Ag layer or depletion region formed.



(a) Cross-section



(b) Close-up under resistor termination

Figure 4-17. Cross section of PdAg (Supplier B) with Ag metallized substrate aged at 300°C for 1000 hours.

Aging studies with PdAg terminated resistors (Supplier B) on PdAg and Au+Ag thick film metallized substrates are ongoing. Shear tests after the first 100 hours of aging at have been completed. For PdAg metallized substrate, the average shear strength was 64.4N. The shear strength for PdAg terminated resistors on Au+Ag thick film metallized substrate was 76.1N.

Conclusion

A post-print drying method was developed to reduce Ag paste squeeze-out during resistor placement and obtain a sintered Ag thickness of approximately 20 μ m.

While the PtAu terminated resistors had good initial shear force results, the shear force decreased with 300°C aging on both Au and Ag thick film metallized substrates. The degradation in shear force was more rapid on Au metallized substrates.

The PdAg terminated resistors with a plated Ni/Au finish, had low shear forces as-built. With Au substrates, increasing the sintering temperature resulted in lower shear force.

The PdAg terminated resistors results varied with supplier. In the case of Supplier A, the failure mode was at the resistor termination-to-ceramic body interface. With Supplier B this failure mode did not occur. No degradation in resistor shear force occurred with PdAg terminated resistors (Supplier B) after 1500 hours at 300°C on Ag thick film substrates. Tests with PdAg and Au+Ag thick film substrates are still underway.

CHAPTER 5 PRESSURE SINTERING

With an increasing demand for SiC and GaN high power devices that operate at high temperature, traditional solder materials are reaching their limitations in performance. In addition, there is a strong desire to eliminate high lead containing solders in Si power device packaging for use over conventional temperature range. Low temperature Ag sintering technology is a promising method for high performance lead-free die attachment. In a previous study, a pressureless sintering process and suitable metallization were demonstrated to provide high reliability die attach by using micro-size Ag sintering. The resulting die attach layer had approximately 30% porosity.

In this work, a low temperature pressure-assisted fast sintering process was examined. The porosity was decreased from 30% to 15% with application of a low pressure (7.6MPa) during a one minute sintering process. The shear strength for a 3 mm x 3 mm die was 70 MPa and the 8 mm x 8 mm die could not be sheared off due to a 100 kg shear module force limit. Both the Ag and Au metallization (die and substrate) were studied. Furthermore, a new substrate metallization combination was found that allows the use of Au thick film metallized substrates. High temperature (300°C) storage tests for up to 2000 hours aging were conducted and results are presented.

5.1 Review of Pressure Sintering Methodology

Driven by an increasing range of applications in geothermal wells, deep oil and gas well logging, aircraft, automotive and nuclear power instrumentation, high-temperature and high-power electronics are needed to operate at or above 300°C. Correspondingly, high temperature packaging to interface with the elements of the electrical system is required [104-106]. Die

attach is the joining of the die to the package or substrate to provide a mechanical connection of the die to the substrate, electrical connection and a thermal path for removing heat during the operation. For decades, high lead solders have been used for high temperature ($\leq 225^{\circ}\text{C}$) die attach. Expensive AuSi and AuGe eutectics and liquid phase transient (LPT) bonding with AuSn have been used for higher temperatures. Due to worldwide regulations banning lead from electronics, Ag sintering technology has been considered a promising replacement for high lead solder for high temperature and high power applications [107-109].

Efforts have been made to develop low temperature, pressureless Ag sintering processes to achieve high reliability and high performance die attach. For small die (1.71 mm x 1.38 mm and 2.26 mm x 2.26 mm), a pressureless sintering process yielded high shear strength up to 38 MPa [110] and could support high temperature operation of SiC power devices [111]. Ag substrate metallization provided better adhesion (40 MPa) than Au substrate metallization (20 MPa) [112]. But for large die (6 mm x 6 mm [113] and 10 mm x 10 mm die [114],[115]), pressure during the sintering process was still needed. To reach a shear strength $>30\text{MPa}$ and good electrical performance, 3 MPa of lamination pressure was needed during sintering [113].

Pressureless sintering for large die has been presented in previous work [116]. The assembly process required one-hour sintering at temperatures ranging from 200°C to 300°C . The porosity was approximately 30%; higher than with pressure sintering. Also, the sintered Ag had a reliability issue (degradation of adhesion with aging at 300°C) with Au metallization on either the thick film Au substrate or the die backside.

In order to decrease the porosity of the sintered Ag layer, the application of pressure has been explored. Lei, et al. [117] evaluated four drying steps at 50, 75, 100 and 125°C for 50 minutes, followed by 20 minutes of 275°C sintering for attaching large-area die. With 5 MPa

pressure, a relative low pore density of about 20 % and shear strength of 31.6 MPa were achieved. Xiao, et al. [114] developed a two-step Ag layer process. The first Ag layer was pre-dried under 3 MPa at 180 °C for 5 minutes. A second thin Ag layer was printed and the die was sintered without pressure for 30 minutes at 275°C. A die-shear strength greater than 30 MPa was obtained. Zheng et al. also used a double print method [118], [119] that dried a first layer of Ag sintering paste in N₂ at 180°C for 5 minutes and sintered a second 10 µm layer at 275°C for 3 minutes with 5 MPa applied. The pore density was 23.48 %. Applying a sintering pressure above 3 MPa was sufficient for die shear strengths in excess of 40 MPa. Nitrogen during sintering was confirmed by Nishikawa, et al [120] to lower the sintering pressure from 20 MPa to 10 MPa while achieving 20 MPa shear strength. The process included a 130°C, 5 minutes pre-dry and a 300°C, 10 minute sintering. Recently, Li et al. experimented with a combination of pre-dry time from 10 to 45 minutes and sintering time from 1 minute to 8 minutes with pressure from 1 MPa to 15 MPa. The shear strength varied in a wide range from 10 MPa to 100 MPa. The porosity was approximately 24 % [121]. All the publications cited above and summarized in Table 5-1 used a hot press to apply pressure during sintering, with a sheet of silicone rubber to protect the die.

Table 5-1. Summary of recent literature on pressure-assisted Ag sintering processes.

Predry	Sintering	Pressure	Porosity	Shear Strength	Ref.
50, 75, 100 and 125°C for 50 min	20 minutes of 275°C sintering	5 MPa	20%	31.6 MPa	[14]
5 min 180°C	Second layer 30 min	3 MPa		30 MPa	[11]
Nitrogen, 180°C for 5 min	Second layer at 275°C for 3 min	5 MPa	23.48%	40 MPa	[15,16]
130°C, 5 min (Bare copper)	300°C, 10min	10 MPa		20 MPa	[17]

150° 1min	300° 1min	7.6 MPa	15%	70.7 MPa	This work
-----------	-----------	---------	-----	----------	-----------

In this work, sintering conditions: pre-dry, sintering time, sintering temperature, and sintering pressure were experimentally optimized. A 150°C, one-minute pre-dry and a 300°C one-minute sintering process was developed. The reduction in the sintering time allowed the use of a flip chip thermocompression bonder for automated die attach. Also, a new substrate metallization was developed to allow the use of Au thick film substrate metallization.

5.2 Test Vehicles

Substrate Metallization: The 5.08 cm x 5.08 cm x 0.64 mm thick, 96 % alumina (Al_2O_3) substrates used for this experiment were purchased from Coorstek. The substrates were metallized with three different thick film conductors. For Au or Ag metallized substrates, one layer of Au or Ag thick film conductor paste was printed onto the substrates and dried at 150°C for 10 minutes, then fired at a peak temperature of 850°C for 10 minutes. A third group of substrates was first metallized with a layer of Au thick film using the same procedure. The use of Au thick film for the die attach pad and interconnect routing eliminates the risk of Ag migration at high temperature and is compatible with Au wire bonding. In order to provide a “Ag” surface layer for the sintered Ag die attach, a layer of thick film Ag was printed on the previously printed and fired Au die attach pad. The Ag was dried and fired, creating a Ag top surface on the die attach pad. Die attach pads were fabricated for both 3 mm x 3 mm die and 8 mm x 8 mm die.

Die Metallization: Si wafers and SiC wafers were metallized on the backside by electron-beam thermal evaporation. For Au metallized die, Ti (50 nm), Ni (200 nm), and Au (200 nm) were sequentially deposited. Ag metallized die were fabricated by sequential deposition of Ti (50 nm), Ni (200 nm), and Ag (300 nm). The Si wafers were diced into 8 mm x 8 mm test die and SiC wafers were diced into 3mm x 3mm test die.

5.3 Assembly and Characterization Process

Ag Paste Deposition: The die attach material was Ag sintering paste containing micrometer-size Ag particles. A 50 μm thick laser cut stencil was used to print the silver sintering paste on the metallized substrate with an MPM semiautomatic printer using a metal squeegee.

Rapid Pressure-Assisted Sintering Process: The pressure sintering process included three stages: pre-dry, die placement and sintering. After the Ag sintering paste was printed, the substrates with fresh patterns were placed into an oven to carry out the pre-dry process. The die placement and sintering steps were accomplished with an FC150 die/flip chip bonder. The sintering process included a temperature ramp to a desired temperature, dwell time at the desired temperature and cool down. The temperature was ramped at the maximum rate and a force was gradually applied to the die to reach the desired value in 100 seconds (Figure 5-1). When the temperature reached the desired peak, 60 seconds of dwell time was initiated. After 160 seconds from cycle initiation, the cooling process was activated and the force was gradually reduced as shown in Figure 5-1.

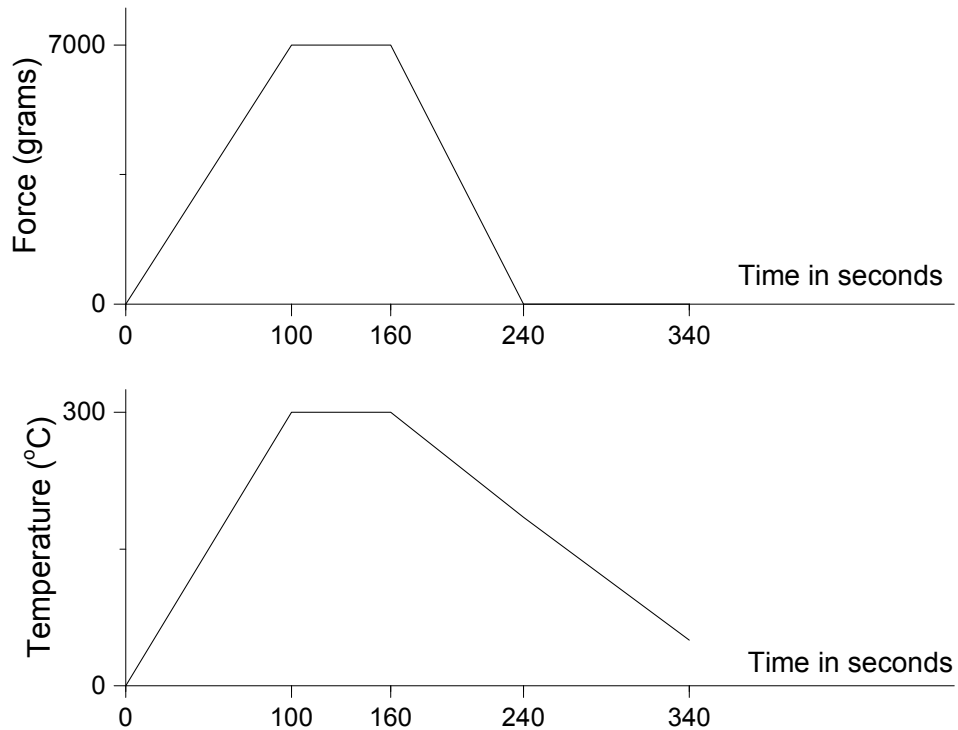


Figure 5-1 Temperature and force profile of pressure-assisted sintering, exhibiting a 3 °C/s ramp rate and sintering/force application dwell time of 60 seconds.

Characterization Process: In order to evaluate the different metallization and process options, as-sintered samples were analyzed by shear testing and sample cross sectioning and then examined using scanning electron microscopy (SEM). In addition, sintered samples were aged at 300°C for 1 hour, then analyzed by shear testing, cross sectioning and microscopy. Previous work has shown this to be an effective screening method [116].

Die Shear Testing: A Dage 2400PC shear tester with a 100 kg die shear module was used for die shear testing. In some instances the die could not be sheared with the force from the 100 kg module. For an 8 mm x 8 mm die, this corresponds to a maximum shear test limit of 15.3 MPa.

SEM Analysis: SEM cross sectional analysis was used to examine the microstructure of the sintered Ag layers. Samples were diced into two pieces along the center of the die. For samples known to have low shear strength, the die was encapsulated with epoxy prior to dicing to maintain the integrity of the die attach layers. Cross sections were then prepared for SEM examination using a Gatan ion milling machine with an Ion Tech 22cm Linear Ion Gun.

5.4 Process Optimization

5.4.1 Pre-dry Condition:

The goal of the pre-drying process was to remove solvent from the paste, increasing the viscosity to prevent paste squeeze out during the pressure application step. Figure 5-2 is a thermogravimetric analysis (TGA) scan of the Ag paste at a rate of 50°C per minute in air (50 ml/min) using a Shimadzu TGA-50. Significant weight loss begins at 100°C and most of the solvent has been removed by the time 200°C is reached. The pre-drying process used a preheated box oven. The substrate with freshly printed Ag paste was placed into the oven and the door was closed. The drying time was defined as the time from closing the oven door until opening the oven door to remove the substrate. To evaluate drying temperatures, Ag metallized die were assembled on Ag metallized substrates using a pressure-assisted (7.6 MPa) process at 300° for one minute. With drying at 100°C for one minute, samples had an average shear strength of 44.7 MPa, while samples dried at 200°C for one minute had an average shear strength of 48.0 MPa. In contrast, samples dried for one minute at 150° had average shear strength of 70.7 MPa. A drying time of 2 minutes decreased the shear strength to 1.07 kg (0.16 MPa), with failure at the die metallization-to-Ag paste interface. A drying time of two minutes over dried the Ag paste and the paste did not “wet” the die metallization during die placement. A one-minute drying time at

150°C was selected for further process development. In production, an inline oven or hotplate drying option could also be used instead of a box oven.

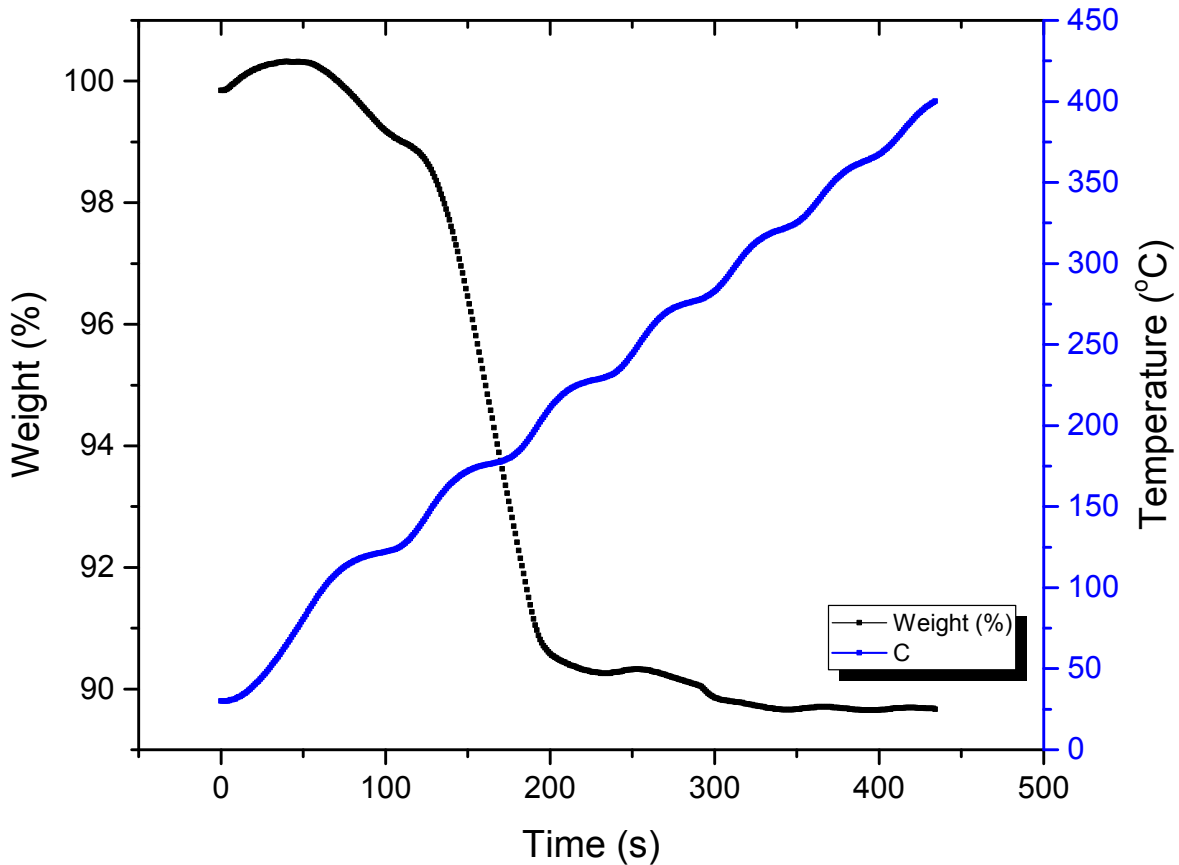


Figure 5-2. TGA of weight loss of Ag sintering paste. Ag paste was placed in a platinum pan with a temperature ramp of 50 °C/min and with air flow rate of 50ml/min.

5.4.2 Sintering Temperature and Sintering Time:

3 mm x 3 mm Ag-metallized SiC die were assembled with Ag metallized substrates after the 150°C, one-minute pre-dry. Three different sintering temperature, 200°C, 250°C, and 300°C, were evaluated.

The maximum force the FC150 die/flip chip bonder could apply was 50 kg. For an 8 mm x 8 mm die, the maximum pressure obtained from FC150 die/flip chip bonder during sintering

was 7.66 MPa, which corresponds to 7.03 kg for a 3 mm x 3 mm die. Therefore, a 7 kg (7.62 MPa) pressing force was selected and programmed into the FC150 for small die assembly. In order to explore the influence of sintering temperature and sintering time, pressure was held at 7.66 MPa for large die and 7.62 MPa for small die during this experiment.

Die subjected to 200° sintering for one minute reached a mean shear strength of 10.3 MPa (Figure 5-3). From the fracture surface analysis, the failure occurred between the die metallization and the sintered Ag. The paste was not fully sintered in one minute, as evidenced by the observation of some Ag powder at the fracture surface. Increasing the sintering time to 2 minutes, did not significantly increase the shear strength (12.0 MPa).

Die subjected to a 250°C, 1-minute sintering time yielded a mean shear strength of 39.8 MPa. Furthermore, by increasing the sintering time to 2 minutes, the mean shear strength increased to 48.9 MPa. The failures were in the sintered Ag near the die side. No unsintered Ag was observed.

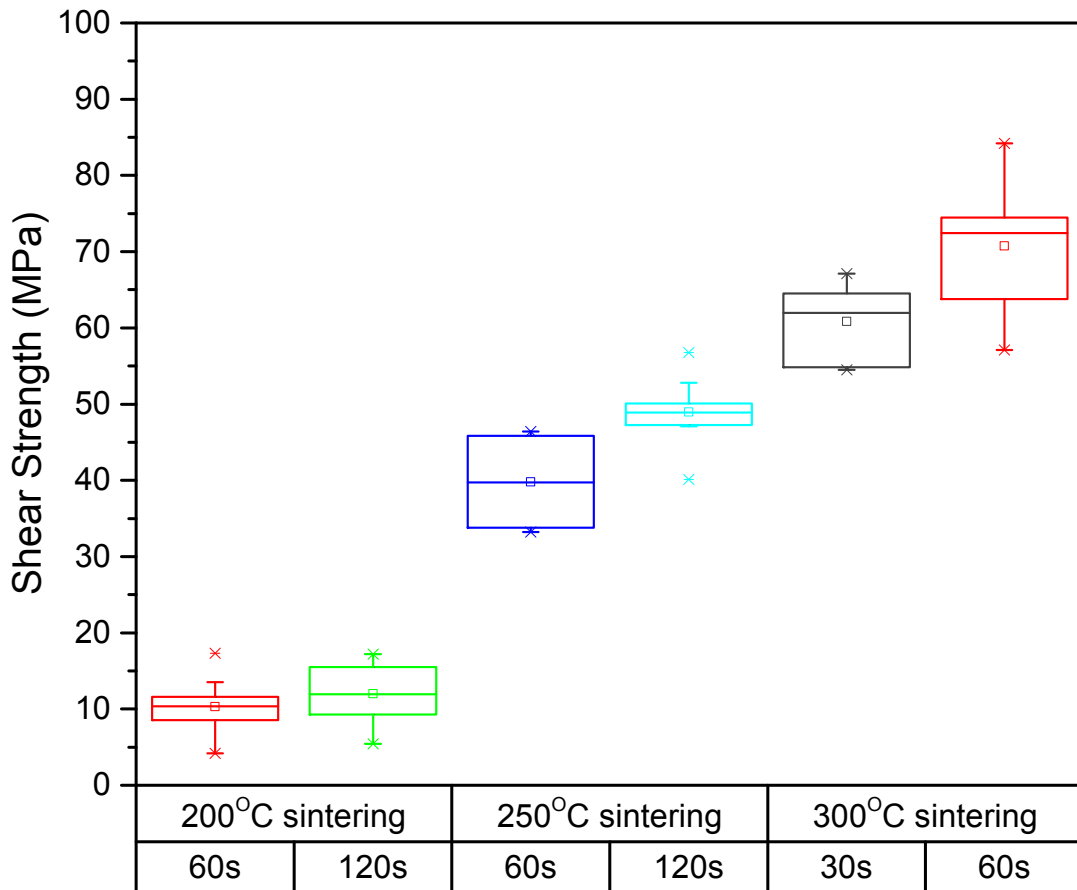


Figure 5-3. Box plot of shear strength versus sintering temperature and sintering time at 7.6 MPa sintering pressure. 3mm x 3 mm Ag metallized SiC die assembled on Ag thick film metallized substrates following a 150°C one-minute pre-dry.

With a 300°C sintering temperature, the 1-minute sintering process resulted in a shear strength of 70.7 MPa. Based on this high shear strength, a reduced sintering time of 30 seconds was evaluated and a mean shear strength of 60.8 MPa was achieved. Fracture surface analysis on these parts showed that the shear test failures for both sintering times were in the sintered Ag near the die side. Compared to 250°C, the higher sintering temperature of 300°C resulted in better attachment and slightly more sintered Ag on the die side of the fracture surface. After aging for 1 hour, the failure mode moved to the middle of the sintered Ag.

5.4.3 Sintering Pressure vs. Shear Strength:

As described above, pressure was applied during sintering with a FC150 flip chip/die binder. Ag metallized, 3mm x 3mm SiC die and Ag metallized substrates were used in this portion of the experiment. Four force (pressure) settings: 3.5 kg (3.8 MPa), 7 kg (7.6 MPa), 25 kg (27.2 MPa), 50 kg (54.4 MPa) were studied.

The stencil printed substrates were first pre-dried at 150°C for one minute. Based on the time-temperature study in the previous section, the sintering process used was 300°C for one minute.

The shear strength had an increasing relation to the sintering pressure (Figure 5-4). Samples, which were sintered at 3.8 MPa during the one-minute, 300°C sintering process, had a mean shear strength of 52.9 MPa. Failures were in the sintered Ag near the die side. Increasing the pressure to 7.6 MPa and 27.2 MPa corresponded to mean shear strengths of 70.7 MPa and 93.4 MPa, respectively. The die shear failed in the sintered Ag near the die side. Samples assembled with 54.4 MPa pressure could not be sheared due to the Dage shear module limit, which is 100 kg, corresponding to shear strength higher than 108.9 MPa.

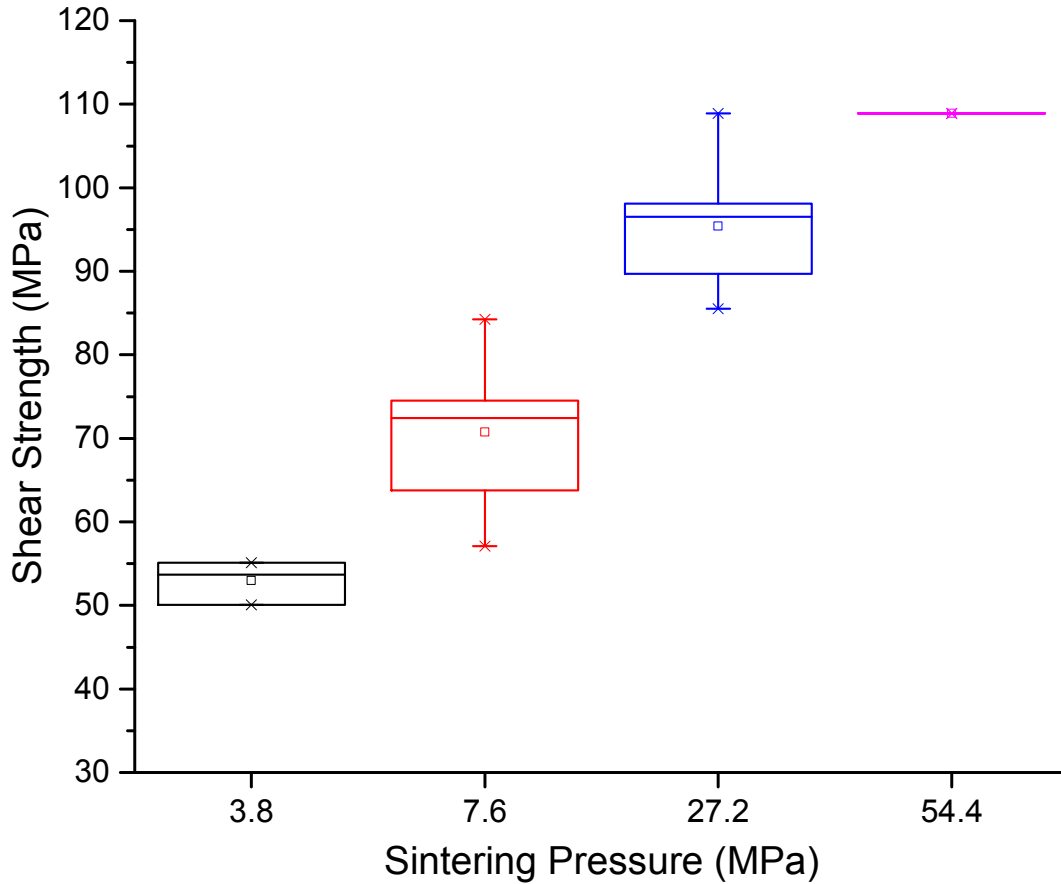


Figure 5-4. Box plot of shear strength versus sintering pressure.

5.4.4 Porosity versus Sintering Pressure

To further examine and verify the quality of die bonding, the porosity of the sintered Ag layer was studied (refer to Figure 5-5). For each sintering pressure group, three samples were cross-sectioned and evaluated by SEM. The SEM images were gray-scaled and pore area was calculated via Matlab code. The tolerance of the porosity calculation is estimated to be $\pm 2\%$ due to the sample surface topology, definition of boundary and image quality of the SEM images. Though, this analysis does provide a relative comparison of densification among different sintered Ag die attachment processes. Other research groups have encountered the same porosity determination accuracy issue [11],[122].

For 3.8 MPa sintering pressure, the porosity of the sintered Ag area ranged from 18% to 21%. Larger voids were found at the die metallization-to-Ag die attach interface as shown in Figure 5-6. This corresponds to lower shear strength and failure interface. For 7.6 MPa sintering pressure, the porosity was approximately 17%. The maximum sintering pressure of 54.4 MPa yielded ~10% porosity.

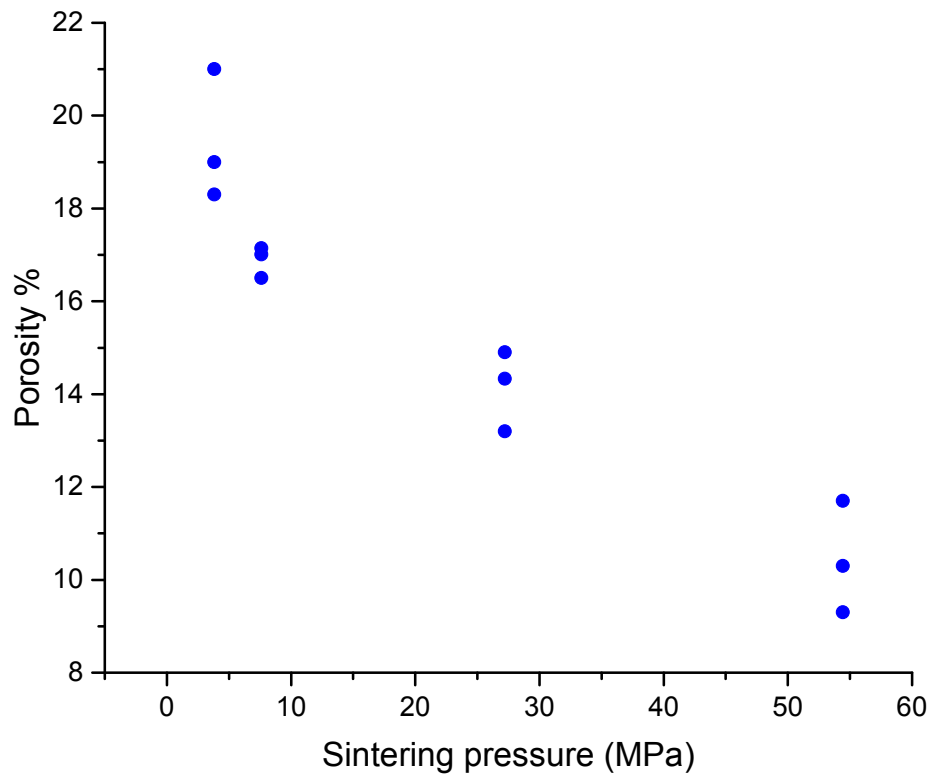


Figure 5-5. Porosity of sintering Ag under different sintering pressure.

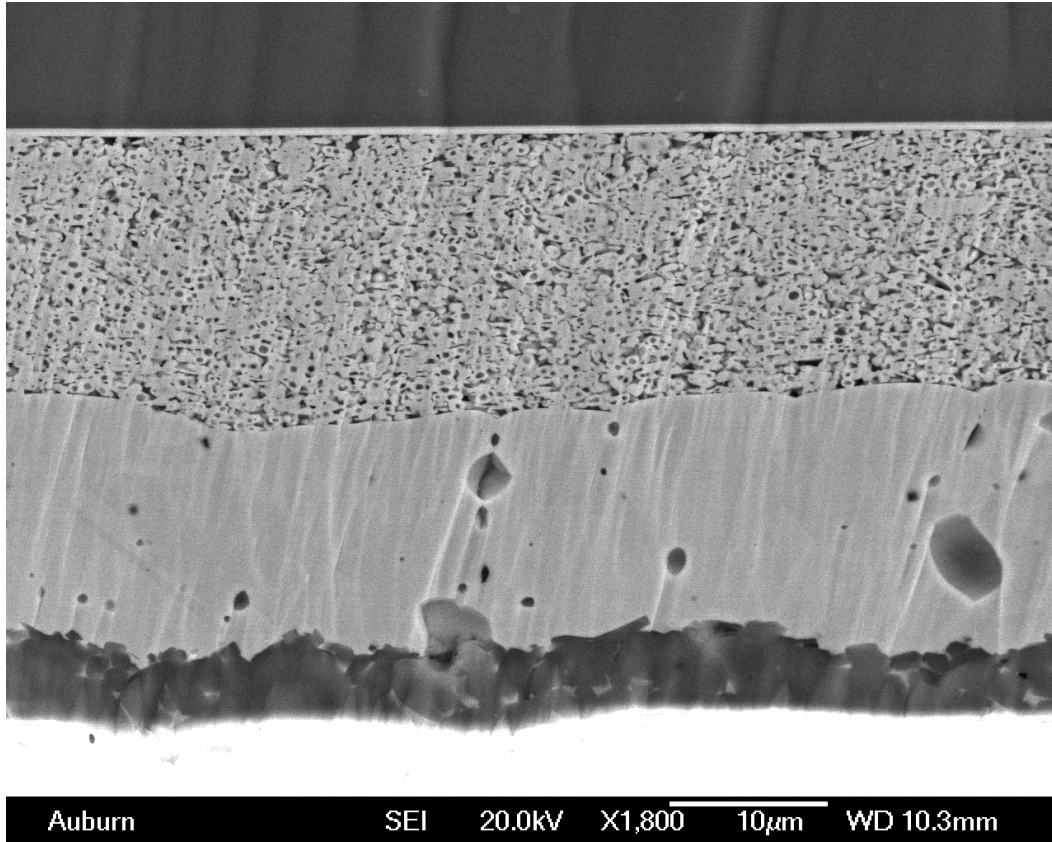


Figure 5-6. Cross-sectional SEM image of die attach layer for as-built sample with 3 mm x 3 mm Ag metallized die on a Ag thick film substrate sintered at 300°C with 3.8 MPa for one minute.

5.5 Assembly Results with Different Metallization

For large die (8 mm x 8 mm), the same pre-dry (150°C for one minute) and sintering conditions (300°C for one minute, 7.66 MPa) were used for die attach. The die attach evaluation matrix included two types of die metallization (Au and Ag) and three types of substrate metallization (Au, Ag and Ag + Au).

5.5.1 Ag Die Metallization, Au Substrate Metallization

For Ag metallized die assembled on Au thick film metallized substrates, the mean shear strength of as-built samples was as low as 7 MPa. As shown in Figure 5-7, the sintered Ag had

minimal attachment to the Au thick film metallization, which can be seen from the fracture surface; all of the sintered Ag was on the die side after shear testing.

By increasing the sintering time to 90 seconds, the mean shear strength increased to 11.1 MPa with the same failure at the Au thick film surface. With 120 seconds of sintering time, the shear strength was 12.5 MPa. The die could not be sheared (> 15.3 MPa) with a sintering time of 180 seconds. To obtain measurable shear strength, 3 mm x 3 mm Ag metallized die with Au thick film substrates were assembled. The average shear strength, for a sintering time of 180 seconds, was 32.2 MPa. All of the failures were on the Au thick film surface.

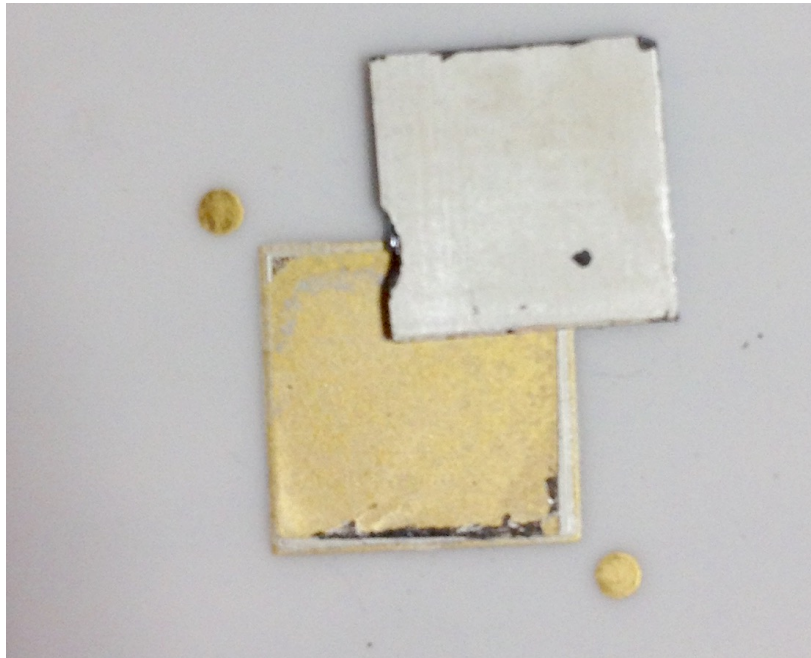


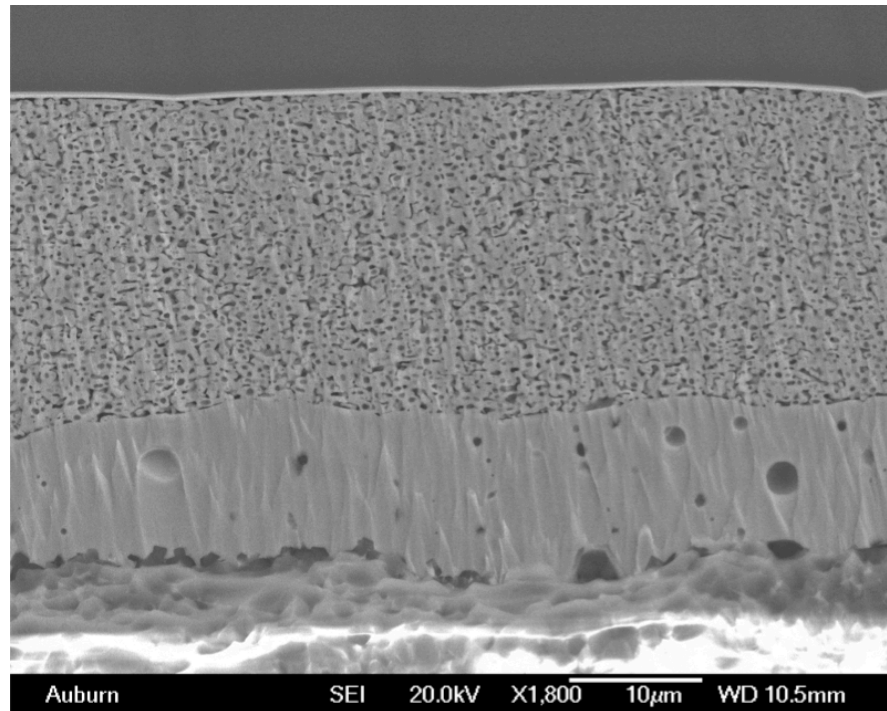
Figure 5-7. Image of fracture surface of 8 mm x 8 mm Ag metallized die with Au thick film metallized substrate.

5.5.2 Au Die Metallization, Ag Substrate Metallization

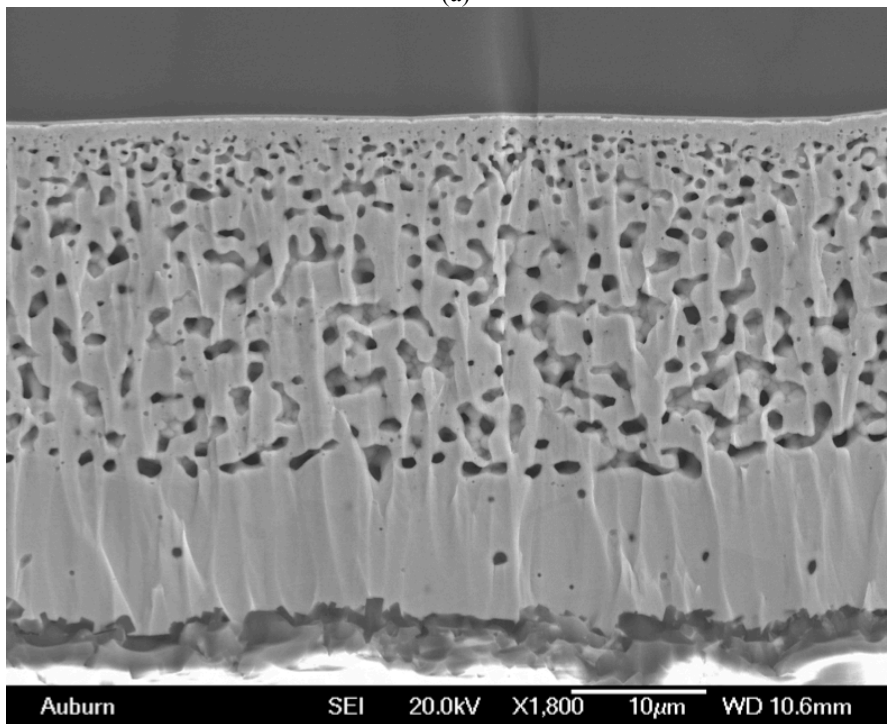
None of the Ti/Ni/Au metallized die assembled on Ag thick film metallized substrates could be sheared when the maximum force of 100 kg was applied (shear strength > 15.3 MPa).

As can be seen in the cross-sectional image shown in Figure 5-8(a), the as-built sample exhibited a die attach layer with a dense microstructure. After 1 hour of aging at 300°C, the die could not be sheared. The small pores merged to form a larger pore structure as shown in Figure 5-8(b). A dense Ag layer, approximately 1 μm thick, formed at the die interface. The porous structure was not homogenous with the pore size smaller on the die side of the Ag die attach layer than on the substrate side.

The formation of a dense Ag layer at the interface to the thin film Au on the die backside was previously observed with pressureless sintering [13]. Unlike the case of pressureless sintering, no depletion layer was found adjacent to the dense Ag layer. This depletion layer resulted in low shear strengths for pressureless sintering. The proposed mechanism was rapid Ag diffusion along the exposed Au surface creating a continuous Ag layer. This consumption of Ag from the bulk resulted in a depletion layer in the case of pressureless sintering. With sintering under pressure, the Ag is significantly denser (84% versus 70%). While Ag is consumed into the dense Ag layer adjacent to the Au layer, the denser bulk Ag obtained with pressure sintering provides a sufficient supply of Ag and no depletion layer develops.



(a)

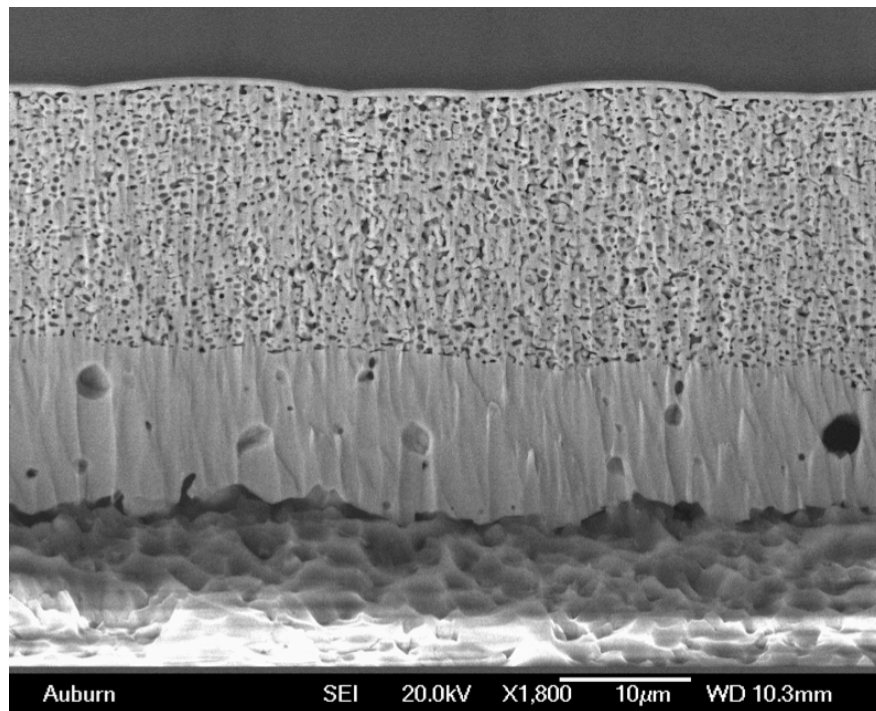


(b)

Figure 5-8. (a) Cross-sectional SEM image of die attach layer for an 8mm x 8mm Au metallized die with Ag thick film substrate that was sintered at 300°C with 7.66 MPa pressure for one minute. (b) Cross-sectional SEM image of sample that was aged at 300 °C for 1 hour.

5.5.3 Ag Die Metallization, Ag Substrate Metallization

Ag metallized die assembled on thick film Ag substrates could not be sheared. Figure 5-9 shows the cross-sectional microstructure of a pressure sintered, as-built sample. A homogenous sintered Ag die bond with a porosity of approximately 15% was observed. After aging at 300° for 1 hour, there was little change in the microstructure and the die still could not be sheared.



(a)

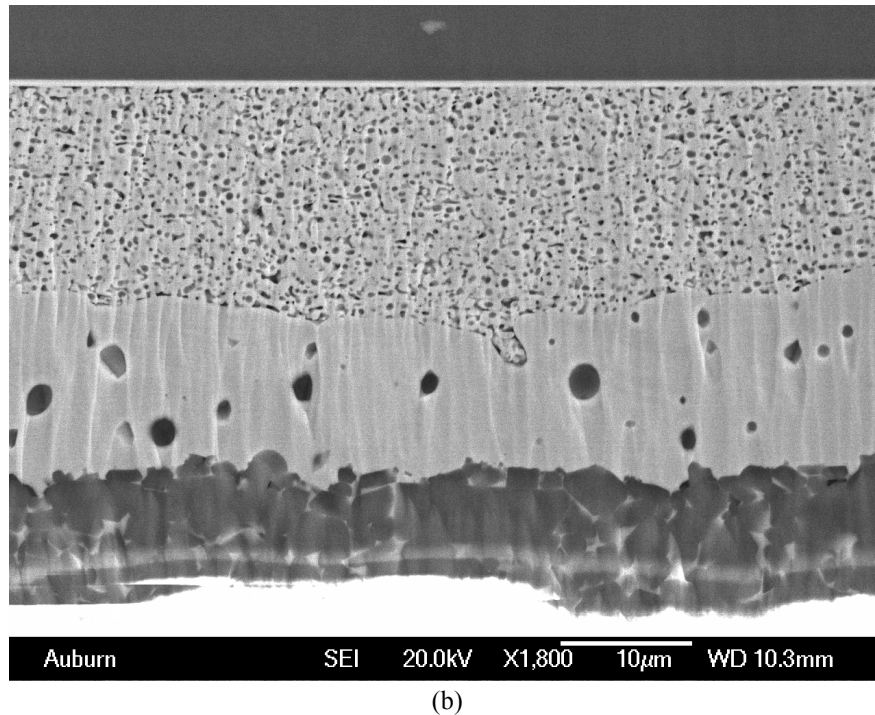
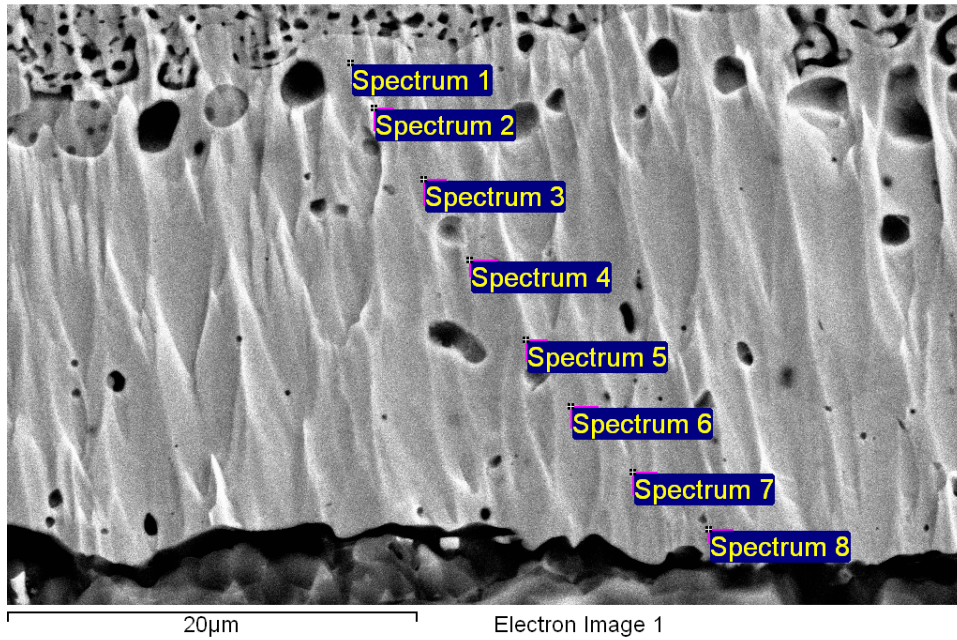


Figure 5-9. (a) Cross-sectional SEM image of die attach layer of as-built sample that was 8 mm x 8 mm Ag metallized die with Ag thick film substrate sintered at 300°C with 7.66 MPa for one minute. (b) Cross-sectional SEM image of sample aged at 300°C for 1 hour.

5.5.4 Ag Die Metallization, Au + Ag Substrate Metallization

Due to Ag migration concerns, thick film Au metallized substrates are more commonly used in high temperature electronics packaging. Au thick film for die attach pads and interconnect routing eliminates the risk of Ag migration at high temperature and is compatible with Au wire bonding. It has been shown that sintered micro-scale Ag has a reliability issue with 300° storage when assembled on Au substrates with pressureless sintering [13]. As described in section V.A above, low initial shear results were obtained for pressure assisted sintering on thick film Au substrates. To provide a “Ag” surface layer for the sintered Ag die attach, a layer of thick film Ag was printed only on the previously printed and fired Au die attach pad. The Ag was dried and fired, creating a Ag top surface on the die attach pad. The Au thick film pattern

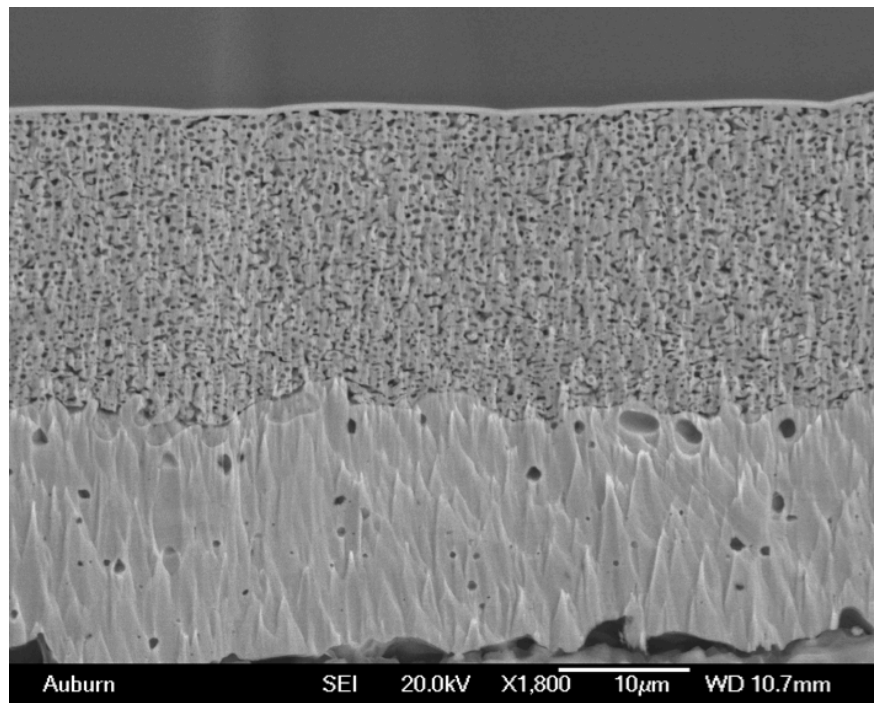
was 16 mm x 16 mm; the Ag thick film pattern was 8 mm x 8 mm. After 850 °C firing for 10 minutes, the 8 mm x 8 mm die pattern of Au + Ag thick film showed signs of interdiffusion. As shown in Figure 5-10, the energy dispersive x-ray spectroscopy (EDS) reveals the results of Au-Ag interdiffusion. The Ag does not completely diffuse through the Au layer.



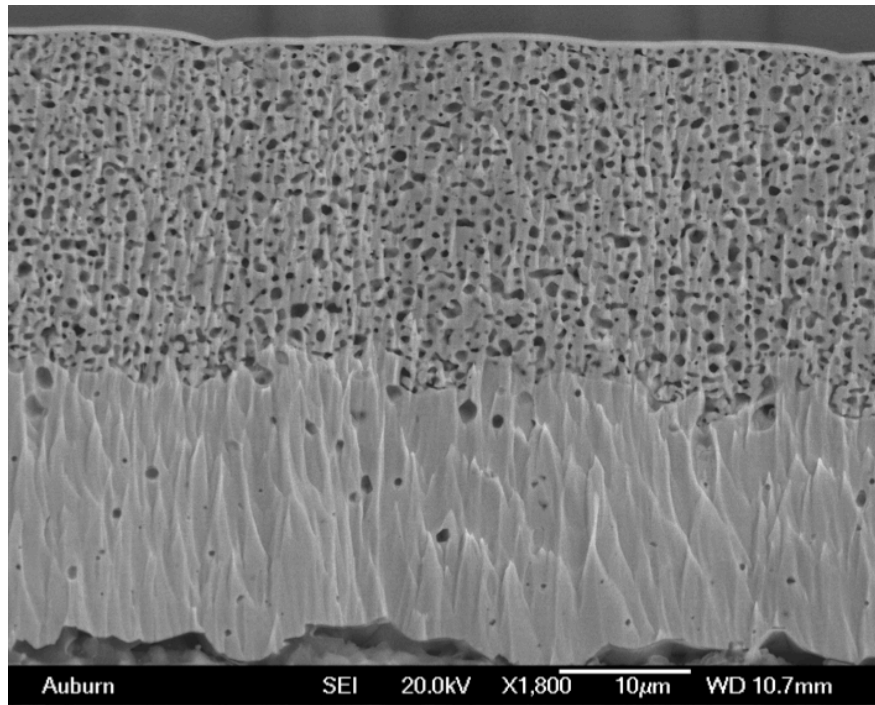
Spectrum	Ag	Au	Total
Spectrum 1	45.87	54.13	100.00
Spectrum 2	47.82	52.18	100.00
Spectrum 3	46.56	53.46	100.00
Spectrum 4	44.65	55.35	100.00
Spectrum 5	44.48	55.52	100.00
Spectrum 6	48.45	51.55	100.00
Spectrum 7	0.00	100.00	100.00
Spectrum 8	0.00	100.00	100.00

Figure 5-10. SEM image and EDS elemental analysis of Au + Ag thick film layer of an as-built sample. The spectra are given in weight percent.

Die assembled on the Au + Ag substrates could not be sheared after a one-minute pressure-assisted sintering process, nor after one hour aging at 300°C. In the cross section shown in Figure 5-11, the sintered Ag layer had a homogeneous porous structure. It is clear that the Ag grains in the die attach layer grew somewhat larger during the 1 hour aging at 300°C. The pore size increased, while the number decreased with aging: the pore area percentage remained constant as determined from image analysis. No depletion region or continuous, dense Ag layer was observed.



(a)



(b)

Figure 5-11. (a) Cross-sectional SEM image of die attach layer of as-built sample that was 8 mm x 8 mm Ag metallized die with Au + Ag thick film substrate sintered at 300°C with 7.66 MPa for one minute. (b) Cross-sectional SEM image of sample aged at 300°C for 1 hour.

5.6 Conclusion

A pressure-assisted Ag sintering process has been developed for large die (8 mm x 8 mm) and small die (3 mm x 3 mm). Compared to a no-pressure process, the porosity percentage decreased from 30% to 15% using a low pressure, one-minute sintering process for both large and small die. To use sintered Ag on Au thick film metallized substrates, printing of a thick film Ag layer on top of the Au die attach pad has been explored and was shown to increase die shear strength. Pressure-assisted, sintering of micro-scale Ag die attach paste with Ag die metallization and Ag or Au + Ag thick film substrate metallization is a viable assembly process for high temperature die attach.

CHAPTER 6 RELIABILITY OF PRESSURE SINTERING

Low temperature Ag sintering provides a lead-free die attachment compatible with high temperature (300°C) power electronics applications. The reliability of sintered Ag die attach for Si and SiC die has been studied on both thick film substrates for lower power applications and direct bond copper (DBC) substrates for higher power applications. Pressureless and low pressure sintering were evaluated. Sintering with low pressure yielded lower porosity (15-17%) versus pressureless sintering (~30%). Reliability was evaluated with thermal aging (300°C) and thermal cycling (-55°C to +300°C) tests. The reliability test results showed good die shear strength reliability with Ag metallized die and substrates, but the shear strength degraded if the die or substrate metallization were Au. The thermal cycle reliability on DBC substrates was limited by failure at the Cu-to-alumina interface over the wide temperature range.

6.1 Literature Review of Reliability for sintered Ag

Low temperature Ag sintering technology is a promising method for high performance lead-free die attachment. Due to its high thermal and electrical conductivity and high melting point, sintered Ag die attach has received much attention for assembly of power modules and for high temperature applications.

The properties of the sintered silver joint have been extensively investigated, but long term reliability has not been confirmed. Ning etc. [123] conducted both thermal aging and cycling test with 2.7 x 2.7 mm² SiC die on DBC substrate. The initial shear strength of 25 MPa decrease to 20 MPa after aging at 250°C for 500 hours. After 800 cycles (-55°C to 250°C), the die shear test value dropped from 25 MPa to 11 MPa. Navarro etc. [124] assembled 2.8 x 2.8 mm² Au metallized SiC Schottky diodes and Si dummy die with Cu substrate by using 3 MPa or

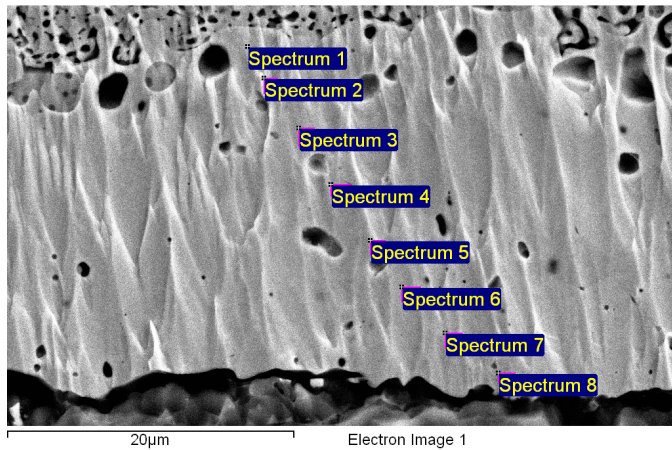
7 MPa sintering process. After 100-200 cycles of $-65^{\circ}\text{C}/275^{\circ}\text{C}$, the shear strength degraded rapidly to 0.1 kgf.

This paper examined the reliability of sintered Ag for both large $8 \times 8 \text{ mm}^2$ and small $3 \times 3 \text{ mm}^2$ die attach on various finishes and substrates by pressure or pressureless Ag sintering process. To achieve high viable and reliable die attach (>2000 hours thermal aging at 300°C and >1000 cycles thermal cycling $-55^{\circ}\text{C}/300^{\circ}\text{C}$), the preferable metallization, assembly process and packaging material selection were reported.

6.2 Test vehicles (Materials/Substrates)

6.2.1 Substrate Metallization

Both thick film and direct bond copper (DBC) metallized alumina substrates were used. The thick film substrates were $5.08 \text{ cm} \times 5.08 \text{ cm} \times 0.64\text{mm}$ thick, 96% alumina (Al_2O_3) substrates purchased from Coorstek. The substrates were metallized with three different thick film conductor options. For Au or Ag metallized substrates, one layer of Au or Ag thick film conductor paste was printed onto the substrates and dried at 150°C for 10 minutes, then fired at a peak temperature of 850°C for 10 minutes. Die attach pads were fabricated for both $3 \text{ mm} \times 3 \text{ mm}$ die and $8 \text{ mm} \times 8 \text{ mm}$ die. The third group of substrates was first metallized with thick film Au ($16 \text{ mm} \times 16 \text{ mm}$ pads) using the same thick film deposition procedure. The use of Au thick film for the die attach pad and interconnect routing eliminates the risk of Ag migration at high temperature and is compatible with Au wire bonding. However, to provide a “Ag” surface layer for the sintered Ag die attach, a layer of thick film Ag was printed ($8 \text{ mm} \times 8 \text{ mm}$ pads) on the previously printed and fired Au die attach pad. The Ag was dried and fired, creating a Ag-bearing top surface on the die attach pad. Figure 6-1 shows a cross section and elemental analysis by Energy Dispersive Spectroscopy (EDS).



Spectrum	Ag	Au
Spectrum 1	45.9	54.1
Spectrum 2	47.8	52.2
Spectrum 3	46.6	53.4
Spectrum 4	44.6	55.4
Spectrum 5	44.5	55.5
Spectrum 6	48.5	51.5
Spectrum 7	0.0	100
Spectrum 8	0.0	100

Figure 6-1. SEM image and EDS elemental analysis of Au + Ag thick film layer of an as-built sample. The spectra are given in weight percent.

DBC substrates for high power applications were also examined for Ag sintering die attach. Three types of metallization were deposited on DBC substrate by electroplating: Ni (6µm)/Ag (4µm); Ni (6µm)/Pd (0.5µm)/Ag (0.23µm); and Ni (6µm)/Pd (0.5µm)/Au (0.076µm). For the high temperature aging test, DBC alumina substrates with 203µm thick copper were used. For the thermal cycling test, DBC alumina substrates with thinner 127µm copper were patterned to form 12mm x 12mm square pads with dimples for better substrate thermal cycling reliability [125]. The dimples were proven to enhance attachment and increase the number of cycles to failure [126], by decreasing the stress density at the singularities.

6.2.2 Die Metallization

Si wafers and SiC wafers were metallized on the backside by e-beam evaporation. In the case of TiW, the TiW was sputtered without breaking vacuum. For Au metallized die, Ti (50 nm), TiW (50 nm), Au (200 nm) were sequentially deposited. Ag metallized die were fabricated by sequential deposition of Ti (50 nm), Ni (200 nm), and Ag (300 nm). The wafers were diced into 8 mm x 8 mm test die and 3 mm x 3 mm test die. SiC die were used for high power DBC substrate attachment and 3 mm x 3 mm die attachment.

6.3 Assembly and Characterization Process (Process summary)

6.3.1 Ag Paste Deposition

The die attach material was Ag sintering paste containing micrometer-size Ag particles. A 50 μ m thick laser cut stencil was used to print the silver sintering paste on the metallized substrate with an MPM semiautomatic printer using a metal squeegee.

6.3.2 Pressureless Sintering Process [116]

After printing the Ag paste, test dies were placed in the paste within 10 minutes. A Palmour Products Model 3500 pick and place system was used for controlled die placement. After the die placement, the assembled test vehicle was sintered at 300°C. The oven was programmed to rise to peak temperature at a ramp rate of 10°C/min and dwell for one hour. No pressure was applied during sintering in air.

6.3.3 Fast Pressure-Assisted Sintering Process [127]

The fast, pressure sintering process included three stages: pre-dry, die placement and sintering. The goal of the pre-drying process was to remove solvent from the paste, increasing the viscosity to prevent paste squeeze-out during the pressure application step. After the Ag sintering paste was printed, the substrates with fresh patterns were placed in to a 150°C preheated

oven to carry out the one minute pre-dry process. The drying time was defined as the time from closing the oven door until opening the oven door to remove the substrate. In production, an inline oven or hotplate drying option could also be used instead of a box oven. The placement and sintering steps were accomplished with an FC150 die/flip chip bonder. The temperature was ramped at the maximum rate and a ramping force was applied to the die as it reached 300°C in 100 seconds (Figure 2). The maximum pressure was 7.6 MPa (7 kg-force for 3 mm x 3 mm die and 50 kg-force 8 mm x 8 mm die). Once 300°C and full force were achieved, 60 seconds of dwell time was initiated. After 160 seconds from cycle initiation, the cooling process was activated and the force was gradually reduced as shown in Figure 6-2.

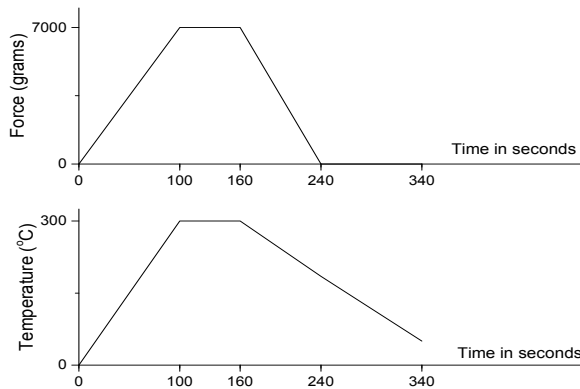


Figure 6-2. Temperature and force profile for pressure-assisted fast sintering, exhibiting a 3°C/s ramp rate and sintering/force application dwell time of 60 seconds.

6.3.4 Die Shear Testing

After being aged or thermal cycled, samples were analyzed by shear. A Dage 2400PC shear tester with a 100 kg die shear module was used for die shear testing. In some cases the die could not be sheared with the 100 kg applied force. For a 8mm x 8mm die, this corresponds to a maximum shear test limit of 15.3 MPa.

6.3.5 SEM Analysis

SEM cross sectional analysis was used to examine the microstructure of the sintered Ag layers. Samples were diced into two pieces along the center of the die. For samples known to have low shear strength, the die was encapsulated with epoxy prior to dicing to maintain the integrity of the die attach. Cross sections were then prepared for SEM examination utilizing a Gatan ion milling machine with an Ion Tech 22cm Linear Ion Gun.

6.4 Reliability of pressureless sintering

6.4.1 Thermal Aging and Thermal Cycling Test Conditions

In order to evaluate the reliability of the different substrates, metallizations and process options, samples were subjected to two test conditions: aging at 300°C in air and thermal cycling from -55°C to +300°C. In the case of thermal cycling, the Delta Design oven was controlled with Labview to execute continuous cycles with dwell times of 10 minutes at -55°C and 300°C (Figure 6-3). The cooling stage was achieved by purging with gaseous nitrogen from a liquid nitrogen tank.

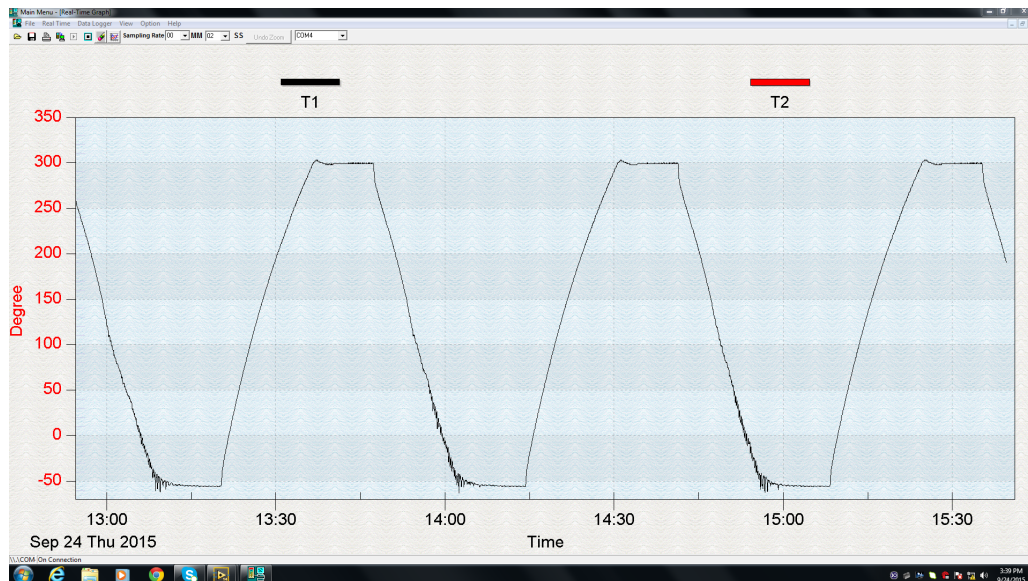


Figure 6-3. Thermal cycling temperature profile.

6.4.2 Thick Film Substrates: Aging

In the previous study [116], Au thick film metallized substrates or Au metallized Si die were found to have a reliability issue with sintered Ag during the 300°C thermal aging test. The mechanism was sintered Ag surface diffusion along the Au metallization surface. Ag metallization on the substrate and the die had good reliability with sintered Ag, as 8000 hours of thermal aging at 300°C did not exhibit degradation of the die shear strength. PdAg thick film substrate metallization was another viable solution, which was evaluated for 2000 hours of aging test at 300°C.

To address the degradation in shear strength of sintered Ag on Au thick film metallization, a Au + Ag thick film die attach pad was evaluated. The Ag metallized Si die (8 mm x 8 mm) were sintered without pressure on the Au + Ag metallized substrates at 300°C for 1 hour. The die could not be sheared for the as-built samples. After aging for 2000 hours at 300°C, die still cannot be sheared due to the 100 kg shear module limit. The cross section of 1500 hours aged is shown in Figure 6-4. There is an increase in pore size, but no dense Ag layer or depletion region was found.

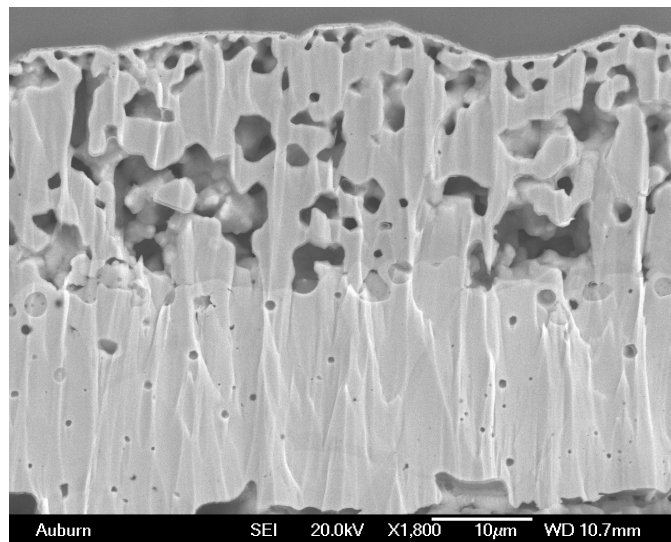
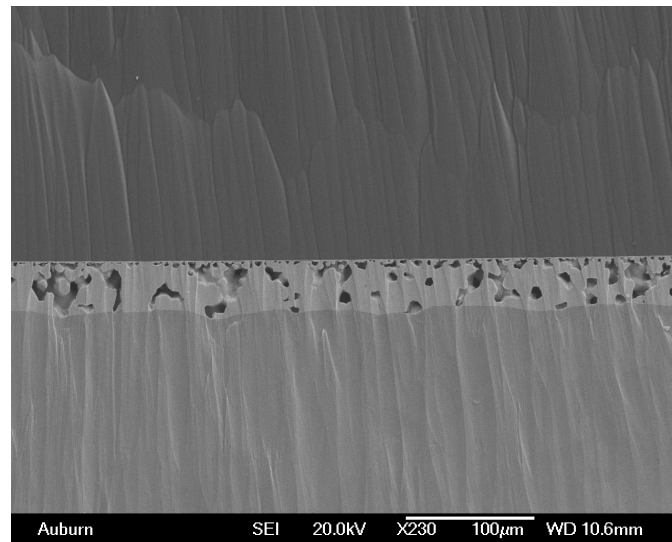


Figure 6-4. Cross sectional SEM image of die attach layer for 300°C 1500 hours aged sample with Ag metallized Si die on Au+Ag metallized substrate.

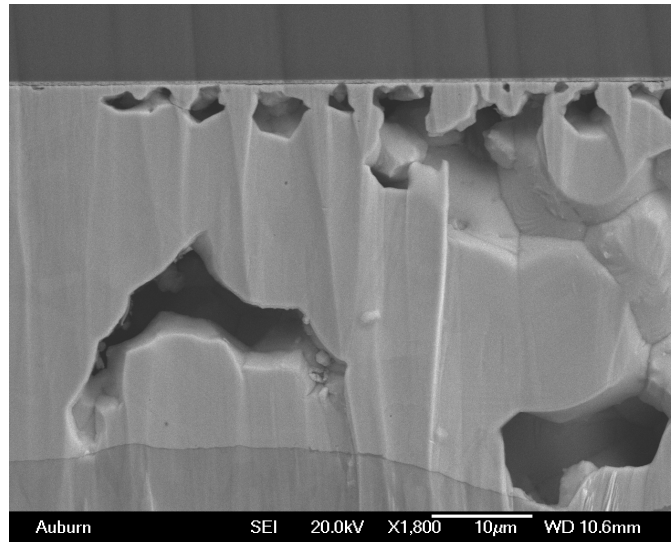
6.4.3 DBC: Aging

Ag SiC die metallization, Ni-Ag DBC metallization

DBC substrates with Ni (6 μm)/Ag (4 μm) were sintered without pressure using Ti/Ni/Ag metallized SiC die (8 mm x 8 mm). As-built the die could not be sheared. After aging at 300°C for 2000 hour, the die still could not be sheared. After aging, homogenous porous sintered Ag die bond was observed (Figure 6-5). The pore size had increased, but the pore percentage had remained nearly constant.



(a)

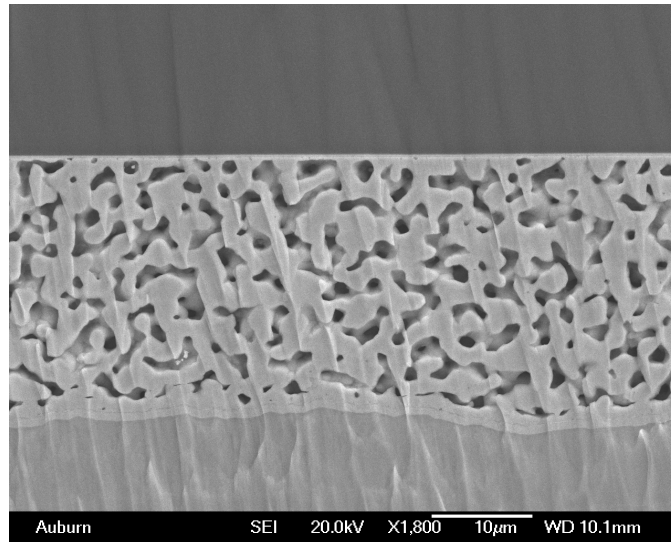


(b)

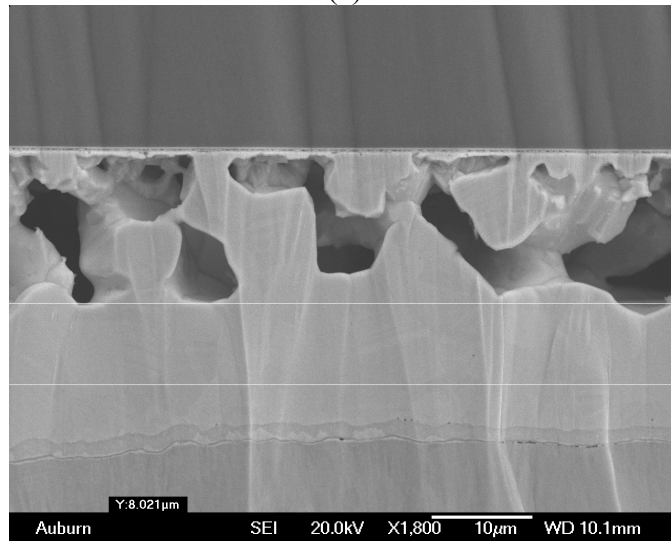
Figure 6-5. Cross sectional SEM image of die attach layer after 2000 hours aging at 300°C. Sample was Ag metallized SiC die on Ni/Ag metallized DBC substrate (a) overview, (b) close-up

Ag SiC die metallization, Ni/Pd/Ag DBC metallization

Ti/Ni/Ag metallized SiC die (8 mm x 8 mm) sintered without pressure on Ni/Pd/Ag metallized DBC substrates could not be sheared as-built. Figure 6-6(a) shows the cross-sectional microstructure of a pressureless sintered, as-built sample. The die could not be sheared after 2000 hours aging at 300°C. The small pores merged to form a larger pore structure as shown in Figure 6-6(b). The sintered Ag diffused to the Ni/Pd/Ag metallization side, forming a thick non-porous Ag layer on the substrate side and a region with a higher void percentage on the die side. No depletion region formed and the shear strength remained >15.3MPa (limit of shear test module).



(a)



(b)

Figure 6-6. (a) Cross-sectional SEM image of die attach layer of sample that was 8mm x 8mm Ag metallized die with Ni/Pd/Ag metallized DBC substrate sintered at 300°C 1 hour without pressure. (b) Cross-sectional SEM image of sample aged at 300°C for 2000 hours.

6.4.4 Thick Film metallization: Thermal cycle

8mm x 8mm Ag metallized Si die were sintered (300°C for 1 hour) without pressure on thick film Ag metallized ceramic substrates. None of the as-built samples could be sheared. After 1000 thermal cycles from -55°C to +300°C, the die still could not be sheared. The cross sectional

SEM image of die attach layer is shown in Figure 6-7. The morphology of the sintered Ag is different than for high temperature aged samples.

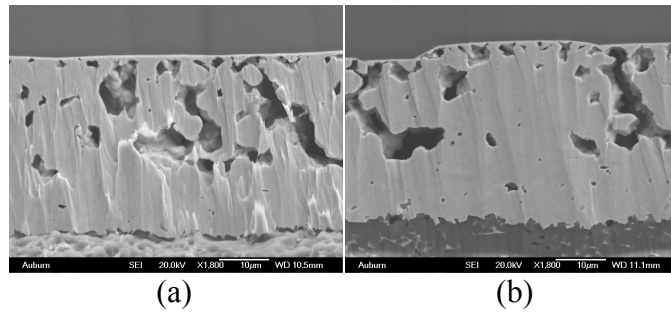


Figure 6-7. Cross-sectional SEM image of die attach layer of sample with 8mm x 8mm Ag metallized Si die and Ag thick film metallized substrate after cycles from -55°C to 300°C (a) 750 cycles, (b) 1000 cycles.

6.4.5 DBC: Thermal cycle

Ti/Ni/Ag metallized SiC die (8 mm x 8 mm) sintered without pressure on Ni/Ag metallized DBC substrates could not be sheared as-built. Even with patterned dimples and reduced Cu thickness, the copper-to-ceramic interface started to fail by 100 cycles from -55°C to 300°C. The fracture started from the edge of the substrate where the highest stress was located (Figure 6-8).

Due to the curve of copper, the shear tool could not fully contact the die bottom to conduct the die shear test. None of the die detached after 100 cycles, while after 300 cycles, 49 out of 72 die fell off from patterned copper without applied force. As shown in Figure 9 no weak point or depletion region was observed. Compared to thick film substrate, sintered Ag with DBC has lower reliability under thermal cycling due to substrate failure of the copper-to-alumina.

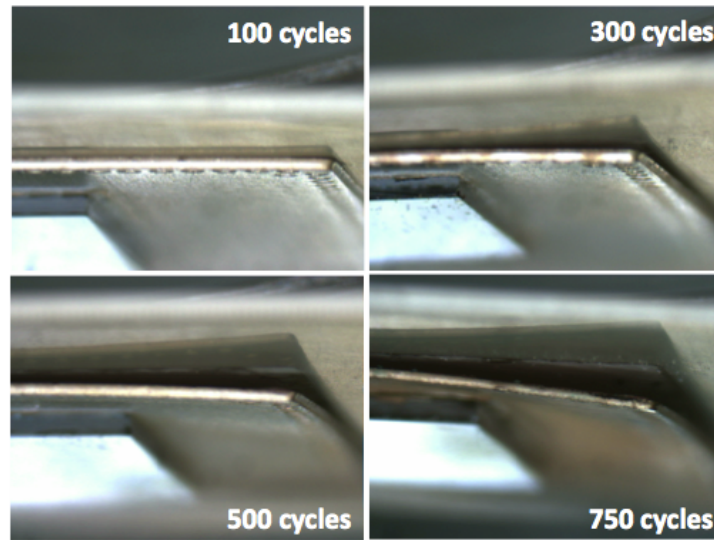


Figure 6-8. DBC substrate showing progressive failure of Cu-to-alumina interface with increasing number of thermal cycles.

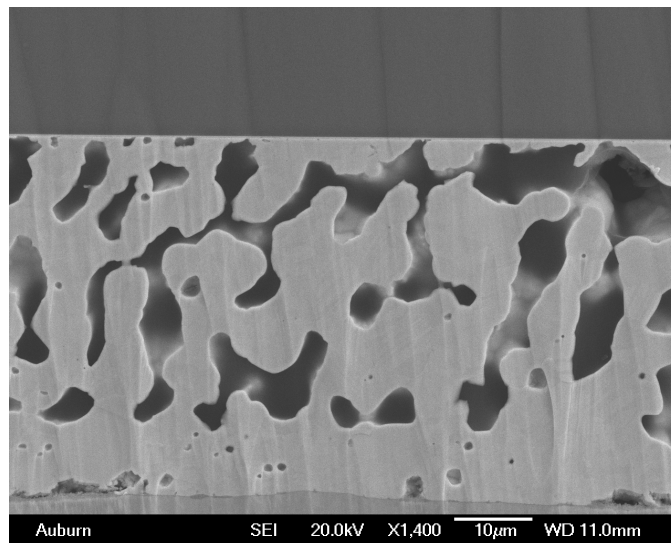


Figure 6-9. Cross-sectional SEM image of die attach layer of sample that was 8mm x 8mm Ag metallized SiC die with Ag metallized DBC substrate after 300 cycles from -55°C to 300°C.

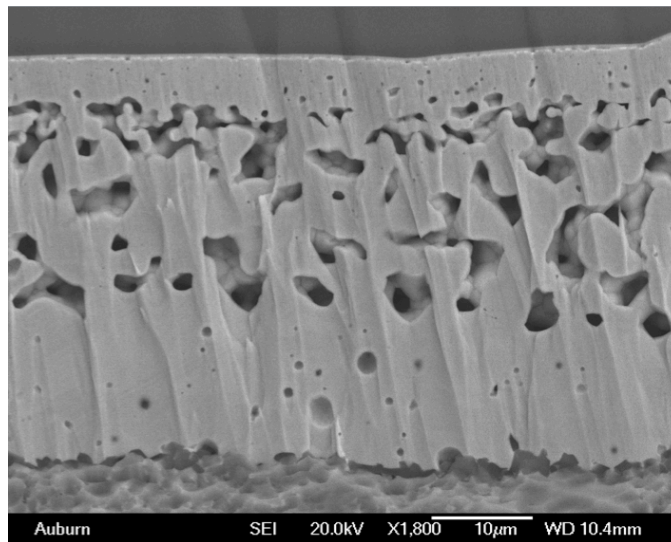
6.5 Reliability of pressure sintering

All sample groups were assembled using a 300°C, one-minute pressure-assisted (7.6 MPa) sintering process.

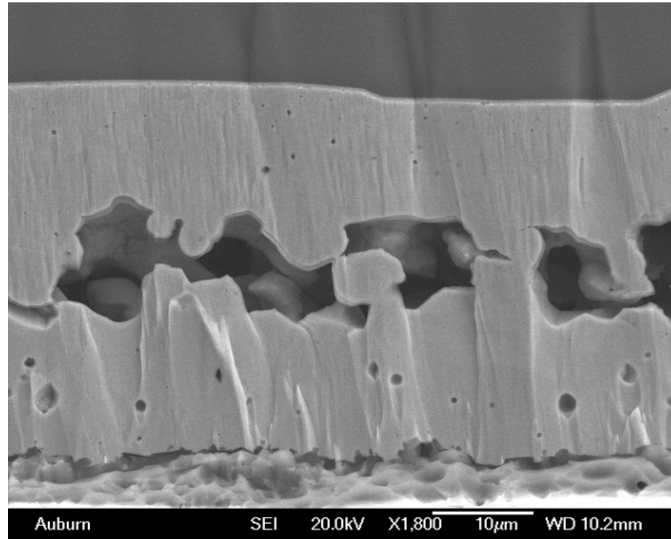
6.5.1 Thick Film metallization: Aging

Au Die Metallization, Ag Substrate Metallization

For Au metallized die with Ag thick film substrates, after 24 hours, the pore size increased and a non-porous layer of sintered Ag ($\sim 6 \mu\text{m}$) formed at the Au metallized die side of the attach layer as shown in Figure 10(a). This phenomenon was also observed in pressureless assembled samples. However, compared to the pressureless assemblies, there was no depletion region observed with pressure-assisted assembly and the continuous, non-porous Ag layer was much thicker on the die side after 24 hours aging. The die could not be sheared until 500 hours, when the shear strength dropped to 12.8 MPa. In the cross section of the 500 hours aged sample (Figure 6-10(b)), a very thick, dense layer of Ag had formed on the die side of the sintered Ag layer and a significant void/depletion region was formed near the substrate side. The lower shear strength was a result of this void/depletion layer.



(a)

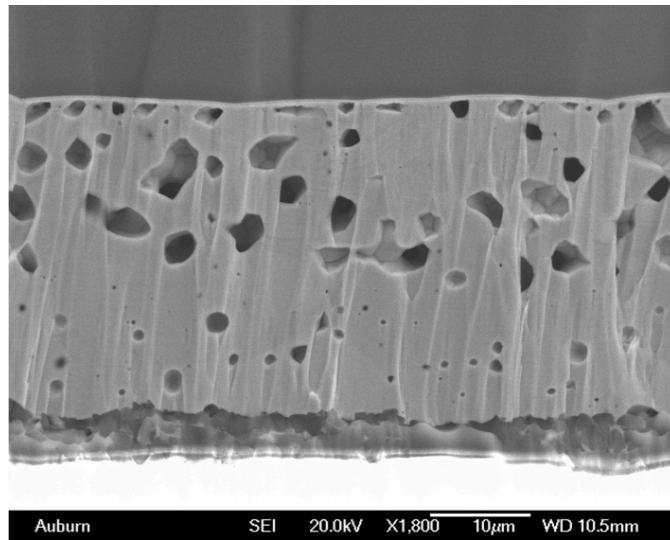


(b)

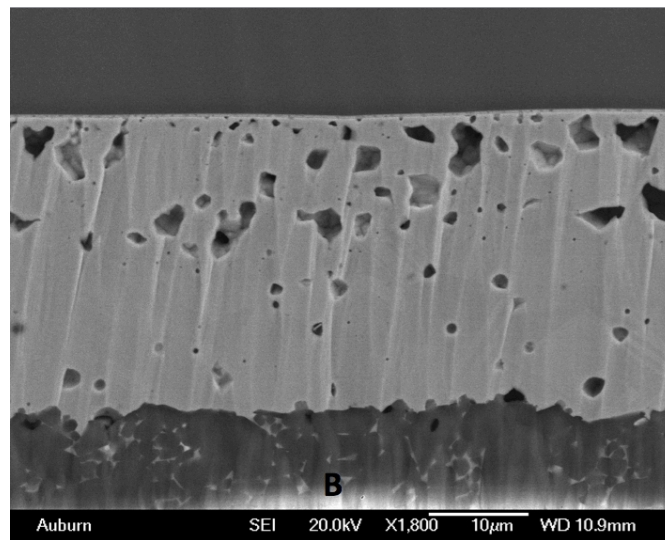
Figure 6-10. Cross-sectional SEM image of die attach layer of sample that was 8mm x 8mm Au die with Ag substrate sintered at 300°C with 7.6 MPa pressure for one minute and aged at 300°C for (a) 24 hours, (b) 500 hours.

Ag Die Metallization, Ag Substrate Metallization

For the Ag metallized die and substrate combination, the die could not be sheared (the shear strength was higher than 15.3 MPa) after 2000 hours of aging at 300°C. The microstructure of samples after 24 hour aging and 1500 hours of aging is shown in Figure 6-11. The morphology of the porous structure remained stable after 24 hours.



(a)



(b)

Figure 6-11. Cross-sectional SEM image of die attach layer of sample that was 8mm x 8mm Ag die with Ag substrate sintered at 300°C for one minute and aged at 300°C for: (a) 24 hours, (b) 1500 hours.

Since the 8 mm x 8 mm dies could not be sheared, 3 mm x 3 mm die were assembled and aged at 300°C. The shear strength data was stable and consistent, remaining at approximately 72 MPa during aging (Figure 6-12). The porous structure of the small die samples was similar to the larger die (8 mm x 8 mm) samples. The porosity of the sintered Ag area was calculated using

Matlab code from cross section SEM images. Three 3 mm x 3 mm die samples were prepared and the mean porosity was calculated to be 17%, which was similar to the 8 mm x 8 mm die samples (15%). The tolerance of the porosity calculation is estimated to be $\pm 2\%$ because of the surface topology, definition of boundary and image quality of the SEM images. However, it does provide a relative comparison of densification among different sintered Ag die attachment. Other research groups have encountered the same porosity accuracy issue [128, 129].

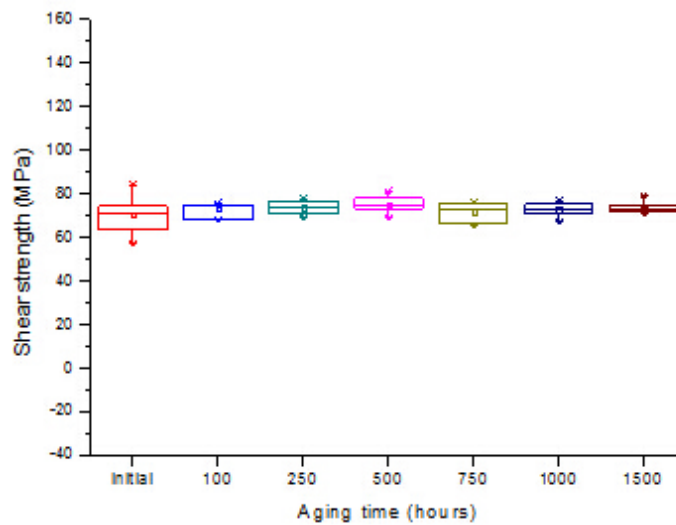
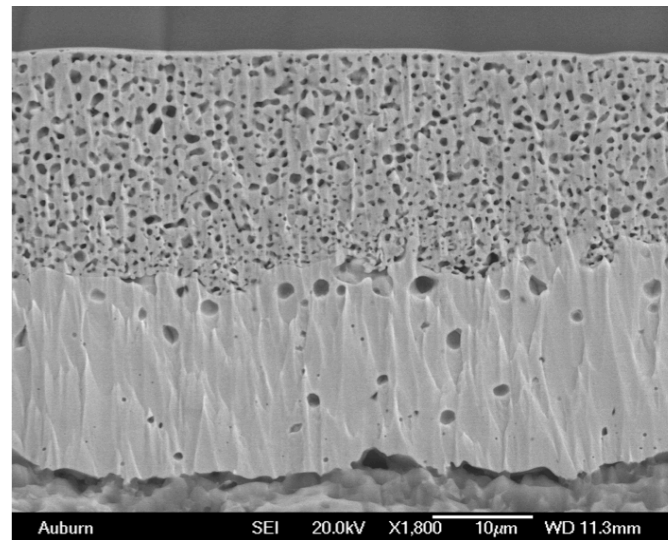


Figure 6-12. Shear strength of 3 mm x 3 mm Ag metallized die with Ag thick film substrate pressure-assisted (7.6 MPa) sintered at 300°C for one minute and aging time from initial to 1500 hours.

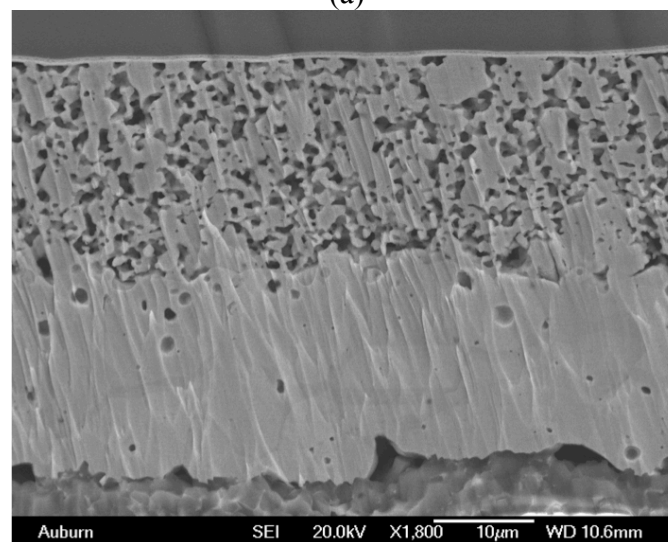
Ag Die Metallization, Au + Ag Substrate Metallization

After 2000 hours of 300°C aging, all the dies (8 mm x 8 mm) on the Au + Ag thick film substrates could not be sheared from the substrates. Figure 6-13 (a) shows the cross section of a sample after 24 hours at 300°C. Figure 6-13 (b) is a SEM cross-section image after 2000 hours at 300°C. While the pore size increased somewhat and the structure was significantly different from

the Ag thick film sample after 1500 hours (Figure 6-11 (b)), no depletion region was observed. This is consistent with the inability to shear the die after 2000 hours at 300°C.



(a)



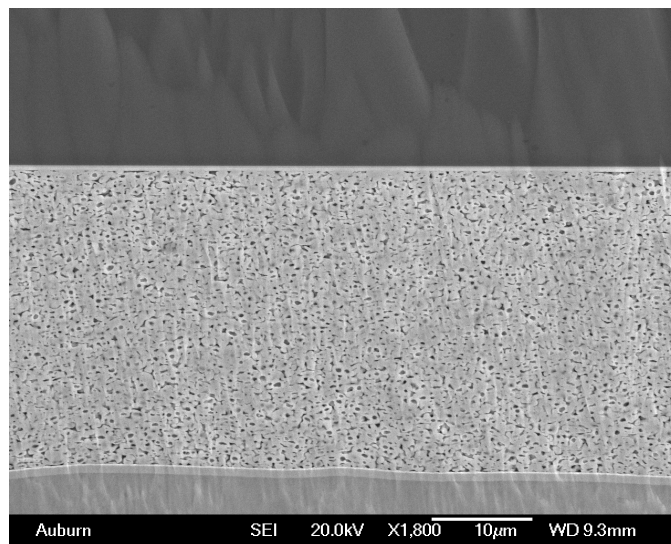
(b)

Figure 6-13. Cross-sectional SEM image of die attach layer of 8mm x 8mm Ag metallized die with A Ag thick film substrate pressure-assisted (7.6 MPa) sintered at 300°C for one minute and aged at 300°C for: (a) 24 hours. (b) 2000 hours.

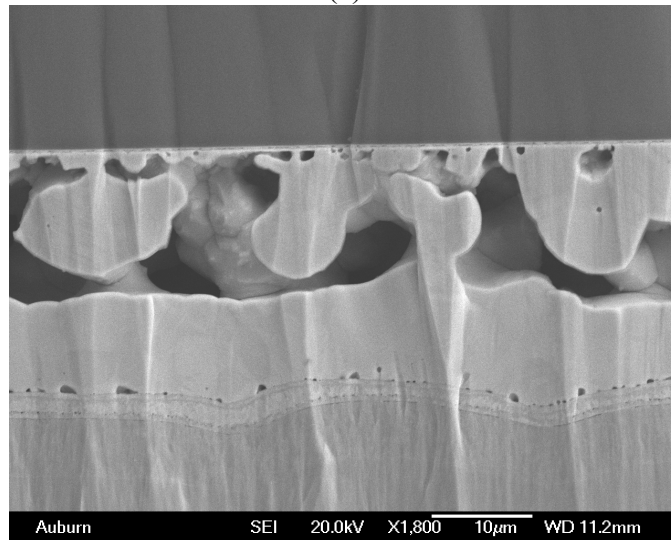
6.5.2 DBC: Aging

Ag die metallization + Ni/Pd/Au DBC metallization

8mm x 8mm Ag metallized SiC die were pressure sintered on Ag metallized DBC substrates. The die could not be sheared as-built, but after 250 hours aging at 300°C, the shear strength dropped to 4.02 MPa. In the cross section of the 250 hours aged sample (Figure 6-14 (b)), a very thick, dense layer of Ag had formed on the Au metallized DBC substrate side of the sintered Ag layer and a porous depletion region formed adjacent to the non-porous Ag layer. The lower shear strength was a result of this porous depletion layer, which was a weak attachment.



(a)



(b)

Figure 6-14. Cross-sectional SEM image of die attach layer of 8mm x 8mm Ag metallized SiC die with Ni/Pd/Au metallized DBC substrate pressure-assisted (7.6 MPa) sintered at 300°C for one minute. (a) As-built, (b) Aged for 250 hours at 300°C.

Ag die metallization + Ag DBC metallization

8mm x 8mm Ag metallized SiC die were pressure-assisted assembled with Ag metallized DBC substrates. The die could not be sheared both for as-built samples and samples aged for 2000 hours 300°C. The cross-sectional microstructure of 2000 hours aged sample is shown in Figure 6-15. The pore size has grown, but the pore percentage is relatively unchanged.

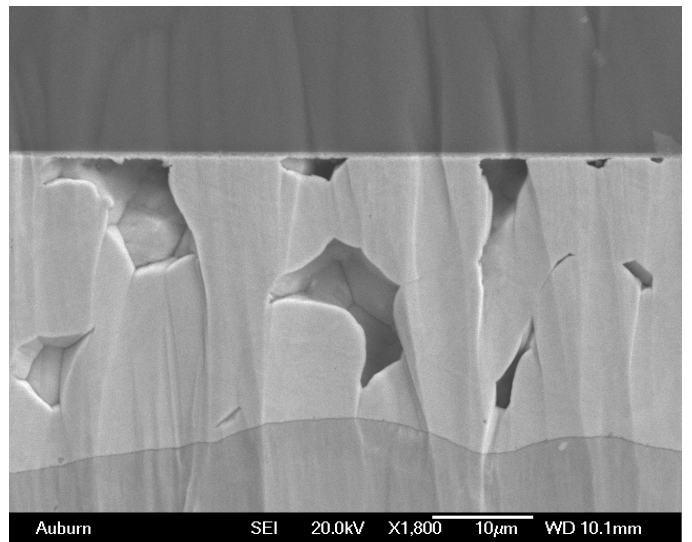


Figure 6-15. Cross-sectional SEM image of die attach layer of 8mm x 8mm Ag metallized SiC die with Ag metallized DBC substrate pressure-assisted (7.6 MPa) sintered at 300°C for one minute and aged at 300°C for 2000 hours.

6.5.3 DBC: Thermal cycling

8mm x 8mm Ag metallized SiC die were sintered with pressure on Ag metallized DBC substrates. The die could not be sheared after 500 thermal cycles over the temperature range from -55°C to 300°C. After 750 cycles, 29 out of 38 die fell off from patterned DBC substrate. Due to the DBC substrate failure at the Cu-to-alumina interface, the shear tool could not fully

contact the die edge to conduct the shear testing. Compared to the failure of pressureless sintering after 300 cycles, the pressure-assisted showed higher resistance to thermal cycling and longer lifetime even as the DBC substrate failed.

6.6 CONCLUSION

Au metallized surfaces (die or substrate) had lower die shear strength with sintered Ag after short-term thermal aging at 300°C. By applying pressure during sintering, the time-to-failure was increased compared to pressureless sintering, however, failure still occurred. To achieve good high temperature reliability for thick film Au metallized substrates, a new metallization combination, Au+Ag, was demonstrated for the die attach pad.

Ag metallized Si die on Ag metallized thick film substrates with pressure had high shear strength after 2000 hours at 300°C. Ag metallized SiC die on Ag metallized DBC substrates assembled with and without pressure also had high shear strength after 2000 hours at 300°C.

Ag metallized Si die with Ag thick film metallized ceramic substrate exhibited good reliability during thermal cycling from -55°C to 300°C. Large, 8 mm x 8 mm die could not be sheared after 1000 cycles. For DBC substrates with dimples, failure near the Cu-to-ceramic interface were observed at the corners of the Cu die attach pads after 100 cycles. In the case of pressureless sintering, 68% die fell off from substrate after 300 cycles. As to the samples assembled by pressure sintering, die was fastened until 750 cycles. Failure of the die attach was driven by the substrate failure.

CHAPTER 7 CONCLUSION AND FUTURE WORK

7.1 Pressureless Sintering

A pressureless Ag sintering process has been demonstrated for larger die (8 mm x 8 mm). While a higher void percentage was observed compared to a pressure process, for non-power device applications the increased porosity is less of an issue. Degradation of shear strength was observed with high temperature sintering and high temperature aging of samples with Au metallization on the die, the substrate or both. Ag surface diffusion was proposed to explain this phenomenon. We observed the formation of a Ag depletion region in the die attach sintered Ag layer with 250°C and 300°C aging and corresponding low shear strength was found with Au metallized die. With storage at 200°C, the depletion region did not form and the shear strength remained high for Au metallized die on thick film Au substrates after 1500 hours.

For Ag metallized die and Ag or PdAg thick film metallized, high shear strengths were maintained after high temperature aging at 300°C. Pressureless sintering of micro-scale Ag die attach with Ag die metallization and Ag and PdAg thick film metallization is a viable assembly process for high temperature die attach of non-power device. For power devices, the impact of the increased porosity on electrical and thermal performance must be determined.

7.2 Component Attach with Pressureless sintering

A post-print drying method was developed to reduce Ag paste squeeze-out during resistor placement and obtain a sintered Ag thickness of approximately 20µm.

While the PtAu terminated resistors had good initial shear force results, the shear force decreased with 300°C aging on both Au and Ag thick film metallized substrates. The degradation in shear force was more rapid on Au metallized substrates.

The PdAg terminated resistors with a plated Ni/Au finish, had low shear forces as-built. With Au substrates, increasing the sintering temperature resulted in lower shear force.

The PdAg terminated resistors results varied with supplier. In the case of Supplier A, the failure mode was at the resistor termination-to-ceramic body interface. With Supplier B this failure mode did not occur. No degradation in resistor shear force occurred with PdAg terminated resistors (Supplier B) after 1500 hours at 300°C on Ag thick film substrates. Tests with PdAg and Au+Ag thick film substrates are still underway.

Pressureless sintered Ag resistor attach is a viable approach for high temperature applications, but selection of resistor termination and substrate metallizations is critical for reliability.

7.3 Pressure Sintering

A low temperature, pressure-assisted fast sintering process was developed. Process optimization decreased the sintering time to one minute, which allowed the use of an FC150 thermocompression flip chip/die bonder for automated die attach instead of a hydraulic press, improving the manufacturability.

The porosity was decreased from 30% to 15% with application of a low pressure (7.6MPa) during a one minute sintering process. The shear strength for a 3 mm x 3 mm die was 70 MPa and the 8 mm x 8 mm die could not be sheared off due to a 100 kg shear module force limit.

Both the Ag and Au metallizations (die and substrate) were studied. For Ag metallized die assembled on Au thick film metallized substrates, the mean shear strength of as-built samples was as low as 7 MPa, with all the failures on the Au thick film surface. None of the Ti/Ni/Au metallized die assembled on Ag thick film metallized substrates could be sheared when the

maximum force of 100 kg was applied. A dense Ag layer approximately 1 μm thick formed at the die interface after aged for one hour. The porous structure was not homogenous with the pore size smaller on the die side of the Ag die attach layer than on the substrate side. The Ag metallized die assembled on thick film Ag substrates could not be sheared.

Furthermore, a new substrate metallization combination was found that allows the use of Au thick film metallized substrates.

7.4 Future Work

In the case of PtAu resistor attachment, the post-printing dry process increased the thickness of the sintered Ag layer, which mitigated the degradation of bonding strength on Au metallized substrate with aging time up to 250 hours. However, the post-printing dry did not play an obvious effect on the shear strength of PtAu resistor on Ag metallized substrates. For PdAg terminated resistor attach, the necessity for the post-printing dry needs to be confirmed through control experiments. Thermal cycle testing is recommended to study the reliability of increased component standoff height.

Another interesting topic is the sintered Ag with Pd finish on the DBC. After 2000 hours aging, a thick non-porous thick Ag layer (approximately 10 μm) was found adjacent to the Pd metallization on DBC without a depletion region. The shear strength was still above 13.5 MPa (cannot shear), whereas the actual bonding strength is unknown. Also a longer aging storage (>2000 hours) is expected to show all of the sintered Ag diffused to the Pd metallization side. So smaller size die attach needs to be tested to verify the influence of microstructure change on the shear strength.

REFERENCES

- [1] F. P. McCluskey, T. Podlesak, R. Grzybowski “Overview of high temperature electronics”, *High temperature electronics*, CRC press, 1996, ch. 1, sec 1, pp. 1-2.
- [2] J. Watson, G. Castro, “High-Temperature Electronics Pose Design and Reliability Challenges”, *Analog Dialogue* 46-04, April, 2012
- [3] [http://www.eia.gov/forecasts/aeo/pdf/0383\(2013\).pdf](http://www.eia.gov/forecasts/aeo/pdf/0383(2013).pdf)
- [4] [http://www.eia.gov/forecasts/aeo/pdf/0383\(2015\).pdf](http://www.eia.gov/forecasts/aeo/pdf/0383(2015).pdf)
- [5] Ásmundsson, R., Normann, R., Lubotzki, H. and Livesay, B., “High Temperature Downhole Tools-Recommendations for Enhanced and Supercritical Geothermal Systems”, IPGT High Temperature Tools Working Group, January 2011, (25 February 2016)
- [6] Ásmundsson, R., Normann, R., Lubotzki, H. and Schill, E., “High Temperature Downhole Tools for Enhanced and Supercritical Geothermal Systems,” *Geothermal Research Council (GRC) Transactions*, Vol. 35, pp. 149-150 (2011)
- [7] R. W. Johnson, J. L. Evans, P. Jacobsen, J. R. Thompson, and M. Christopher, “The changing automotive environment: High temperature electronics,” *IEEE Trans. Electron. Packag. Manuf.*, vol. 27, no. 3, pp. 164–176, Jul. 2004.
- [8] Wang, Y., Dai, X., Liu, G., Wu, Y., Li, D. and Jones, S., "Integrated Liquid Cooling Automotive IGBT Module for High Temperatures Coolant Application," *PCIM Europe 2015; International Exhibition and Conference for Power Electronics, Intelligent Motion, Renewable Energy and Energy Management; Proceedings of, Nuremberg, Germany*, pp. 1-7. (2015)

[9] Higuchi, K., Kitamura, A., Arai, H., Ichimura, T., Gohara, H., Dietrich, P. and Nishiura, A., "An intelligent power module with high accuracy control system and direct liquid cooling for Hybrid system," PCIM Europe 2014; International Exhibition and Conference for Power Electronics, Intelligent Motion, Renewable Energy and Energy Management; Proceedings of, Nuremberg, Germany, pp. 1-8. (2014)

[10] Kurosu, T., Sasaki, K., Nishihara, A. and Horiuchi, K., "Packaging technologies of direct-cooled power module," Power Electronics Conference (IPEC), 2010 International, Sapporo, pp. 2115-2119. (2010)

[11] J. Wallace, "Introducing ... Boeing's electric 7E7", By, SEATTLE POST-INTELLIGENCER, Thursday, May 20, 2004

[12] I. S. Mehdi, A. E. Brockschmidt, and K. K. J., "A case for high temperature electronics for aerospace," in Proceedings of the High Temperature Electronics Conference (HiTEC), (Santa Fe, NM), IMAPS, may 2006.

[13] Chen, Y., Del Castillo, L., Aranki, N., Mazzola, M., Mojarradi, M., and Kolawa, E., "Reliability assessment of high temperature electronics and packaging technologies for Venus mission," *Reliability Physics Symposium, 2008. IRPS 2008. IEEE International*, Phoenix, AZ, pp. 641-642 (2008)

[14] D. C. Linda , V. S. Donald , T. Carissa , H. Toshiro , C. Yuan , M. Mojarradi and E. Kolawa, "Extreme environment electronic packaging for Venus and Mars landed missions", *Proc. 4th Int. Planetary Probe Workshop*, pp. 1-7, 2006

- [15] P. G. Neudeck, R. S. Okojie, and L. Chen, “High-temperature electronics—A role for wide bandgap semiconductors,” *Proc. IEEE*, vol. 90, no. 6, pp. 1065–1076, Jun. 2002.
- [16] P. G. Neudeck, R. S. Okojie, and L. Y. Chen, “High-temperature electronics—A role for wide bandgap semiconductors?,” *Proc. IEEE*, vol. 90, no. 6, pp. 1065–1076, Jun. 2002.
- [17] R. Kirschman, “High Temperature Electronics”, Wiley-IEEE Press, August 18, 1998
- [18] P. L. Dreike, D. M. Fleetwood, D. B. King, D. C. Sprauer and T. E. Zipperian, “An overview of high-temperature electronic device technologies and potential applications”, *IEEE Trans. Comp, Hybrids, Manufact. Technol. A*, vol. 17, pp. 594–609, Dec. 1994.
- [19] B. Ozpineci, L. M. Tolbert, “Comparison of wide-bandgap semiconductors for power electronics applications”, Oak Ridge National Laboratory, ORNL/TM-2003/257.
- [20] J. Homberger, A. B. Lostetter, K. J. Olejniczak, T. McNutt, S. M. Lal, and A. Mantooth, “Silicon-carbide (SiC) semiconductor power electronics for extreme high-temperature environments,” in *Proc. IEEE Aerospace Conf.*, vol. 4. Mar. 2004, pp. 2538–2555.
- [21] T. Nomura, M. Masuda, N. Ikeda, and S. Yoshida, “Switching characteristics of GaN HFETs in a half bridge package for high temperature applications,” *IEEE Trans. Power Electron.*, vol. 23, no. 2, pp. 692–697, Mar. 2008.
- [22] R. F. Davis, G. Kelner, M. Shur, J. W. Palmour, and J. A. Edmond, “Thin film deposition and microelectronic and optoelectronic device fabrication and characterization in monocrystalline alpha and beta silicon carbide,” *Proc. IEEE*, vol. 79, pp. 677–701, May 1991.

[23] J. L. Hudgins, G. S. Simin, E. Santi, and M. A. Khan, "An assessment of wide bandgap semiconductors for power devices," *IEEE Trans. Power Electron.*, vol. 18, no. 3, pp. 907–914, May 2003.

[24] M. R. Werner and W. R. Fahrner, "Review on materials, microsensors, systems, and devices for high-temperature and harsh-environment applications," *IEEE Trans. Ind. Electron.*, vol. 48, no. 2, pp. 249–257, Apr. 2001.

[25] J. B. Casady, W. C. Dillard, R. W. Johnson, and U. Rao, "A hybrid 6H-SiC temperature sensor operational from 25 C to 500 C," *IEEE Trans. Compon., Packaging, and Manufacturing Technology*, vol. 19, no.

[26] D. B. Slater, L. A. Lipkin, G. M. Johnson, A. V. Suvorov, and J. W. Palmour, "High temperature enhancement-mode NMOS and PMOS devices and circuits in 6H-SiC," *53rd Device Research Conf.*, pp. 100–101, Jun. 19–21, 1995.

[27] <http://www.electronics-cooling.com/2006/02/integrated-circuit-package-types-and-thermal-characteristics/>

[28] Johnson, R. W., Pan, S., Palmer, M. and Dean, R., "Conductive Adhesives for Under-the-Hood Automotive Applications," *Proceedings of the 5th International High Temperature Electronics Conference*, June 12-15, Albuquerque, NM. (2000)

[29] E. P. Wood and K. L. Nimmo, "In search of new lead-free electronic solders," *J. Electron. Mater.*, vol. 23, no. 8, pp. 709–713, 1994.

[30] Hagler, P., Henson, P. and Johnson, R. W., "Packaging Technology for Electronics Applications in Harsh, High Temperature Environments," *IEEE Transactions on Industrial Electronics*, Vol. 58, Issue 7, pp. 2673 – 2682.

[31] Palmer, M. J. and Johnson, R. W., "Thick Film Modules for 300° Applications," *Proceedings of the International High Temperature Electronics Conference*, Santa Fe, NM, May 16-18, pp. 118-124 (2006)

[32] Chidambaram, V., Rong, E. P. J., Lip, G. C. and Rhee, M. W. D., "Performance enhancement of Au-Ge eutectic alloys for high-temperature electronics," *Electronics Packaging Technology Conference (EPTC 2013), 2013 IEEE 15th*, Singapore, pp. 202-207 (2013)

[33] Sousa, M.F., Riches, S., Johnston, C., and Grant, P. S., "Assessing the Reliability of Die Attach Materials in Electronic Packages for High Temperature Applications," *Proceedings of the International High Temperature Electronics Conference*, May 11-13, Albuquerque, NM, pp. 1-6 (2010)

[34] Johnson, R. W., Zheng, P., Wiggins, A., Rubin, S. and Peltz, L., "High Temperature Electronics Packaging," *Proceedings of the HITEN International Conference on High Temperature Electronics*, St. Catherine's College Oxford, England, September 17-19 (2007)

[35] Sousa, M. F., Riches, S., Johnston, C. and Grant, P. S., "Optimizing the Performance of the Au-Si System for High Temperature Die Attach Applications," *Proceedings of the IMAPS High Temperature Electronics Network (HiTEN 2011)*, July 18-20, Oxford, UK, pp. 68-76 (2011)

[36] Zheng, P., Wiggins, A., Johnson, R. W., Frampton, R. V., Adam, S. J. and Peltz, L., "Die Attach for High Temperature Electronics Packaging," Proceedings of the International High Temperature Electronics Conference, May 13-15, Albuquerque, NM, pp. 213-219 (2008)

[37] Rettenmayr, M., Lambracht, P., Kempf, B. and Tschudin, C., "Zn-Al Based Alloys as Pb-free solders for Die Attach," Journal of Electronic Materials, Vol. 31, No.4, pp. 278–285 (2002)

[38] Egelkraut, S., Frey, L., Knoerr, M. and Schletz, A., "Evolution of shear strength and microstructure of die bonding technologies for high temperature applications during thermal aging," *Electronics Packaging Technology Conference (EPTC), 2010 12th*, Singapore, pp. 660-667 (2010)

[39] S. J. Kim, K. S. Kim, S. S. Kim, and K. Suganuma, "Interfacial reaction and die attach properties of Zn-Sn high-temperature solders," J. Electron. Mater., vol. 38, no. 2, pp. 266–272, 2009.

[40] P. Quintero and F. P. McCluskey, "Silver–indium transient liquid phase sintering for high temperature die attachment," IMPAS J. Microelectron. Electron. Packag., vol. 6, pp. 66–74, 2009.

[41] Johnson, R. W., Wang, C., Liu, Y. and Scofield, J. D., "Power Device Packaging Technologies for Extreme Environments," IEEE Transactions on Electronics Packaging Manufacturing, Vol. 30, No. 3, pp. 182-191 (2007)

[42] C. L. Chin, Y. W. Chen, and G. Matijasevic, "Au-In bonding below the eutectic temperature," *IEEE Trans. Compon. Hybrids, Manuf. Technol.*, vol. 16, no. 3, pp. 311–316, May 1993.

[43] Grummel, B., Mustain, H. A., Shen, Z. J. and Hefner, A. R., "Comparison of Au-In Transient Liquid Phase bonding Design for SiC Semiconductor Device Packaging," *Proceedings of the IMAPS High Temperature Electronics Network (HiTEN 2011)*, July 18-20, Oxford, UK, pp. 77-83 (2011)

[44] Zheng, P., Henson, P. and Johnson, R. W., "Packaging Technology for Electronics Applications in Harsh, High Temperature Environments," *IEEE Transactions on Industrial Electronics, Special Section on Electronic Devices and Systems in Harsh Environments*, Vol. 58, No. 7, pp. 2673 – 2682 (2011)

[45] Qu, S., Pham, K., Nguyen, L., Prabhu, A., Poddar, A., Athavale, S. and Xu, A., "Electroless over pad metallization for high temperature interconnections," *Electronic Manufacturing Technology Symposium (IEMT), 2010 34th IEEE/CPMT International*, Melaka, pp. 1-7 (2010)

[46] Qu, S. *et al.*, "Over pad metallization for high temperature interconnections," *Electronic Components and Technology Conference (ECTC), 2011 IEEE 61st*, Lake Buena Vista, FL, pp. 1496-1501 (2011)

[47] Ng, B. T., Ganesh, V. P. and Lee, C., "Optimization of gold wire bonding on electroless nickel immersion gold for high temperature applications," *Electronics Packaging Technology Conference, 2006. EPTC '06. 8th*, Singapore, pp. 277-282 (2006)

[48] Burla, R. K., Chen, L., Zorman, C. A. and Mehregany, M., "Development of Nickel Wire Bonding for High-Temperature Packaging of SiC Devices," in *IEEE Transactions on Advanced Packaging*, vol. 32, no. 2, pp. 564-574 (2009)

[49] Freytag, J. and Wennemuth, I., "Wire bonding technique for high temperature applications," *Solid-State and Integrated Circuit Technology, 1998. Proceedings. 1998 5th International Conference on*, Beijing, pp. 219-221 (1998)

[50] Woo, D. R. M., Yun, J. A. K., Jun, Y., Ching, E. W. L. and Che, F. X., "Extremely high temperature and high pressure (x-HTHP) durable SOI device & sensor packaging for deep sea, oil and gas applications," *Electronics Packaging Technology Conference (EPTC), 2014 IEEE 16th*, Singapore, pp. 16-21 (2014)

[51] Delatte, P., Vanzielegem, E., Francois, T. and Doucet, J. C., "VEGA & RIGEL: New tiny high temperature adjustable voltage regulators for reduced PCB footprint and extended reliability of medium and high temperature systems," in *IMAPS High Temperature Electronics Conference (HiTEC)*, pp.93-98 (2012)

[52] Mouawad, B., Buttay, C., Soueidan, M., Morel, H., Bley, V., Fabregue, D. and Mercier, F., "Sintered molybdenum for a metallized ceramic substrate packaging for the wide-bandgap devices and high temperature applications," *Power Semiconductor Devices and ICs (ISPSD), 2012 24th International Symposium on*, Bruges, pp. 295-298 (2012)

[53] Woo, D. R. M., Yun, J. A. K., Jun, Y., Ching, E. W. L. and Che, F. X., "Extremely high temperature and high pressure (x-HTHP) durable SOI device & sensor packaging for

deep sea, oil and gas applications," *Electronics Packaging Technology Conference (EPTC), 2014 IEEE 16th*, Singapore, pp. 16-21 (2014)

[54] Chen, L. Y., Beheim, G. M. and Meredith, R. D., "Packaging Technology for high Temperature Capacitive Pressure Sensor," Proceedings of the International High Temperature Electronics Conference, May 11-13, Albuquerque, NM, pp. 367-372 (2010)

[55] Chen, L.-Y., Hunter, G. W., Neudeck, P. G., Beheim, G. M., Spry, D. J., Meredith, R. D., "Packaging technologies for high temperature electronics and sensors," Joint Conference on 67th Machinery Failure Prevention Technology, MFPT 2013 and 59th International Society of Automation, ISA 2013, 2013.

[56] Okojie, R. S., Beheil, G. M., Saad, G. J. and Savrun, E., "Characteristics of a Hermetic 6H-SiC Pressure Sensor at 600°C," Proceedings of the AIAA Space 2001 Conference and Exposition, Albuquerque, NM, August 28-30, Paper No. 2001-4652 (2001)

[57] <http://www.bulliondesk.com/>

[58] <https://en.wikipedia.org/wiki/Sintering>

[59] http://www.ipmd.net/Introduction_to_powder_metallurgy/Sintering

[60] H. Schwarzbauer, "Method of securing electronic components to a substrate," U.S. Patent 4810672, Mar. 1989.

[61] H. Schwarzbauer, Method and apparatus for fastening electronic components to substrates, US4903885, Siemens, USA (1990).

[62] H. Schwarzbauer, Apparatus for fastening electronic components to substrates, US5058796, Siemens, USA (1991).

[63] U. Scheuermann and P. Wiedl, "Low temperature joining technology—A high reliability alternative to solder contacts," in Proc. Workshop Metal Ceramic Compos. Funct. Appl., Vienna, Austria, 1997, pp.1-5

[64] C. Gobl and J. Faltenbacher, "Low temperature sinter technology die attachment for power electronic applications," in Proc. 6th Int. Conf. Intergr. Power Electron. Syst., Nuremberg, Germany, 2010, pp.1-5

[65] K. S. Siow, "Are sintered silver joints ready for use as interconnect material in microelectronic packaging?", J Electron. Mater., vol. 43, pp. 947- 961, 2014.

[66] H. Schwarzbauer, Heat conducting adhesive joint with an adhesive-filled porous heat conductor, US6823915B2, Siemens, USA (2004).

[67] W. Baumgartner, J. Fellingner, US4856185, Siemens AG, 1989

[68] U. Scheuermann, P. Wiedl, "Low temperature joining technology a high reliability alternative to solder contacts", Workshop on metal ceramics composites for function applications Vienna 4/5. June 1997

[69] W. Schmitt, M. Schafer, and H. W. Hagedorn, Controlling the porosity of metal pastes for pressure free, low temperature sintering process, US2010/0051319A1, W.C. Heraeus, Germany (2010).

[70] W. Schmitt, T. Dickel and K. Stenger, Process and paste for contacting metal surfaces, US2009/0134206A1, W.C. Heraeus, Germany (2009).

[71] M. Kuramoto, S. Ogawa, M. Niwa, K.-S. Kim, and K. Suganuma, “Die bonding for a nitride light-emitting diode by low-temperature sintering of micrometer size silver particles,” IEEE Trans. Compon. Packag. Manuf. Technol., vol. 33, no. 4, pp. 801–808, Dec. 2010.

[72] P. Atkins, D. Shirver et al. “Oxidation and reduction”, Inorganic Chemistry, Fifth edition, Oxford University Press, 2009, ch. 5, pp. 172,

[73] G.Q. Lu, G. Lei, and J. Calata, Nanoscale Metal Paste for Interconnect and Method of Use, WO2009/094537A2 (Blacksburg: Virginia Tech Intellectual Properties, 2009).

[74] M. Tobita and Y. Yasuda, Interconnect material and inter-connect formation method, US2009/0180914A1, Hitachi, USA (2009).

[75] J. G. Bai, Z. Z. Zhang, J. N. Calata, and G. Q. Lu, “Low-temperature sintered nanoscale silver as a novel semiconductor device-metallized substrate interconnect material,” IEEE Trans. Compon. Packag. Technol., vol. 29, no. 3, pp. 589–593, Sep. 2006.

[76] H. Zheng, D. Berry, J. Calata, K. Ngo, “Low-temperature Joining of Large-area Chips on Copper Using Nanosilver Paste”, Components and Packaging Technologies, IEEE Transactions on 33.1 (2010): 98-104.

[77] K. Xiao, J. Calata, H Zheng, K. Ngo, “Simplification of the Nanosilver Sintering Process for Large-Area Semiconductor Chip Bonding: Reduction of Hot-Pressing Temperature

Below 200/spl deg/C”, Components, Packaging and Manufacturing Technology, IEEE Transactions on 3.8 (2013): 1271-1278.

[78] K Xiao, S Luo, K Ngo, G-Q Lu, "Low-temperature sintering of a nanosilver paste for attaching large-area power chips", *Advanced Packaging Materials (APM), 2013 IEEE International Symposium on*. IEEE, 2013.

[79] H Zheng, D Berry, JN Calata, KDT Ngo, S Luo, GQ Lu, "Low-Pressure Joining of Large-Area Devices on Copper Using Nanosilver Paste", Components, Packaging and Manufacturing Technology, IEEE Transactions on 3.6 (2013): 915-922.

[80] D. W. Palmer, and R. Heckman, "Extreme Temperature Range Microelectronics," *Components, Hybrids, and Manufacturing Technology, IEEE Transactions on* , vol.1, no.4, pp.333,340, Dec 1978.

[81] S. T. Riches, C. Warn, K. Cannon, G. Rickard, L. Stoica and C. Johnston, "Design and Assembly of High Temperature Distributed Aero-engine Control System Demonstrator," Proceedings of the International Conference on High Temperature Electronics, May 13-15, 2014, Albuquerque, NM, pp. 285-290.

[82] U. Scheuermann and P. Wiedl, " Low temperature solder contacts," in Proc. Workshop Metal Ceramic Compos. Funct. Appl., Vienna, Austria, 1997, pp.1-5

[83] H. Schwarzbauer, "Method of securing electronic components to a substrate," U.S. Patent 4810672, Mar. 1989.

[84] C. Gobl and J. Faltenbacher, "Low temperature sinter technology die attachment for power electronic applications," in Proc. 6th Int. Conf. Intergr. Power Electron. Syst., Nuremberg, Germany, 2010, pp.1-5

[85] J.G Bai, G.Q Lu, "Thermomechanical Reliability of Low-Temperature Sintered Silver Die Attached SiC Power Device Assembly", *Device and Materials Reliability, IEEE Transactions on* 6.3 (2006): 436-441.

[86] J-G Bai, J Yin, Z Zhang, G-Q Lu, "High-Temperature Operation of SiC Power Devices by Low-Temperature Sintered Silver Die-Attachment", *Advanced Packaging, IEEE Transactions on* 30.3 (2007): 506-510.

[87] JG Bai, JN Calata, GQ Lu, "Processing and Characterization of Nanosilver Pastes for Die-Attaching SiC Devices" *Electronics Packaging Manufacturing, IEEE Transactions on* 30.4 (2007): 241-245.

[88] H. Zheng, D. Berry, J. Calata, K. Ngo, "Low-temperature Joining of Large-area Chips on Copper Using Nanosilver Paste", *Components and Packaging Technologies, IEEE Transactions on* 33.1 (2010): 98-104.

[89] K. Xiao, J. Calata, H Zheng, K. Ngo, "Simplification of the Nanosilver Sintering Process for Large-Area Semiconductor Chip Bonding: Reduction of Hot-Pressing Temperature Below 200/spl deg/C", *Components, Packaging and Manufacturing Technology, IEEE Transactions on* 3.8 (2013): 1271-1278.

[90] K Xiao, S Luo, K Ngo, G-Q Lu, "Low-temperature sintering of a nanosilver paste for attaching large-area power chips", *Advanced Packaging Materials (APM), 2013 IEEE International Symposium on*. IEEE, 2013.

[91] H Zheng, D Berry, JN Calata, KDT Ngo, S Luo, GQ Lu, "Low-Pressure Joining of Large-Area Devices on Copper Using Nanosilver Paste", *Components, Packaging and Manufacturing Technology*, IEEE Transactions on 3.6 (2013): 915-922.

[92] G. Lewis, G. Dumas, S. H. Mannan, "Evaluation of pressure free nanoparticle sintered silver die attach on silver and gold surface," IMAPS conference & Exhibition on HiTEN 2013, July 8-10, 2013, pp. 237 – 245.

[93] R. Wayne Johnson and Rene Cote, "Thermosonic Gold Wire Bonding to Silver Bearing Conductors," *Proceedings of the 1980 International Microelectronics Symposium*, October 1980, pp. 313-321.

[94] M. F. Sousa, S. Riches, C. Johnston and P. S. Grant, "Assessing the Reliability of Die Attach Materials in Electronic Packaging for High Temperature Applications," *Proceedings of the International Conference and Exhibition on High Temperature Electronics*, May 11-13, 2010, pp. 1-6.

[95] Guo-Quan Lu, Yunhui Mei, Xu Chen Dimeji Ibitayo and Susan Luo, "Migration of Sintered Nanosilver Die-Attach Material on Alumina Substrate at High Temperature,"

[96] U. Scheuermann and P. Wiedl, "Low temperature joining technology —A high reliability alternative to solder contacts," in *Proc. Workshop Metal Ceramic Compos. Funct. Appl.*, Vienna, Austria, 1997, pp.1-5.

[97] H. Schwarzbauer, "Method of securing electronic components to a substrate," U.S. Patent 4810672, Mar. 1989.

[98] C. Gobl and J. Faltenbacher, "Low temperature sinter technology die attachment for power electronic applications," in *Proc. 6th Int. Conf. Intergr. Power Electron. Syst.*, Nuremberg, Germany, 2010, pp. 1-5.

[99] J. G. Bai, and G-Q Lu, "Thermomechanical Reliability of Low-Temperature Sintered Silver Die Attached SiC Power Device Assembly", *IEEE Trans. Device Mater. Rel.*, vol. 6, no. 3, pp. 436-443, Sep. 2006.

[100] J. G. Bai, J Yin, Z Zhang, and G-Q Lu, "High-Temperature Operation of SiC Power Devices by Low-Temperature Sintered Silver Die-Attachment", *IEEE Trans. Adv. Packag.*, vol. 30, no. 3, pp. 506– 510, Aug. 2007.

[101] J. G. Bai, J. N. Calata, and G-Q Lu, "Processing and Characterization of Nanosilver Pastes for Die-Attaching SiC Devices" *IEEE Trans. Electron. Packag. Manuf.*, vol. 30, no. 4, pp. 241–245, Oct. 2007.

[102] F. Yu, R. W. Johnson and M. C. Hamilton, "Pressureless Sintering of Microscale Silver Paste for 300 °C Applications," in *IEEE Transactions on Components, Packaging and Manufacturing Technology*, vol. 5, no. 9, pp. 1258-1264, Sept. 2015.

[103] C. Hunt, L. Zou et al. "High Temperatures Solder Replacement to Meet RoHS", NPL Report Mat 64, April 2014.

[104] D. W. Palmer and R. Heckman, "Extreme temperature range microelectronics.," *IEEE Trans. Comp, Hybrids, Manufact. Technol.*, vol.1, no.4, pp.333-340, Dec, 1978.

[105] R. W. Johnson, C. Wang, Y. Liu, and J. D. Scofield, "Power device packaging technologies for extreme environments", *IEEE Trans. Electron. Packag. Manuf.*, vol. 30, no.3, pp.182–193, Jul. 2007

[106] R. W. Johnson, et al, "The changing automotive environment: High-temperature electronics," *IEEE Trans. Electron. Packag. Manuf.*, vol. 27, no. 3, pp. 164–176, Jul. 2004.

[107] L. Coppola, D. Huff, F. Wang, R. Burgos, and D. Boroyevich, "Survey on high-temperature packaging materials for SiC-based power electronics modules," in *Proc. IEEE PESC*, Jul. 2007, pp. 2234-2240

[108] V. R. Manikam and K. Y. Cheong, "Die attach materials for high temperature applications: A review", *IEEE Trans. Compon. Packag. Technol.*, vol. 1, no. 4, pp. 457-478, 2011.

[109] K. S. Siow, "Mechanical properties of nano-silver joints as die attach materials." *J. Alloys Compd.*, vol. 514, pp. 6-19, 2012.

[110] J. Bai and G. Lu, "Thermomechanical reliability of low-temperature sintered silver die attached SiC power device assembly", *IEEE Trans. Device Mater. Rel.*, vol. 6, no. 3, pp. 436-441, 2006.

[111] J. G. Bai, J. Yin, Z. Zhang, G. Lu and J. D. van Wyk, "High-temperature operation of SiC power devices by low-temperature sintered silver die-attachment", *IEEE Trans. Adv. Packag.*, vol. 30, no. 3, pp. 506-510, 2007.

[112] J. Bai, J. Calata and G. Lu, "Processing and characterization of nanosilver pastes for die-attaching SiC devices", *IEEE Trans. Electron. Packag. Manuf.*, vol. 30, no. 4, pp. 241-245, 2007.

[113] H. G. Zhang, D. Berry, J. N. Calata, K. D. T. Ngo, S. Luo and G. Q. Lu, "Low-pressure joining of large-area devices on copper using nanosilver paste", *IEEE Trans. Compon. Packag. Manuf. Technol.* vol. 3, no. 6, pp. 915-922, 2013.

[114] K. Xiao, J. N. Calata, H. Zheng, K. D. T. Ngo and G. Lu, "Simplification of the nanosilver sintering process for large-area semiconductor chip bonding: Reduction of hot-pressing temperature below 200 °C", *IEEE Trans. Compon. Packag. Manuf. Technol.*, vol. 3, no. 8, pp. 1271-1278, 2013.

[115] K Xiao, S. Luo, K Ngo and G. Lu, "Low-temperature sintering of a nanosilver paste for attaching large-area power chips", *Int. Sym. Adv. Pkg. Mat.*, Irvine, CA, 2013, pp. 192-202.

[116] F. Yu, R. W. Johnson, and M. C. Hamilton, 'Pressureless Sintering of Microscale Silver Paste for 300°C Applications', *IEEE Trans. Compon. Packag. Manuf. Technol.*, vol. 5, no. 9, pp. 1258-1264, 2015.

[117] T. G. Lei, J. N. Calata, G. Q. Lu, X. Chen and S. Luo, "Low-temperature sintering of nanoscale silver paste for attaching large-area ($> 100 \text{ mm}^2$) chips", *IEEE Trans. Comp. Packag. Technol.*, vol. 33, pp. 98-104, 2010.

[118] H. G. Zheng, J. Calata, N. Khai, S. Luo and G. Q. Lu "Low-pressure ($< 5 \text{ MPa}$) low-temperature joining of large-area chips on copper using nanosilver paste", *Proc. CIPS*, pp.1-6, 2012.

[119] H. Zheng, D. Berry, J. N. Calata, K. D. Ngo, S. Luo and G. Lu, "Low-pressure joining of large-area devices on copper using nanosilver paste," *IEEE Trans. Compon. Packag. Manuf. Technol.*, vol. 3, pp. 915-922, 2013.

[120] H. Nishikawa, X. Liu, X. Wang, A. Fujita, N. Kamada, M. Saito, "Bonding Strength of Cu/Cu Joints Using Micro-sized Ag Particle Paste for High-temperature Application", *International Conference and exhibition on High Temperature Electronics Network (HiTEN)*, Cambridge, UK, July 6-8, 2015.

[121] J. Li, C. M. Johnson, C. Buttay, W. Sabbah, and S. Azzopardi, "Bonding strength of multiple SiC die attachment prepared by sintering of Ag nanoparticles." *J. Mater. Process. Technol.*, vol. 215, pp. 299-308, 2015.

[122] M. Abbasgholipourghadim and M. Malilah, "Porosity and Pore Area Determination of Hollow Fiber Membrane Incorporating Digital Image Processing." *Recent Advances in Mechanics and Mechanical Engineering*, 2015, pp. 118-123.

[123] P. Ning, "Design and development of high density high temperature power module with cooling system," Ph.D. dissertation, Faculty of the Virginia Polytechnic, 2010.

[124] L. Navarro, X. Perpina, P. Godignon, J. Monteserrat, V. Banu, M. Vel- lvehi, and X. Jorda, "Thermomechanical assessment of die attach ma- terials for wide bandgap semiconductor devices and harsh environment applications," *IEEE Trans. Power Electron.*, vol. 29, no. 5, pp. 2261–2271, May 2014.

[125]http://www.dchopkins.com/professional/open_seminars/DirectBondedCopper.pdf

[126] J. Schulz-Harder, "Advantages and new development of direct bonded copper substrates," *Microelectron. Rel.*, vol. 43, no. 3, pp. 359–365, 2003.

[127] F. Yu, R. W. Johnson, and M. C. Hamilton, "Low Temperature, Fast Sintering of Micro-Scale Silver Paste for Die Attach for 300° C Applications", *International Symposium on Microelectronics*, 2015

[128] K. Xiao, J. N. Calata, H. Zheng, K. D. T. Ngo and G. Lu, "Simplification of the nanosilver sintering process for large-area semiconductor chip bonding: Reduction of hot-pressing temperature below 200 °C", *IEEE Trans. Compon. Packag. Manuf. Technol.*, vol. 3, no. 8, pp. 1271-1278, 2013

[129] M. Abbasgholipourghadim and M. Malilah, "Porosity and Pore Area Determination of Hollow Fiber Membrane Incorporating Digital Image Processing." *Recent Advances in Mechanics and Mechanical Engineering*, 2015, pp. 118-123.